

Spring 2000

Carbon and nitrogen dynamics of northeastern United States forests in response to environmental stress: Measurements and models at local to regional scales

Scott V. Ollinger

University of New Hampshire, Durham

Follow this and additional works at: <https://scholars.unh.edu/dissertation>

Recommended Citation

Ollinger, Scott V., "Carbon and nitrogen dynamics of northeastern United States forests in response to environmental stress: Measurements and models at local to regional scales" (2000). *Doctoral Dissertations*. 2125.
<https://scholars.unh.edu/dissertation/2125>

This Dissertation is brought to you for free and open access by the Student Scholarship at University of New Hampshire Scholars' Repository. It has been accepted for inclusion in Doctoral Dissertations by an authorized administrator of University of New Hampshire Scholars' Repository. For more information, please contact nicole.hentz@unh.edu.

INFORMATION TO USERS

This manuscript has been reproduced from the microfilm master. UMI films the text directly from the original or copy submitted. Thus, some thesis and dissertation copies are in typewriter face, while others may be from any type of computer printer.

The quality of this reproduction is dependent upon the quality of the copy submitted. Broken or indistinct print, colored or poor quality illustrations and photographs, print bleedthrough, substandard margins, and improper alignment can adversely affect reproduction.

In the unlikely event that the author did not send UMI a complete manuscript and there are missing pages, these will be noted. Also, if unauthorized copyright material had to be removed, a note will indicate the deletion.

Oversize materials (e.g., maps, drawings, charts) are reproduced by sectioning the original, beginning at the upper left-hand corner and continuing from left to right in equal sections with small overlaps.

Photographs included in the original manuscript have been reproduced xerographically in this copy. Higher quality 6" x 9" black and white photographic prints are available for any photographs or illustrations appearing in this copy for an additional charge. Contact UMI directly to order.

**Bell & Howell Information and Learning
300 North Zeeb Road, Ann Arbor, MI 48106-1346 USA
800-521-0600**

UMI[®]

**CARBON AND NITROGEN DYNAMICS OF NORTHEASTERN U.S. FORESTS IN
RESPONSE TO ENVIRONMENTAL STRESS: MEASUREMENTS AND MODELS
AT LOCAL TO REGIONAL SCALES.**

BY

SCOTT V. OLLINGER

B.S. Purchase College, 1989

M.S. University of New Hampshire, 1992

DISSERTATION

**Submitted to the University of New Hampshire
In Partial Fulfillment of the
Requirements for the Degree of**

**Doctor of Philosophy
in
Natural Resources**

May, 2000

UMI Number: 9969210

UMI[®]

UMI Microform 9969210

Copyright 2000 by Bell & Howell Information and Learning Company.

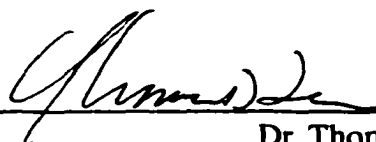
All rights reserved. This microform edition is protected against
unauthorized copying under Title 17, United States Code.

Bell & Howell Information and Learning Company
300 North Zeeb Road
P.O. Box 1346
Ann Arbor, MI 48106-1346

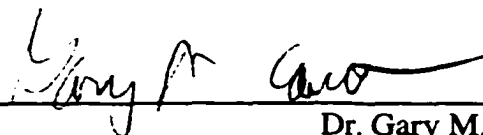
This dissertation has been examined and approved.



Dissertation Director, Dr. John D. Aber
Professor of Natural Resources
Complex Systems Research Center
University of New Hampshire



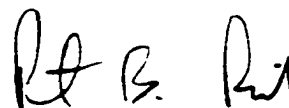
Dr. Thomas D. Lee
Associate Professor of Plant Biology
University of New Hampshire



Dr. Gary M. Lovett
Scientist, Plant Ecologist
Institute of Ecosystem Studies



Dr. Mary Martin
Research Assistant Professor
Complex Systems Research Center
University of New Hampshire



Dr. Peter B. Reich
Professor and F.B. Hubachek, Sr. Chair in Forestry
Department of Forest Resources
University of Minnesota

4/12/2000

Date

**Dedicated to
Rodney M. Ollinger Jr.
for years of friendship and encouragement.**

ACKNOWLEDGEMENTS

First and foremost, I would like to send a million thanks to Dr. John Aber, who has provided unwavering support, encouragement and enthusiasm since my early days as a master's student and has helped make my graduate education an altogether positive experience. He and my other committee members, Drs. Tom Lee, Gary Lovett, Mary Martin, and Peter Reich, have provided many enlightening discussions on subjects ranging from photosynthesis to plant succession to ecosystem biogeochemistry to broad-scale patterns in climate and atmospheric chemistry. I have benefited greatly from these interactions and extend my sincere appreciation to all of them.

Individual chapters of this work were prepared as manuscripts for submission to various scientific journals. I am indebted to all of my co-authors and have retained the plural voice in acknowledgement of their contributions. They are: John D. Aber, C. Anthony Federer, Rita Freuder, Christine L. Goodale, Richard A. Hallett, Mary E. Martin, Peter B. Reich, and Marie-Louise Smith. I also wish to acknowledge the help of a number of individuals who assisted with lab and field work, including Jim Muckenhoupt, Gloria Quigley, Jennifer Pontius, Maggie Leffer, Alison Magill, Matt Kizlinski, Steve Newman, Ralph Perron and Melissa Sytek. Special thanks go to Christy Goodale, Scott Bailey and Jim Hornbeck for their help with plot location and selection and discussions regarding land use history. Thanks are also owed to J.W. Munger and R. Poirot for providing ozone data used in regional and canopy-level analyses.

I have been extremely fortunate to be part of a unique collaboration known as the White Mountain MAPBGC project and am indebted to my co-conspirators and co-leaf shooters, including Christy Goodale, Rich Hallett, Mary Martin and ML Smith. Special thanks go to ML Smith and Mary Martin for their hard work, helpful discussions and generous contributions, particularly regarding remote sensing and canopy chemistry portions of the project.

I am also indebted to the organizations that provided financial support for this work, including the U.S.D.A. Forest Service Northern and Southern Global Change Programs, the National Aeronautics and Space Administration (through NASA TECO grant # NAG5-3527) and the U.S. Environmental Protection Agency (through EPA grant # 825865).

TABLE OF CONTENTS

DEDICATION.....	iii
ACKNOWLEDGEMENTS.....	iv
LIST OF TABLES.....	ix
LIST OF FIGURES.....	x
ABSTRACT	xiii

CHAPTER	PAGE
----------------	-------------

**CHAPTER 1: ESTIMATING REGIONAL PATTERNS OF FOREST
PRODUCTIVITY AND WATER YIELD FOR THE NORTHEASTERN**

U.S.....	1
Abstract.....	1
Introduction.....	2
Methods.....	4
PnET-II.....	4
Regional Data Base.....	5
Regional Model Runs.....	8
Sensitivity Analyses.....	9
Validation.....	10
Results and Discussion.....	12
Model Predictions.....	12
Sensitivity Analyses.....	18
Validation.....	21
Conclusion.....	24

CHAPTER 2: SIMULATING OZONE EFFECTS ON FOREST GROWTH: SCALING LEAF AND STAND-LEVEL PROCESSES TO REGIONAL PATTERNS OF PRODUCTIVITY.....	26
---	-----------

Abstract.....	26
Introduction.....	27
Methods.....	30
PnET-II.....	30
Ozone Response Relationships.....	32
Photosynthesis.....	32
Stomatal Conductance.....	36
Allocation.....	37
Canopy Ozone Gradients.....	38
Interactions Between Ozone and Drought.....	42
Model Application.....	44
Ozone Data.....	44
Model Application Using Mean Climate and Ozone.....	46
Model Application Using Monthly Climate and Ozone.....	47
Sensitivity Analyses.....	48
Results and Discussion.....	50
Mean Climate and Ozone.....	50
Interactions between Climate and Ozone.....	54
Sensitivity Analyses.....	57
Conclusion.....	60

**CHAPTER 3: TROPOSPHERIC OZONE AND LAND USE HISTORY
AFFECT FOREST CARBON UPTAKE IN RESPONSE TO CO₂ AND**

N DEPOSITION.....	63
Abstract.....	63
Introduction.....	63
Methods.....	65
Ozone.....	66
Nitrogen Deposition.....	66
CO ₂	67

Model Analyses	70
Results and Discussion	73
CHAPTER 4: FOLIAR CHEMISTRY IN RELATION TO NITROGEN CYCLING AND NITRATE PRODUCTION ACROSS A TEMPERATE FOREST LANDSCAPE: INFLUENCE OF DISTURBANCE HISTORY AND SPECIES COMPOSITION	
Abstract	80
Introduction	82
Methods	84
Study Area	84
Field Sample Collection and Analysis	87
Soils	87
Foliar Chemistry	89
Remote Sensing	90
Results	92
Soil N Transformations	92
Foliar Chemistry and Soil N Status	102
Species Interactions with N Cycling and Foliar Chemistry	105
Remote Detection of Canopy Chemistry and Soil C:N Ratios	110
Discussion	113
Plant-Soil Interactions	113
Disturbance History	116
Remote Detection of Canopy Chemistry and Regional Ecological Analysis	118
 REFERENCES	 121

LIST OF TABLES

TABLE 1.1.	Results of randomized Monte Carlo sensitivity analyses indicating model sensitivity to climate, soils and foliar nitrogen.....	18
TABLE 1.2.	Validation of predicted biomass production.....	21
TABLE 2.1.	Solutions to equations describing canopy ozone gradients	40
TABLE 2.2.	Locations of ozone monitoring stations used for analysis of interannual variation in ozone effects.....	47
TABLE 2.3.	Predicted net primary production and wood growth with and without ozone at 5 levels of soil water holding capacity.....	53
TABLE 4.1.	Plot characteristics, foliar nitrogen and lignin, soil C:N ratios, net N mineralization and nitrification and soil pH for 30 plots sampled across the White Mountain National Forest.....	94
TABLE 4.2.	Correlation matrix for relationships between N cycling variables, soil C:N ratios and soil pH within and between soil horizons.....	100
TABLE 4.3.	Results of stepwise regressions showing best-fit predictions of soil nitrogen variables using foliar chemistry and disturbance history.....	103
TABLE 4.4.	Fractional species abundance in the canopies of sample plots by forest type and disturbance history.....	106
TABLE 4.5.	Regression coefficients for relationships between species abundance in the canopy and soil nitrogen variables for three species that exhibited significant trends.....	107

LIST OF FIGURES

FIGURE 1.1:	AVHRR-derived Land Use/Land Cover map of the northeast study region.	7
FIGURE 1.2:	Predicted annual net primary production, wood production and runoff generated by PnET-II in conjunction with the northeast regional GIS data base.	13
FIGURE 1.3:	Histograms of predicted annual net primary production, wood production and runoff showing the distributions of values given in Figure 1.2.	16
FIGURE 1.4:	Relationships between predicted net primary production and climate variables for hardwood, pine and spruce-fir forest types across the northeast region.	17
FIGURE 1.5:	Predicted versus observed runoff for gauged watersheds across the study region with greater than 90% forest cover and no barriers to natural flow rates.	23
FIGURE 1.6:	Differences between predicted and observed runoff (Figure 1.5) in relation to the mean basin elevation.	23
FIGURE 2.1:	Percent reduction in net photosynthesis in relation to ozone uptake for hardwoods (From Reich 1987).	33
FIGURE 2.2:	Ozone dose > 40ppb in relation to canopy position at the Harvard Forest in Central Massachusetts.	39
FIGURE 2.3:	Coefficients describing canopy ozone gradient in relation to monthly leaf area index.	41
FIGURE 2.4:	Simplified flow diagram of processes included in PnET-O ₃	43
FIGURE 2.5:	Locations of EPA ozone monitoring stations.	45
FIGURE 2.6:	Predicted change in annual net primary production and wood growth at 64 sites across the study region in response to mean ozone levels from 1987-1992.	51

FIGURE 2.7:	Predicted change in annual net primary production due to ozone in relation to latitude.....	52
FIGURE 2.8:	Distributions of ozone dose, annual precipitation, percent change in net primary production and percent change in wood production across the 12 study sites for individual years from 1987 to 1992.	54
FIGURE 2.9.	Distributions of ozone dose, annual precipitation, percent change in net primary production and percent change in wood production across the 6 year period from 1987 to 1992 for 12 study sites.....	55
FIGURE 2.10.	Results of Monte Carlo sensitivity analyses showing regional ozone effects on net primary production in relation to foliar N and soil WHC under different assumptions for carbon allocation and ozone-drought interactions.....	58
FIGURE 3.1.	Photosynthesis in relation to internal leaf CO ₂ concentrations for conifer and hardwood species taken from the literature.	68
FIGURE 3.2.	Locations of ozone monitoring sites where model simulations were performed.....	71
FIGURE 3.3.	Predicted mean net primary production and net ecosystem production under different combinations of CO ₂ , O ₃ and N deposition and two land use history scenarios.	74
FIGURE 3.4.	Predicted change in current annual net ecosystem production in response to ambient ozone concentrations across the northeastern U.S. under two land use history scenarios	77
FIGURE 3.5.	Mean ozone Dose > 40 ppb in relation to annual wet + dry nitrogen deposition across the northeastern U.S. region.....	78
FIGURE 4.1.	Map of the White Mountain National Forest showing locations of sample sites.	85
FIGURE 4.2.	Comparison of lab incubated and annual field measured rates of net N mineralization and net nitrification.	93
FIGURE 4.3.	Net nitrification in relation to net N mineralization.....	98
FIGURE 4.4.	Soil C:N ratios in relation to net N mineralization and net nitrification.....	99

FIGURE 4.5.	Comparison of N mineralization and nitrification and soil C:N ratios between undisturbed and disturbed stands.	101
FIGURE 4.6.	Net nitrification in relation to canopy N concentrations for disturbed and undisturbed stands.....	102
FIGURE 4.7.	Soil C:N ratios in relation to mass-based canopy lignin:N ratios.	105
FIGURE 4.8.	Mass-based foliar N concentrations for individual species in relation to N mineralization rates.	109
FIGURE 4.9.	Predicted soil C:N ratio for the White mountain National Forest, derived by combining the trend in figure 4.7 with AVIRIS-estimated canopy lignin:N ratios.....	111
FIGURE 4.10.	Soil C:N ratios as predicted from AVIRIS imagery in relation to measured values at 10 plots that were not used in AVIRIS foliar chemistry calibrations.....	112
FIGURE 4.11.	Distribution of predicted soil C:N ratios across the White Mountain National Forest.....	112

ABSTRACT

CARBON AND NITROGEN DYNAMICS OF NORTHEASTERN U.S. FORESTS IN RESPONSE TO ENVIRONMENTAL STRESS: MEASUREMENTS AND MODELS AT LOCAL TO REGIONAL SCALES.

by

SCOTT V. OLLINGER

University of New Hampshire, May, 2000

This thesis stems from several ongoing efforts to characterize patterns of productivity and nitrogen cycling in northeastern US forests and to address the effects of nitrogen deposition, tropospheric ozone and rising atmospheric CO₂. The work reported on involves two related projects; 1) an ecosystem model analysis that integrates physiological and biogeochemical processes with important environmental variables across the northeast region and 2) a field and remote sensing analysis that examines landscape-level patterns of forest biogeochemistry in the White Mountains of New Hampshire.

Chapter 1 presents a regional analysis of forest productivity using the PnET forest ecosystem model and discusses the relative importance of water, temperature and nitrogen on predicted spatial patterns. Chapter 2 integrates ozone effects on leaf-level carbon gain and describes interactions with canopy and stand-level processes. Using

ambient ozone data from across the northeast region, the model predicted declines in annual forest production of between 3% and 16% and demonstrated an interaction with water availability whereby ozone damage declined during periods of drought. In chapter 3, a physiological response to CO₂ is added to the model and applied with historical changes in N deposition and ozone. This analysis suggested that increased CO₂ and N deposition have stimulated forest carbon uptake, but to different degrees following agriculture and timber harvesting. Further, the concurrent increases in ozone offset a large fraction of the predicted growth enhancement. This result is particularly relevant given the related spatial distributions of ozone and N deposition.

The final chapter presents a field study in the White Mountain National Forest that examines relationships between nitrogen cycling and foliar chemistry among forests of diverse history and composition. Across a wide range of conditions, foliar lignin:N ratios were correlated with soil C:N ratios, providing a means of assessing soil N status using hyperspectral remote sensing. Relationships between foliar chemistry and soil N transformations (mineralization and nitrification) were also observed, but these trends differed between historically disturbed versus undisturbed stands. Disturbed stands had significantly lower rates of mineralization and nitrification and higher soil C:N ratios than undisturbed stands, but these trends were not clearly reflected in stand-level foliar chemistry.

CHAPTER I

ESTIMATING REGIONAL PATTERNS OF FOREST PRODUCTIVITY AND WATER YIELD FOR THE NORTHEASTERN U.S.

Abstract

We used the PnET-II model of forest carbon and water balances to estimate regional forest productivity and runoff for the northeastern United States. The model was run at 30 arc-second resolution (approximately 1 km) in conjunction with a Geographic Information System that contained monthly climate data and a satellite-derived land cover map. Predicted net primary production (NPP) ranged from 700 to 1450 g m⁻² yr⁻¹ with a regional mean of 1084 g m⁻² yr⁻¹. Validation at a number of locations within the region showed close agreement between predicted and observed values. Disagreement at two sites was proportional to differences between measured foliar N concentrations and values used in the model. Predicted runoff ranged from 24 to 150 cm yr⁻¹ with a regional mean of 63 cm yr⁻¹. Predictions agreed well with observed values from U.S. Geologic Survey watersheds across the region although there was a slight bias towards overprediction at high elevations and underprediction at lower elevations.

Spatial patterns in NPP followed patterns of precipitation and growing degree days, depending on the degree of predicted water versus energy limitation within each forest type. Randomized sensitivity analyses indicated that NPP within hardwood and pine forests was limited by variables controlling water availability (precipitation and soil

water holding capacity) to a greater extent than foliar nitrogen, suggesting greater limitations by water than nitrogen for these forest types. In contrast, spruce-fir NPP was not sensitive to water availability and was highly sensitive to foliar N, indicating greater limitation by available nitrogen. Although more work is needed to fully understand the relative importance of water versus nitrogen limitation in northeastern forests, these results suggests that spatial patterns of NPP for hardwoods and pines can be largely captured using currently available data sets, while substantial uncertainties exist for spruce-fir.

Introduction

Ecosystem scientists have become increasingly interested in the spatial patterns of important ecological processes and the environmental factors that influence them. This interest stems from the recognition that spatial heterogeneity of environmental and ecological variables interact in ways that make site-specific information alone insufficient for understanding natural systems and coping with the large-scale environmental problems society currently faces.

Several decades of ecosystems research have provided enough information about processes such as photosynthesis, transpiration and decomposition for scientists to build simulation models that predict properties such as biomass production, soil carbon storage and nitrogen cycling rates (e.g. Parton et al. 1988, Raich et al. 1991, Running and Gower 1991, Aber et al. 1997). Along with remote sensing and geographic information systems (GIS), these models can be used to extrapolate predictions across larger spatial scales (Burke et al. 1990, Raich et al. 1991, McGuire et al. 1992, Neilson 1995, Vemapp 1995).

This approach holds great potential for assessing the effects of factors such as air pollution and climate change and also provides a tool for resolving different environmental controls on ecosystem function (e.g. Schimel et al. 1996).

For these goals to be realized, several issues require careful attention. Because ecosystem models (and ecosystems) are very sensitive to the environmental factors that drive them, reliable spatial data sets of important input variables must be obtained from remote or ground-level sources. This can be challenging and often requires making significant assumptions where reliable data are not available. For example, models are often run using potential vegetation where maps of actual vegetation have not been developed. Because human activities have altered the distribution and function of many ecosystems (e.g. Foster 1992), results from these studies may apply to something very different from actual conditions. Where data limitations exist, sensitivity analyses should be performed to test the potential effects of the resulting assumptions. This is a critical, but often overlooked step in ecosystem modeling. Lastly, but of equal importance, model output should be validated at all possible opportunities.

In this paper, we present results from a regional modeling exercise aimed at predicting forest productivity and water balances across the northeastern U.S. using an uncalibrated ecosystem model (PnET-II Aber et al. 1995), a regional climate data set (Ollinger et al. 1995) and a satellite-derived map of current vegetation (Lathrop and Bognar 1994). We also present validation of predicted forest productivity using data from independent field studies, and predicted runoff using data from U.S. Geologic Survey stream gauges. Regional studies are valuable because policy decisions are often made at regional rather than continental or global scales, and because they provide an

important intermediate between detailed plot-level information and coarse-scale modeling of global fluxes.

Methods

PnET-II

PnET-II (Aber et al. 1995) is a monthly time step, canopy- to stand-level model that was built on several generalized relationships. Maximum leaf photosynthetic rate (A_{\max}) is determined as a linear function of foliar nitrogen content, following a strong relationship between the two across species from diverse ecosystems (Field and Mooney 1986, Reich et al. 1995). As such, foliar N serves as a surrogate for site nitrogen availability, assuming that N availability and photosynthetic capacity in foliage are related to N dynamics in soils. Stomatal conductance is related to the actual rate of net photosynthesis, making plant water use efficiency an inverse function of the atmospheric vapor pressure deficit (Sinclair et al. 1984, Baldocchi et al. 1987). This allows transpiration to be predicted from canopy photosynthesis and climate and provides a dynamic link between the carbon and water balance portions of the model.

These relationships are used in the model to construct a multi-layered forest canopy in which available light and specific leaf weight (SLW) decline with canopy depth. Light attenuation is based on the Beers-Lambert exponential decay equation ($y = e^{-k \cdot LAI}$). Changes in SLW are based on Ellsworth and Reich (1993) producing canopy gradients in area-based, but not mass-based foliar nitrogen concentration. Photosynthesis is calculated in a numerical integration over 50 canopy layers in order to capture the effect of gradual light extinction on total canopy carbon gain. Photosynthetic response

curves for light and temperature were derived by Aber and Federer (1992). The photosynthetic response to vapor pressure deficit (VPD) is determined as a power function derived by Aber et al. (1996). Actual evapotranspiration and moisture stress are calculated as functions of plant water demand and available soil water, which is determined using equations from the Brook model (Federer and Lash 1978).

Equations in the model are structured in a series of six subroutines, the first five of which operate in a monthly time step. *AtmEnviron* calculates vapor pressure deficit and cumulative growing degree days, *Psn* determines leaf area display and potential photosynthesis in the absence of drought stress, *WaterBal* calculates available water, drought stress, actual net photosynthesis and runoff, *AllocateMo* calculates tissue respiration and allocation to wood and roots and *SoilResp* calculates CO₂ flux from soils. The final subroutine, *AllocateYr*, allocates accumulated carbon to buds and a wood storage pool for next year's leaf and wood growth.

Regional data base

The northeast study region is the portion of the U.S. north of 41 degrees N latitude and east of 76 degrees west longitude. It includes the New England states, eastern New York and a portion of northeastern New Jersey and Pennsylvania. Environmental inputs required by PnET-II are monthly averages of maximum and minimum daily temperature, vapor pressure and solar radiation, total monthly precipitation, forest type and plant-available soil water holding capacity (WHC). Climate inputs were generated by a statistical model known as Climcalc, developed for the northeast region from long-term (30 year) climate records (Ollinger et al. 1995).

Monthly temperature and precipitation were estimated for each grid cell of a 30 arc-second (approximately 1 km) digital elevation model (DEM) using multiple regression equations based on geographic position and elevation. These equations capture regional and temporal trends in temperature and precipitation, but do not account for local variation such as lake effect precipitation and nighttime valley temperature inversions. Atmospheric vapor pressure was determined as a function of the minimum daily temperature, assuming that nighttime air temperatures decrease only to the point at which dew formation begins. Solar radiation was determined by combining equations for potential radiation with actual radiation measurements made at 11 locations within the study region. Monthly potential radiation was calculated for each grid cell of the DEM using latitude, slope, aspect and time of year. This was then multiplied by the ratio of measured to potential radiation, determined monthly for the 11 measurement stations.

Forest type was determined from a Land Use/Land Cover map (LULC), developed by Lathrop and Bognar (1994) using AVHRR (Advanced Very High Resolution Radiometer) satellite data in combination with existing USGS Land Use/Land Cover data (Figure 1.1). The map identifies hardwood, spruce fir, mixed hardwood/spruce fir and mixed hardwood/pine forest types as well as a number of non-forest categories at 1 km resolution. Approximately 70% of the region is classified as forest; the remainder is mostly agricultural and urban.

Vegetation-specific input parameters such as foliar nitrogen, specific leaf weight and leaf retention time were determined by Aber et al. (1995) for each forest type using data from field measurements within the region. The nitrogen content of foliage is the most important of these parameters because it determines the maximum attainable rate of

photosynthesis. In the absence of a regional foliar N data layer, we assigned a single value to each forest type identified in the LULC map. After Aber et al. (1995), we used values of 2.2% for hardwoods, 1.2% for pines and 0.8% for spruce-fir. Although variation in foliar N within a forest type is generally small with respect to variation across forest types (Newman et al. 1994, Martin and Aber 1997), these are obviously important generalizations.

A plant-available soil water holding capacity (WHC) map for the northeast region has been derived from the U.S. Soil Conservation Service's STATSGO data base (SCS 1991) by Lathrop et al. (1995). However, comparison of these data with the county-level soil survey data from which they were derived showed poor agreement (Lathrop et al.

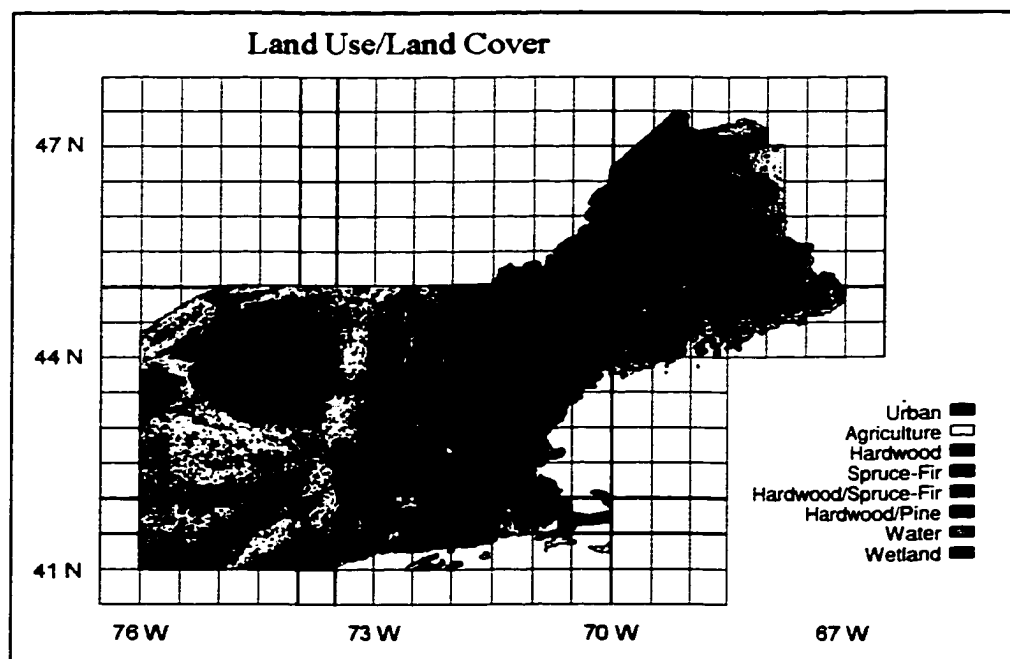


Figure 1.1. AVHRR-derived Land Use/Land Cover map of the northeast study region. (after Lathrop and Bognar 1994).

1995). The authors attributed this to the high degree of spatial variability exhibited by soils in areas of complex terrain combined with the aggregated nature of the STATSGO-derived data. As an alternative, we used the soil hydrology equations of Clapp and Hornberger (1978) to evaluate plant available water under the range of soil properties typically encountered in northeastern forests. Interestingly, for soils ranging from loamy sands to silty clays, texture had a small effect compared with the effects of rooting depth and the fraction of coarse fragments. Assuming a rooting depth of 1 m and 25% coarse fragments, most well drained till soils produced a plant available water holding capacity of 12 cm. Because of uncertainties surrounding the STATSGO-derived data, we held soil WHC at this value for all model runs.

Regional model runs

For regional analyses, all GIS input data layers were georeferenced and converted to a 30 arc second grid (approximately 1 km). For each grid cell, geographic coordinates and elevation were read from the DEM and used by Climcalc to calculate maximum and minimum temperature, vapor pressure, precipitation and solar radiation. Vegetation type was read from the AVHRR-derived Land Use/Land Cover map. Grid cells classified as mixed were run twice and the final output value was calculated as a weighted average of the two runs, assuming a ratio of 40:60 for hardwood/spruce-fir and 40:60 for hardwood/pine. These values were determined by comparing the LULC map with USDA Forest Inventory data for growing stock of these forest types (Kingsley 1985). Because high elevation forests experience stresses that are not included in the model, (e.g. wind damage), we limited model runs to grid cells located below 1200 m, roughly the elevation

at which stresses unique to the subalpine zone begin (Reiners and Lang 1979).

Elevations above 1200 m represent less than one percent of the total land area of the region.

Sensitivity analysis

Predicted patterns of forest productivity reflect how equations in the model respond to climatic gradients across the region. However, these trends are also dependent on assumptions for soil water holding capacity and foliar nitrogen concentrations. In order to assess the importance of these assumptions, we performed sensitivity analyses using a Monte Carlo approach. This involved conducting multiple model runs where inputs for temperature, precipitation, foliar N and soil WHC were determined stochastically using appropriate distribution functions.

For each run, geographic location and elevation were chosen randomly, but were limited for each forest type to the range in which it occurs. For elevation, we used a randomization function that reproduced the skewed distribution of the DEM. This effectively limited variation in climate to values experienced by each forest type within the region. Variation in foliar nitrogen was restricted to values reported in the literature for northeastern hardwoods and conifers. Those values were: 1.8 to 2.6% for hardwoods, 0.9 to 1.5% for pines and 0.7 to 1.2% for spruce-fir (Newman et al. 1994, Bolster et al. 1996). For soil WHC, we used values ranging from 6 cm, representing a sand with 50% stone content, to 18 cm, representing a clay loam with no stones. For foliar N and WHC, we used a randomization function that produced a normal distribution as described by

Hamilton (1989). The model was run a total of 1000 times for each forest type. The relative importance of temperature, precipitation, foliar N and WHC were evaluated by the degree to which each were correlated with predicted NPP.

Validation

There have been relatively few measurements of forest productivity within the study region and at present, there are no data-driven maps with which to test predicted spatial patterns. Nevertheless, comparison of predicted values with existing measurements can still provide insight into the model's performance. Forest productivity (total or aboveground) has been measured for mature pine and hardwood forests at the Harvard Forest in Massachusetts (Magill et al. 1997), for hardwood forests at the Bear Brook watershed in Maine (Magill et al. 1996), for hardwood and mixed forests at three elevations in the Hubbard Brook Experimental Forest in New Hampshire (Whittaker et al. 1974), for young pin cherry stands in northcentral New Hampshire (Marks 1974) and for a high-elevation balsam fir stand on Whiteface Mountain, New York (Sprugel 1984).

We validated the model for these locations by generating pixel values for the latitude, longitude, elevation and forest type of each site. Specifying the correct forest types removed the regional land cover map as a potential source of error, but allowed a greater number of validation points to be used since several sites included measurements for more than one forest type. Potential sources error come from the model, the climate inputs generated by Climcalc and the parameter values used in the regional model runs. No adjustments were made to any of these for the site-level validation. Predictions were

generated for total NPP or aboveground only (ANPP) depending on the data available.

Where both were reported (Whittaker et al. 1974), we used ANPP only because fine roots were not measured, but are included in the model and can be an important fraction of belowground production.

Runoff predictions were validated against observations from gauged watersheds within the region that are part of the USGS Hydro-Climatic Data Network (HCDN, Slack and Landwehr 1992) and contain long term (> 30 year) streamflow records. We restricted the comparison to watersheds that are at least 90% forested since water balances of nonforested lands can vary considerably from those of forests. We also eliminated watersheds where dams, reservoirs, or other human activities impede natural flow rates. The resulting dataset consisted of 34 watersheds ranging in size from a few to several thousand square kilometers, spread relatively evenly across the region.

Streamflow measurements represent water balances that are spatially-integrated over the entire surface of a watershed. Thus, runoff validation would ideally be conducted by averaging predicted values across all grid cells that lie within a given watershed. At present, this is not possible because the boundaries defining the necessary watersheds are not available in a digital format. As an alternative, we used single pixel values coinciding with the latitude, longitude and mean basin elevation of each watershed as given by HCDN. Model predictions were compared with observed mean annual runoff from the period of 1951-1988 (Slack and Landwehr 1992).

Results and Discussion

Model Predictions

Predicted annual net primary production ranged from approximately 700 to 1450 $\text{g m}^{-2} \text{yr}^{-1}$ with a regional mean of 1084 $\text{g m}^{-2} \text{yr}^{-1}$ (Figure 1.2a). In general, predictions increased from north to south, following a gradient in temperature and growing season length, although maximum values were attained at mid elevations in the Catskill mountains where precipitation was high enough to reduce mid summer drought. Predictions were highest in areas of pure hardwood due to the higher photosynthetic rates of broad-leaf deciduous species, as compared to coniferous evergreen species. Lowest growth rates occurred in northern and high elevation spruce-fir forests which had the shortest growing season and lowest photosynthetic rates. Intermediate NPP occurred in mixed hardwood/pine forests along the coastal lowlands of central New England.

Spatial patterns in wood growth followed patterns of NPP, but exhibited a greater range of variation. Predictions ranged from 250 to 900 $\text{g m}^{-2} \text{yr}^{-1}$ with a regional mean of 550 $\text{g m}^{-2} \text{yr}^{-1}$ (Figure 1.2b). PnET-II calculates wood growth as a function of the difference between total biomass production and leaf plus root production after a portion of the remaining carbon is withheld for a reserve pool. The only constraint on wood growth insures that under stressful conditions, the ratio of wood to leaf growth does not fall below a critical level, specified as a parameter in the model (1.5 for hardwoods and 1.25 for conifers, Aber et al. 1995).

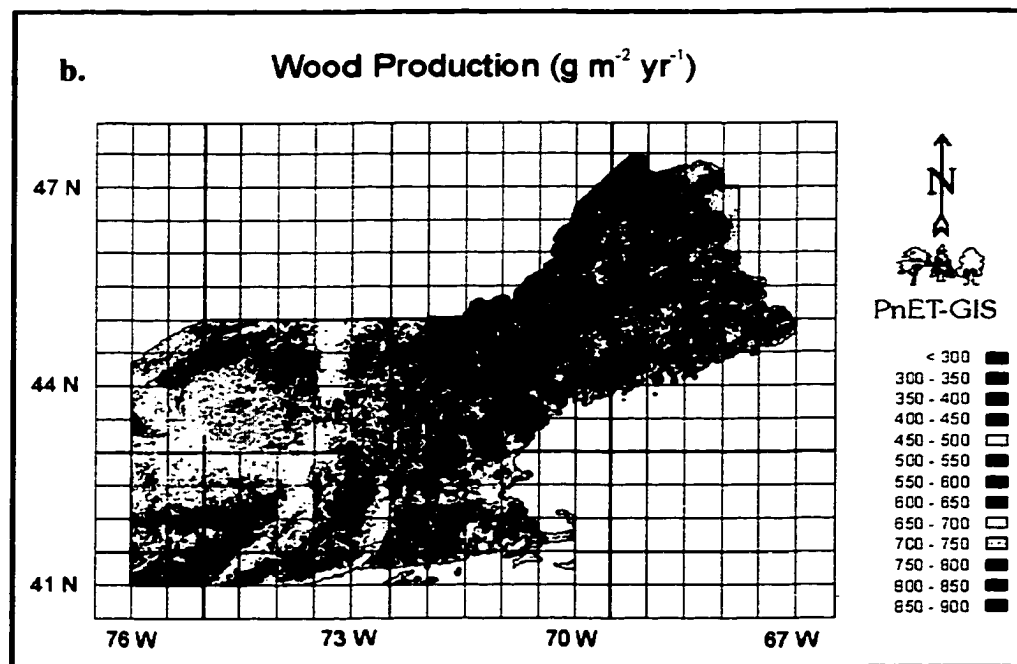
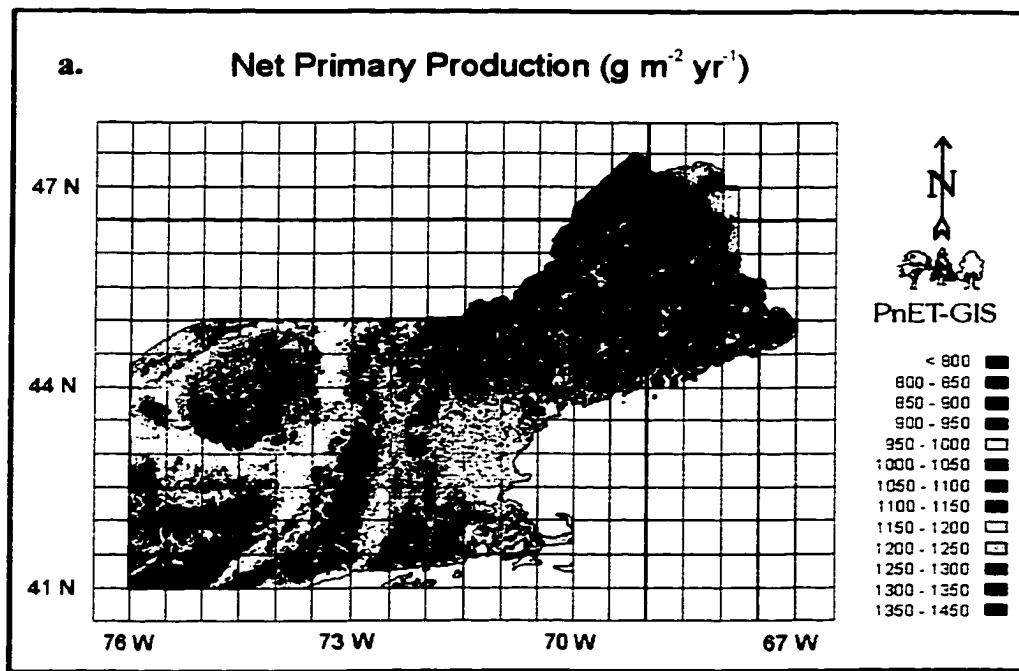


Figure 1.2. Predicted annual NPP (a), wood production (b), and runoff (c) generated by PnET-II in conjunction with the regional GIS data base. Blank areas are non-forest.

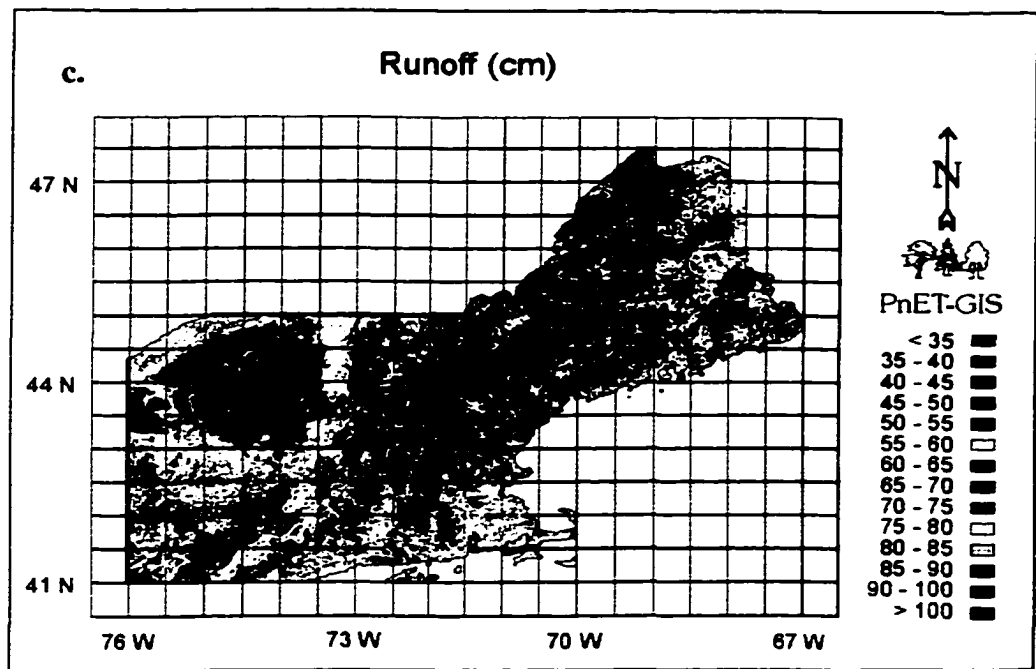


Figure 1.2. Continued.

This serves to prevent foliar production in excess of that which can be supported by new xylem tissue. As such, wood growth is the lowest allocation priority in the model and is least constrained by the model's structure. Hence, it is more sensitive to environmental fluctuations than leaf or root growth.

Predicted annual runoff averaged 63 cm, ranging from approximately 24 cm in the northwest corner of the region to nearly 150 cm at high elevations in the White Mountains of New Hampshire (Figure 1.2c).

The distributions of predicted NPP and wood production show three distinct peaks (Figure 1.3 a, b), corresponding to areas of hardwood (highest values), mixed hardwood/conifer (intermediate values) and spruce-fir (lowest values). This discontinuous pattern results from the fixed hardwood/conifer composition assigned to mixed pixels in the AVHRR land cover map. In reality, these areas undoubtedly contain

a range of hardwood/conifer ratios which would produce a more continuous distribution of values. In contrast, predicted runoff showed a unimodal distribution (Figure 1.3c). Although potential transpiration is driven by photosynthesis, and is generally higher for hardwood than coniferous forests, this was offset by the longer growing season and higher precipitation interception rate of conifers. Differences that do occur between forest types are masked by the greater importance of variation in precipitation.

Comparison of the spatial patterns of predicted growth with those of input climate variables revealed several interesting trends. In general, predicted growth rates were related to precipitation and annual growing degree days as these variables relate to the availability of water and energy. Between vegetation types, however, distinct differences occurred. For hardwoods, the strongest correlation occurred between NPP and precipitation (Figure 1.4a) with a much weaker correlation between NPP and growing degree days. This results from the relatively high photosynthetic rates of hardwoods, which drive transpiration and soil water consumption to a point where water limitations occur. For pine, NPP was correlated with both growing degree days and precipitation, but in different parts of its range. In northern areas, the relationship was strongest with growing degree days because growth rates were low enough that available water supplies were not depleted. Through warmer areas to the south, this trend was replaced by a stronger correlation with precipitation as transpirational demands increasingly depleted available soil water (Figure 1.4b). For spruce-fir, which has the lowest photosynthetic rate and is restricted to northern and high-elevation areas, the only significant trend was with growing degree days (Figure 1.4c).

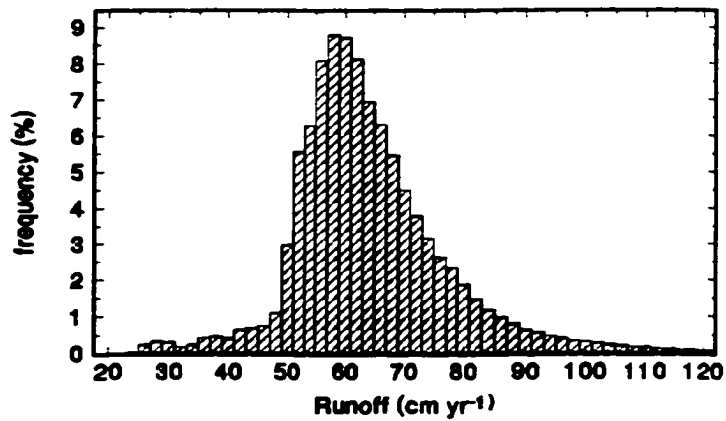
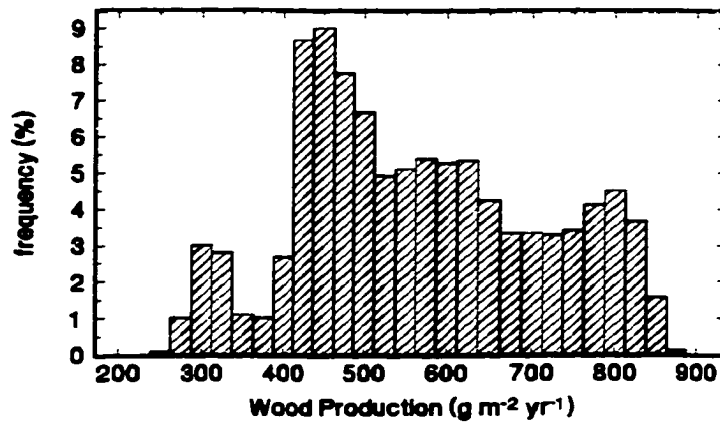
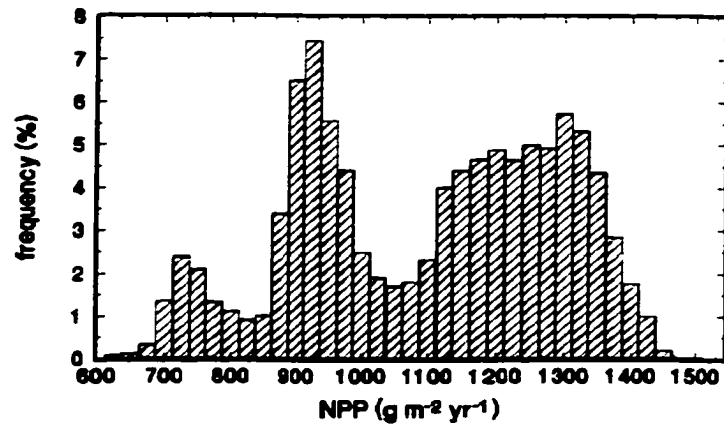


Figure 1.3. Histograms of predicted annual NPP (a), wood production (b), and runoff (c) showing the distributions of values given in Figure 1.2. In (c), a small number of data points representing high elevation areas lie off the scale to the right.

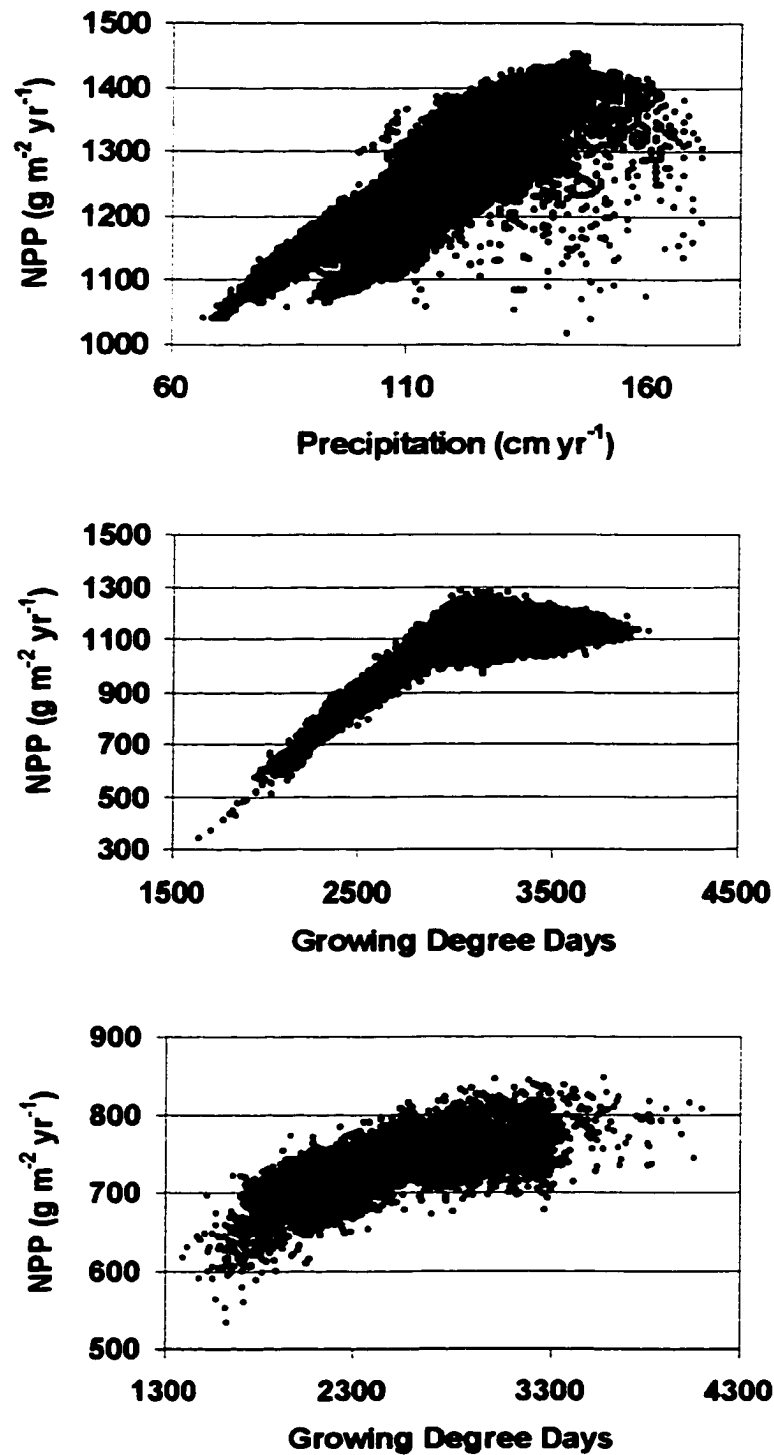


Figure 1.4. Relationships between predicted NPP and climate for each forest type: (a) hardwood NPP vs. annual precipitation, (b) pine NPP vs. annual growing degree days and (c) spruce-fir NPP vs. annual growing degree days. In 1.4a, data points falling off the relationship to the upper right reflect high elevation areas where temperature limitations become increasingly important.

Table 1.1. Results of randomized Monte Carlo analyses indicating sensitivity of predicted NPP to climate, foliar N and soil WHC for each forest type as shown by correlation coefficients (R^2) from regression of NPP against each variable alone and in combination. Climate data are summarized as annual precipitation (PPT) and annual growing degree days (GDD). Foliar N (FolN) is mass-based leaf nitrogen concentration and soil WHC is plant-available soil water at field capacity. $n = 1000$ for each forest type. All variables were significant at $p < 0.05$) except where listed as NS.

	R^2			Standard Error		
	Hardwood	Pine	Spruce-fir	Hardwood	Pine	Spruce-fir
PPT	0.46	0.27	NS	83	92	78
GDD	0.02	0.02	0.10	108	106	74
Fol N	0.16	0.18	0.74	101	100	40
WHC	0.27	0.25	NS	93	93	78
PPT + GDD	0.54	0.32	0.11	81	89	73
Fol N + WHC	0.40	0.38	0.74	83	84	40
ALL	0.90	0.78	0.90	35	51	25

Sensitivity analyses

The relationships in Figure 1.4 indicate an interaction between model sensitivity to temperature and precipitation, variables for which regional data are available. Results of randomized sensitivity analysis (Table 1.1) indicate additional interactions with foliar nitrogen and plant-available soil water holding capacity (WHC), variables for which reliable data layers are not currently available at the regional level. As such, these results represent the degree to which the trends in Figures 1.4a-c depend on assumptions made about these missing data layers.

Within the randomized model runs, the strongest predictors of NPP for hardwood and pine forests were precipitation and soil WHC, indicating that water limitations were common in both forest types under the range of conditions simulated. The stronger correlation with precipitation than WHC indicates that regional variation in precipitation had a greater effect on available water than did our simulated range of WHC. Spruce-fir NPP showed the opposite trend, being unrelated to water availability and strongly correlated with foliar N. This results from the fact that spruce-fir transpiration rates were rarely high enough to exhaust soil water supplies and induce water stress.

The model's relatively low sensitivity to foliar nitrogen for hardwood forests countered our expectations based on earlier, site-level analyses which showed foliar N to be a critical input parameter for this forest type (Aber et al. 1996). These results are not contradictory, but rather demonstrate the influence of scale in determining the relative importance of different ecological processes. Foliar N varies over finer spatial scales than precipitation, and for local areas, appears to control patterns of productivity via its affect on photosynthesis and carbon gain (Martin and Aber 1997). At the broader regional level, however, variation in precipitation overshadowed variation in available N, and water limitation became the dominant factor.

These trends also suggest interactions between water, nitrogen and carbon dynamics that were observed in several previous modeling exercises (Schimel et al. 1996, Aber et al. 1997). Although nitrogen limitations in terrestrial ecosystems often occur locally through both time and space, large scale patterns of productivity are more often related to patterns of temperature and rainfall. Schimel et al. (1996) addressed this conflict by using the Century model to evaluate the relative importance of water and

nitrogen limitations globally. The model predicted that, under steady-state conditions, nitrogen limitations and water limitations become correlated. This was due to the simultaneous control of carbon and nitrogen fluxes by the water budget. Aber et al. (1997), using a version of the PnET model that includes coupled C and N cycles, reached similar conclusions predicting that N cycling rates in the northeastern U.S. were ultimately limited by water or energy, depending on the C fixation efficiencies of different forest types. The paradox of growth limitations by both water and nitrogen was suggested by both authors to be a function of disturbance, whereby periodic perturbations alter rates of C and N cycling which in turn are constantly moving towards - if never achieving - a state of equilibrium with the ultimate controls set by the physical environment.

Overall, the combined influence of precipitation, growing degree days, foliar N and soil WHC explained between 78 and 90% of the variation in predicted NPP within the randomized model runs (Table 1.1). Table 1.1 also shows the degree to which predicted NPP is correlated with PPT and GDD together versus foliar N and WHC together. These combinations are presented to provide an indication of the amount of spatial variation in regional NPP which can be explained by factors for which spatial data bases presently exist versus those for which further data development are required. The strong dependence of NPP on precipitation among hardwoods and pines suggests that regional patterns may be at least partly captured by available data, with uncertainty introduced by the absence of WHC and foliar N data planes. For spruce-fir, the importance of foliar N raises considerable uncertainties in current predicted spatial patterns across the study region.

Validation

Predicted forest production rates were generally in good agreement with measured values (Table 1.2). The mean absolute error between predicted and observed values was 12.5%. The two sites with poorest agreement were the high elevation balsam fir stand, where the predicted value was less than half of that measured, and the Harvard Forest hardwood stand, where the model overpredicted by 20%. In both cases, measured values for foliar nitrogen were reported and appear to explain much of the disagreement.

Table 1.2. Predicted and measured biomass production ($\text{g m}^{-2} \text{ yr}^{-1}$) for several locations across the northeastern U.S. Abbreviations are: BB = Bear Brook watershed, ME; HF = Harvard Forest, MA; HB = Hubbard Brook, NH (low, mid and high elevations); NNH = Northern NH and WF = Whiteface Mt., NY. ANPP is aboveground net primary production, NPP is total net primary production.

Site	Variable Measured	Forest Type	PnET-II	Observed	Source
BB	ANPP	HW	909	893	Magill et al. 1997
HF	ANPP	HW	1010	843	Magill et al. 1996
HF	ANPP	Pine	795	757	Magill et al. 1996
WF	ANPP	Balsam fir	456	960	Sprugel 1984
HB low	ANPP	HW	1032	1094	Whittaker et al. 1974
HB mid	ANPP	HW	1013	1010	Whittaker et al. 1974
HB high	ANPP	HW-SF	876	751	Whittaker et al. 1974
NNH	NPP	Pin Cherry	1295	1264	Marks 1974

Sprugel (1984) measured an average foliar N of 1.59% at Whiteface Mountain, which is high relative to other values reported for balsam fir (Newman et al. 1994, Bolster et al. 1996) and almost twice that used for spruce-fir forests in this study. At Harvard Forest,

Magill et al. (1997) reported a foliar N of 1.9% for the hardwood stand, which is low for this forest type and lower than the value of 2.2% used in the model. Using the measured foliar N values resulted in considerably closer agreement for both Whiteface and Harvard Forest (predicted ANPP = 980 and 905, respectively) and reduced the average absolute error to only 5.2% for all validation sites combined.

Predicted runoff was in good agreement with measured values for forested watersheds in the USGS Hydro-Climatic Data Network (Figure 1.5). Mean annual runoff among the HCDN watersheds was 71.1 cm, compared with the mean predicted value of 72.6 cm. Regression of predicted against observed values produced an r^2 of 0.73, a standard error of 6.0 cm (8.4%), and a slope and intercept not significantly different from 1 and 0, respectively. Although this indicates generally good spatial agreement across the region, residuals indicated a slight elevation bias whereby the model tended to overpredict runoff at higher elevations and underpredict at lower elevations (Figure 1.6). At present, it is unclear whether this bias results from the elevation coefficients used to estimate precipitation, the model's calculation of canopy transpiration, the use of a fixed water holding capacity or the use of single pixel values for each watershed (as opposed to extracting predictions from the entire surface of each watershed). Although any of these may have caused the observed bias, the precipitation-elevation coefficients used by Climcalc are perhaps most suspect because they were derived from relatively few high elevation weather stations. Additional efforts aimed at resolving this issue should lead to improvements in future runoff predictions.

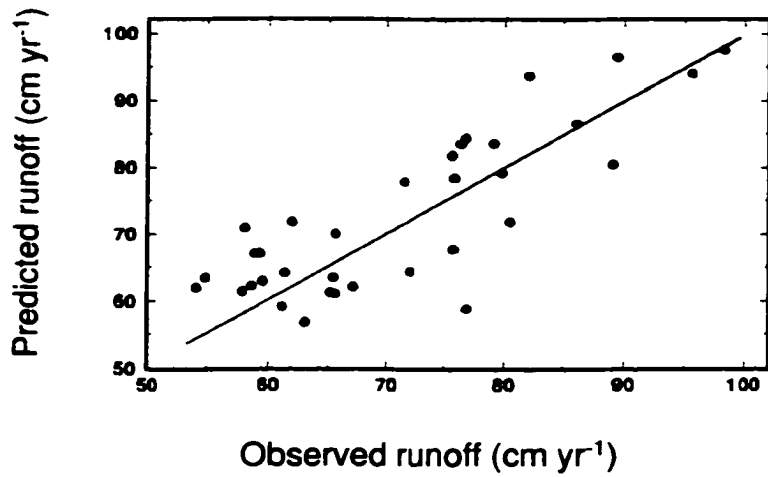


Figure 1.5. Predicted versus observed runoff for gauged watersheds across the study region with > 90% forest cover and no barriers to natural flow rates (dams, reservoirs, etc.). $n = 34$.

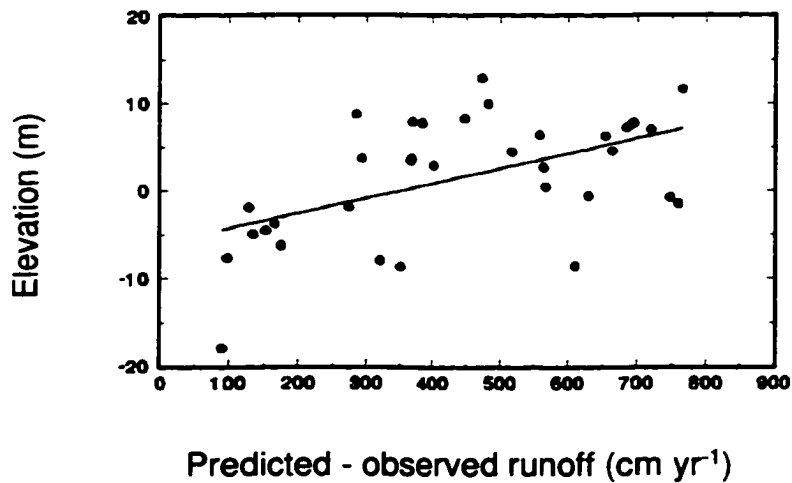


Figure 1.6. Differences between predicted and observed runoff (Figure 1.5) in relation to the mean basin elevation.

Conclusions

This analysis provided regional estimates of forest production and water yield for the northeastern U.S. using a satellite-derived map of current vegetation and an uncalibrated model of forest carbon and water balances. Several interesting trends between forest production and regional gradients in climate were suggested. Among hardwood forests, NPP was strongly correlated with precipitation suggesting water limitation as an important factor controlling regional patterns of productivity. NPP within pine forests was correlated with precipitation across much of the region, except in northern and upper elevation areas where transpirational demands are low. In these areas, stronger relationships were observed between NPP and annual growing degree days. Among spruce-fir forests, which are found only in northern and high elevation areas, NPP was rarely limited by water and was most strongly related to growing degree days.

Randomized sensitivity analyses showed that model sensitivity to inputs for soil water holding capacity (WHC) and foliar nitrogen varied between forest types. Under the range of temperature, precipitation, foliar N and WHC values expected across the region, precipitation was the strongest predictor of NPP among hardwoods and pines, followed by WHC and foliar N. Within spruce-fir forests, water limitations were absent and predicted growth were related only to foliar N. Further research will be needed to determine the actual importance of nitrogen versus water limitation on spatial patterns of productivity.

Model validation showed good agreement between predicted and measured forest productivity and runoff at a number of sites across the region. Differences between

predicted and measured forest productivity at two sites were related to data inputs for foliar nitrogen. Differences between predicted and observed runoff were positively correlated with elevation, suggesting an elevational bias in inputs for water availability (precipitation or soil water holding capacity) or processes simulated by the model (e.g. transpiration). Because water and nitrogen are the two most important factors limiting northeastern forest productivity, future efforts should be directed towards obtaining or improving high-resolution data planes for these variables.

CHAPTER II

SIMULATING OZONE EFFECTS ON FOREST GROWTH: SCALING LEAF AND STAND-LEVEL PROCESSES TO REGIONAL PATTERNS OF PRODUCTIVITY

Abstract

Ozone pollution in the lower atmosphere is known to have adverse effects on forest vegetation, but the degree to which mature forests are impacted has been very difficult to assess directly. In this study, we combined leaf-level ozone response data from independent ozone fumigation studies with a forest ecosystem model in order to simulate the effects of ambient ozone on mature hardwood forests. Reductions in leaf carbon gain were determined as a linear function of ozone flux to the leaf interior, calculated as the product of ozone concentration and leaf stomatal conductance. This relationship was applied to individual canopy layers within the model in order to allow interaction with stand- and canopy-level factors such as light attenuation, leaf morphology, soil water limitations and vertical ozone gradients.

The resulting model was applied to 64 locations across the northeastern United States using ambient ozone data from 1987 to 1992. Predicted declines in annual net primary production ranged from 3 to 16% with greatest reductions in southern portions of the region where ozone levels were highest, and on soils with high water holding capacity where drought stress was absent. Reductions in predicted wood growth were slightly greater (3 to 22%) because wood is a lower carbon allocation priority in the model than

leaf and root growth. Interannual variation in predicted ozone effects was small due to concurrent fluctuations in ozone and climate. Periods of high ozone often coincided with hot, dry weather conditions, causing reduced stomatal conductance and ozone uptake. Within-canopy ozone concentration gradients had little effect on predicted growth reductions because concentrations remained high through upper canopy layers where net carbon assimilation and ozone uptake were greatest.

Sensitivity analyses indicate a tradeoff between model sensitivity to available soil water and foliar nitrogen and demonstrate uncertainties regarding several assumptions used in the model. Uncertainties surrounding ozone effects on stomatal function and plant water use efficiency were found to have important implications on current predictions. Field measurements of ozone effects on mature forests will be needed before the accuracy of model predictions can be fully assessed.

Introduction

Tropospheric ozone is one of the most pervasive and detrimental air pollutants known to affect forest vegetation. Repeated studies have demonstrated that ozone concentrations commonly observed in polluted air masses can have substantial impacts on plant function. Despite regulatory efforts aimed at controlling emissions of the precursor compounds (nitrogen oxides and volatile organics), ozone levels have continually exceeded national ambient air quality standards (NAAQS) across much of the United States and are expected to increase into the foreseeable future (National Research Council 1992).

A large body of research has documented the mechanisms by which ozone affects

plants. A number of reviews are available for comprehensive discussion of these mechanisms (Guderian et al. 1985, Pye 1988, Heck et al. 1988), but in general, observed responses can be viewed as those involving either the acquisition or allocation of carbon. At the physiological level, the most pronounced effect of ozone on plant carbon gain is a reduction in net photosynthesis resulting from the oxidation of pigments and photosynthetic enzymes (Guderian et al. 1985, Reich and Amundson 1985, Pell et al. 1992, Tjoelker et al. 1995). Because injury occurs at the leaf interior, factors affecting leaf gas exchange rates are important in determining plant response to a given level of external exposure (Reich 1987, Taylor and Hanson 1992). Species with high gas exchange rates, such as early-successional hardwoods, exhibit the greatest growth reductions, while slow-growing species such as spruce are less affected (e.g. Reich and Amundson 1985, Wang et al. 1986, Skarby et al. 1995).

Because plant allocation patterns have evolved towards optimized use of available carbon to meet the requirements of a particular growth strategy, any change in C fixation is likely to affect subsequent partitioning into different plant tissues (Mooney and Winner 1991). In seedlings, ozone has been observed to induce reductions in root/shoot ratios as allocation shifts towards the maintenance or replacement of ozone-damaged foliage at the expense of root growth (Hogsett et al 1985, Laurence et al. 1994, Pell et al. 1994, McLaughlin and Downing 1995, McLaughlin et al. 1994).

Although ozone damage mechanisms have been well studied at the seedling and leaf level, it is still difficult to assess impacts on mature forests across real landscapes. Direct application of seedling-level results is problematic for several reasons. Factors such as light availability, leaf morphology and ozone concentrations all vary within a

forest canopy. This complicates estimation of pollutant uptake via their effects on stomatal conductance and ozone exposure levels (Pye 1988). Additional uncertainty stems from differences in growth patterns and resource constraints of seedlings versus mature trees (Pye et al. 1988, Edwards et al. 1994, Fredericksen et al. 1994). Seedlings are at a flexible ontogenetic stage, are often grown in pots with ample water and nutrients and therefore have more dynamic carbon economies than mature trees, which are less allocationally plastic and must compete for light, water and other resources.

One method of addressing these scaling issues is to incorporate ozone-response relationships into process models that simulate tree growth and ecosystem function. Several studies have used models to simulate the plant-level response of conifers (Chen et al. 1994, Laurence et al. 1993, Weinstein and Yanai 1994), but the approach has not been applied to mature hardwood forests under ambient field conditions. The purpose of this study was to integrate physiological ozone response data into a forest ecosystem model known as PnET-II (Aber et al. 1995, 1996) in order to simulate the effects of ozone on mature hardwood forests in the northeastern U.S. PnET-II is a physiologically-based model that was designed to capture important ecosystem processes while retaining enough simplicity to be run on the types of data available across large regions. Our approach was to characterize leaf-level ozone effects on carbon fixation and add the resulting algorithms to individual canopy layers within the model. By combining this with measured canopy ozone gradients, ozone effects are assessed for each canopy layer as influenced by variation in light, water and ozone exposure.

We applied the model using ambient ozone data from 64 locations across the northeastern U.S., a region dominated by hardwood forests that is chronically impacted

by ozone and other urban and industrial air pollutants. Predictions are given for all 64 sites using mean climate and ozone from the period of 1987-1992 and for a subset of 12 of these sites using monthly climate and ozone for the same time period. In addition to estimating ozone effects on regional forest growth, questions we sought to address were 1) how do predictions vary with respect to site moisture status, 2) what are the effects of year-to-year fluctuations in climate and 3) what are the potential consequences of assumptions used in the model.

Methods

PnET-II

PnET-II is a monthly time step model of forest carbon and water balances that is built on several generalized relationships. Maximum leaf photosynthetic rate (A_{max}) is determined as a linear function of foliar nitrogen content, following a strong relationship between the two across species from diverse ecosystems (Field and Mooney 1986, Reich et al. 1995). Stomatal conductance is related to the actual rate of net photosynthesis, making plant water use efficiency an inverse function of the atmospheric vapor pressure deficit (Sinclair et al. 1984, Baldocchi et al. 1987). This allows transpiration to be determined from canopy photosynthesis, providing a link between forest carbon uptake and site water balances.

These relationships are used in constructing a multi-layered forest canopy in which available light and specific leaf weight (SLW) decline with depth through the canopy. Light attenuation is based on the Beers-Lambert exponential decay equation ($y = e^{-k \cdot LAI}$) with a light extinction coefficient of 0.58 for hardwood forests. Changes in SLW

through the canopy are based on Ellsworth and Reich (1993), resulting in a gradient of area-based, but not mass-based foliar nitrogen concentration (Ellsworth and Reich 1993). This allows interaction between mass-based A_{\max} and area-based light interception within each canopy layer. These equations are used in a numerical integration over 50 canopy layers in order to capture the effect of gradual light attenuation on photosynthesis over the entire canopy. Photosynthetic response curves for light and temperature were derived by Aber and Federer (1992). The photosynthetic response to vapor pressure deficit (VPD) is based on a power function described by Aber et al. (1996). Actual evapotranspiration and moisture stress are calculated as functions of plant water demand and available soil water which is determined using equations from Federer and Lash (1978).

Leaf production is initiated as a function of cumulative growing degree days and is drawn from bud carbon reserves accumulated during the previous year. Maximum foliar biomass is a function of available light, foliar N and SLW, but is also affected in a given year by stress-induced reductions in foliar mass during the previous year (Aber et al 1995). This has the effect of minimizing intra-annual variation in leaf area display due, for instance, to mid-summer drought. Root growth is based on the linear relationship between aboveground litter production and root allocation determined by Raich and Nadelhoffer (1989). This relationship produces a decrease in proportional belowground allocation with increasing allocation to foliage. Annual allocation to wood is determined as a fraction of the remaining plant C pool after production of foliage and roots. The only constraint on wood production ensures that the ratio of wood C to bud C does not fall below a critical level, specified as a parameter in the model. For hardwoods,

this parameter is set to 1.5 and serves to prevent foliar growth in excess of that which can be sustained by production of new xylem tissue each year (Aber et al. 1995). When wood growth falls below this level, carbon is drawn from bud C until this ratio is maintained. Thus, wood represents the lowest carbon allocation priority and is the most responsive growth compartment to environmental fluctuations.

The model has performed well at predicting wood growth, net primary production and water runoff at diverse locations across North America (Aber and Federer 1992, Aber et al. 1995), and has also been successfully tested against eddy flux CO₂ exchange measurements (Aber et al. 1996).

Ozone response relationships

Photosynthesis. Data from the literature demonstrate strong relationships between cumulative ozone exposure and reductions in both net photosynthesis and plant growth (e.g. Guderien et al. 1985, Reich and Amundson 1985, Reich 1987, Pell et al. 1992, Volin et al. 1993, Skarby et al. 1995, Tjoelker et al. 1995). These relationship can vary among and even within species, although much of this variation is related to differences in stomatal conductance (Thorne and Hanson 1972, Reich 1987). Because conductance is the most important regulator of ozone uptake under a given external concentration (Taylor and Hanson 1992, Munger et al. 1996), this suggests that ozone effects on photosynthesis can be determined largely as a function of ozone uptake to internal leaf surfaces (Reich 1987, Laisk et al. 1989, Taylor and Hanson 1992). This is not to say that other factors are unimportant. Differences in plant sensitivity per unit ozone uptake have also been noted and are likely related to differences in leaf

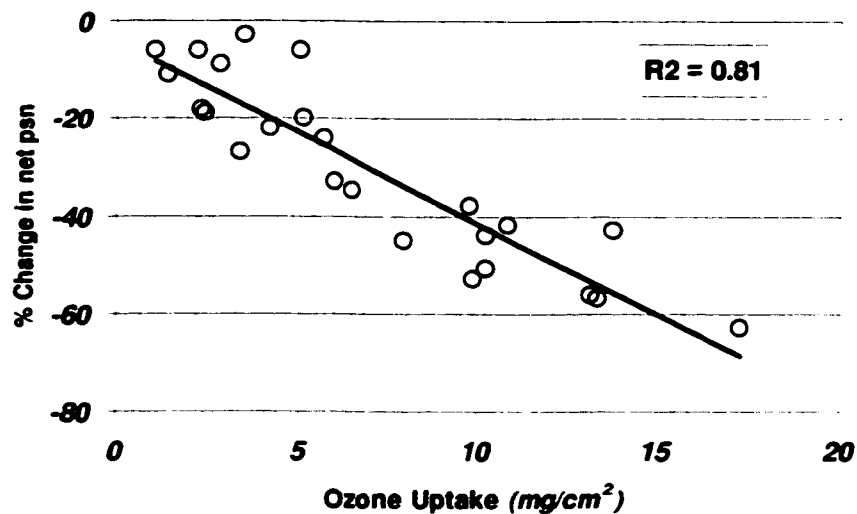


Figure 2.1. Percent reduction in net photosynthesis in relation to ozone uptake for hardwoods. From Reich 1987 using data from independent studies conducted over periods of several days to several months on a variety of hardwood seedlings.

biochemistry or cellular anatomy (Taylor and Hanson 1992). However, when considering the range of species that typically occur across natural landscapes, these differences appear much smaller proportionally than differences attributed to conductance, and hence uptake. Differences in response per unit uptake also tend to be greater in magnitude between functional groups (e.g. hardwoods vs. conifers) where leaf structure and plant growth strategy differ most widely (Reich 1987). If we limit the literature data examined by Reich (1987) to hardwoods, 81% of the variation in observed photosynthetic response can be explained by cumulative ozone uptake alone (Figure 2.1). Given the strength of this relationship and uncertainties surrounding additional sources of variation, examining its implications across natural forested landscapes represents a valuable way to advance current understanding of ozone effects, even while recognizing the limitations of its simplicity.

Although most of the data relating ozone exposure to changes in photosynthesis

come from seedlings, several studies conducted on mature trees indicate similar or perhaps greater responses. Tjoelker et al. (1995) obtained a response consistent with that shown in Figure 2.1 from mature sugar maple leaves, suggesting that at the leaf level, seedlings and mature trees respond similarly. In contrast, Edwards et al. (1994) compared the photosynthetic responses of mature and seedling red oak trees and found mature trees to exhibit greater reductions than seedlings. This was attributed to differences in seedling versus mature-tree carbon allocation. Seedlings consistently produced multiple leaf flushes and exhibited indeterminate stem growth whereas mature trees produced only a single growth flush each spring. Although changes in seedling photosynthesis were not reported with respect to leaf age or ozone uptake, indeterminate growth patterns can result in lower responses at the plant level because only a fraction of the leaves produced are exposed to ozone for the entire growing season. Such differences in ozone exposure have been demonstrated by Fredericksen et al. (1994) between open-grown seedling and mature black cherry trees. Although seedlings exhibited greater instantaneous rates of ozone uptake than mature trees, their indeterminate shoot growth resulted in reduced average exposure times and subsequently lower cumulative uptake.

Indeterminate growth can also lead to lower reductions or even increases in whole-plant photosynthesis by allowing mid-season adjustments in allocation of carbon and nutrients. Pell et al. (1994) reviewed several studies where increased photosynthesis was observed in younger foliage of free-growing seedlings after older foliage suffered damage from ozone. This compensation mechanism was less important for species with a limited number of growth flushes and is not expected to occur in mature, closed-canopy trees which produce all of their foliage at the beginning of the growing season and

typically never flush again.

These results suggest that differences between seedling and mature-tree allocation patterns can cause differences in ozone response at the plant level, but do not indicate differences in the relationship between cumulative ozone uptake and net photosynthesis among individual leaves. This underscores the importance of distinguishing between leaf- and plant-level responses in extrapolating seedling response data to mature, field-grown trees.

For the present study, we pooled data from Figure 2.1 (Reich 1987) and Tjoelker et al. (1995) in order to derive a leaf-level ozone response equation for broad-leaved deciduous species that could be incorporated into the PnET-II model. To minimize differences caused by seedling versus mature-tree allocation patterns, the data were summarized on an individual leaf basis using initial growth flush foliage where possible. Thus, the response of each leaf could be related to cumulative ozone uptake calculated over its own lifespan. From the resulting data set we obtained the following response equation:

$$1) \quad dO_3 = 1 - (.0026 * g * D40)$$

where dO_3 is the ratio of ozone-exposed to control photosynthesis, .0026 is an empirically derived ozone response coefficient, g is mean stomatal conductance to water vapor (in mm s^{-1}) and D40 is the cumulative ozone dose (in ppm-h) above a threshold concentration of 40 ppb. The diffusivity ratio of ozone to water vapor is not explicitly used in the equation, but as a constant, is accounted for by the calculated ozone response

coefficient. The D40 dose is accumulated over the entire growing season and is calculated as the sum of all hourly values > 40 ppb after subtracting 40 from each. We use this threshold because 40 ppb is the approximate level at which negative impacts begin to appear in the pooled data set and because lower concentrations become confused with natural background levels. Other studies have also found 40 ppb to be the level at which growth effects begin to occur (Fuhrer 1994, McLaughlin and Downing 1995) and this was the threshold used by Weinstein and Yanai (1994) in modeling ozone effects on red spruce and ponderosa pine.

Stomatal conductance. Stomatal conductance is calculated as a linear function of net photosynthesis, based on the strong relationship ($r^2 = 0.93$) derived by Aber and Federer (1992) using data from the literature (Abrams et al. 1990, Amthor et al. 1990, Aubuchon et al. 1978 and Hinckley et al. 1978):

$$2) \quad g = -0.3133 + 0.8126 * NetPsn$$

where g is stomatal conductance to water vapor (in mm s^{-1}) and $NetPsn$ is the actual rate of net photosynthesis (in $\mu\text{mol m}^{-2} \text{s}^{-1}$).

Given this relationship, conductance should be expected to decline along with photosynthesis in response to ozone. Among data reported in the literature, the effect of ozone on conductance is reasonably consistent, although there is some indication that the response varies with the light environment of treated foliage (Reich and Lassoie 1984, Volin et al. 1993). In both of these cases, sunlit leaves showed slight declines in conductance with ozone treatment while shaded leaves showed no change or moderate

increases. In other studies, declines in conductance were observed in both sun and shade leaves (Tjoelker et al. 1995), and in sun leaves where only well-lit foliage was examined (Pell et al. 1992). In most cases, changes in conductance were small and occurred after the photosynthetic response. We incorporated this effect into the model by including a simple feedback whereby a reduction in photosynthesis for a given month causes a proportional reduction in conductance during the following month. This was done to reproduce the observed lag between declines in photosynthesis and conductance. In the model, it has the effect of reducing subsequent ozone uptake following damage, assuming that photosynthesis and conductance remain coupled. An uncoupling of these two variables would have important implications for interactions between ozone and water stress as discussed in a following section.

Allocation. In addition to the leaf-level responses of photosynthesis and conductance, many seedling studies have observed reductions in the ratio of below- to above-ground production following exposure to ozone (e.g. Hogsett et al. 1985, Laurence et al. 1994, Pell et al. 1994, McLaughlin et al. 1994). This is often viewed as a compensation mechanism whereby additional carbon is allocated to the replacement of damaged foliage. This can offset or prevent reductions in photosynthesis at the plant level, but comes at the expense of allocation to other plant tissues. For the present exercise, ozone effects on carbon allocation are not explicitly included in the model, but rather, reductions in carbon uptake are allowed to interact with the model's existing allocation priorities. Because the model allocates preferentially to the canopy and lastly to wood, elevated ozone will result primarily in decreased wood growth and increased proportional allocation to foliage. In light of differences between seedling and mature-

tree allocation constraints and available data suggesting that mature trees have a lower capacity for compensation (Edwards et al. 1994), we view this as a more reasonable approach than attempting to reproduce the dynamic root/shoot ratio patterns often observed among seedlings and potted plants. Nevertheless, uncertainties in this area are well recognized and should highlight the need for further experimental work on mature forests.

Canopy ozone gradients

One uncertainty in extrapolating ozone effects to whole forests is the question of how ozone concentrations vary within a forest canopy (Pye, 1988). Canopy ozone gradients are expected to result from several factors, but their importance in moderating growth reductions has not been rigorously tested. To address this, we used ozone data from Munger et al. (1996) collected over a three year period at 8 positions within a mixed hardwood canopy at the Harvard Forest eddy correlation tower in central Massachusetts. The tower is located in a 24 m tall hardwood forest that consists mainly of 50 to 70 year-old red oak and red maple. Hourly ozone concentrations were measured by UV-absorbance.

For the present study, we calculated ozone D40 values for each tower position and plotted the resulting patterns for all months of the growing season (Figure 2.2). In typical results from May and July of 1992, D40 values below the canopy decreased to 72 and 18% of the above-canopy values, respectively. These patterns are consistent from month to month, whereby the rate of depletion increases with depth through the canopy. For all

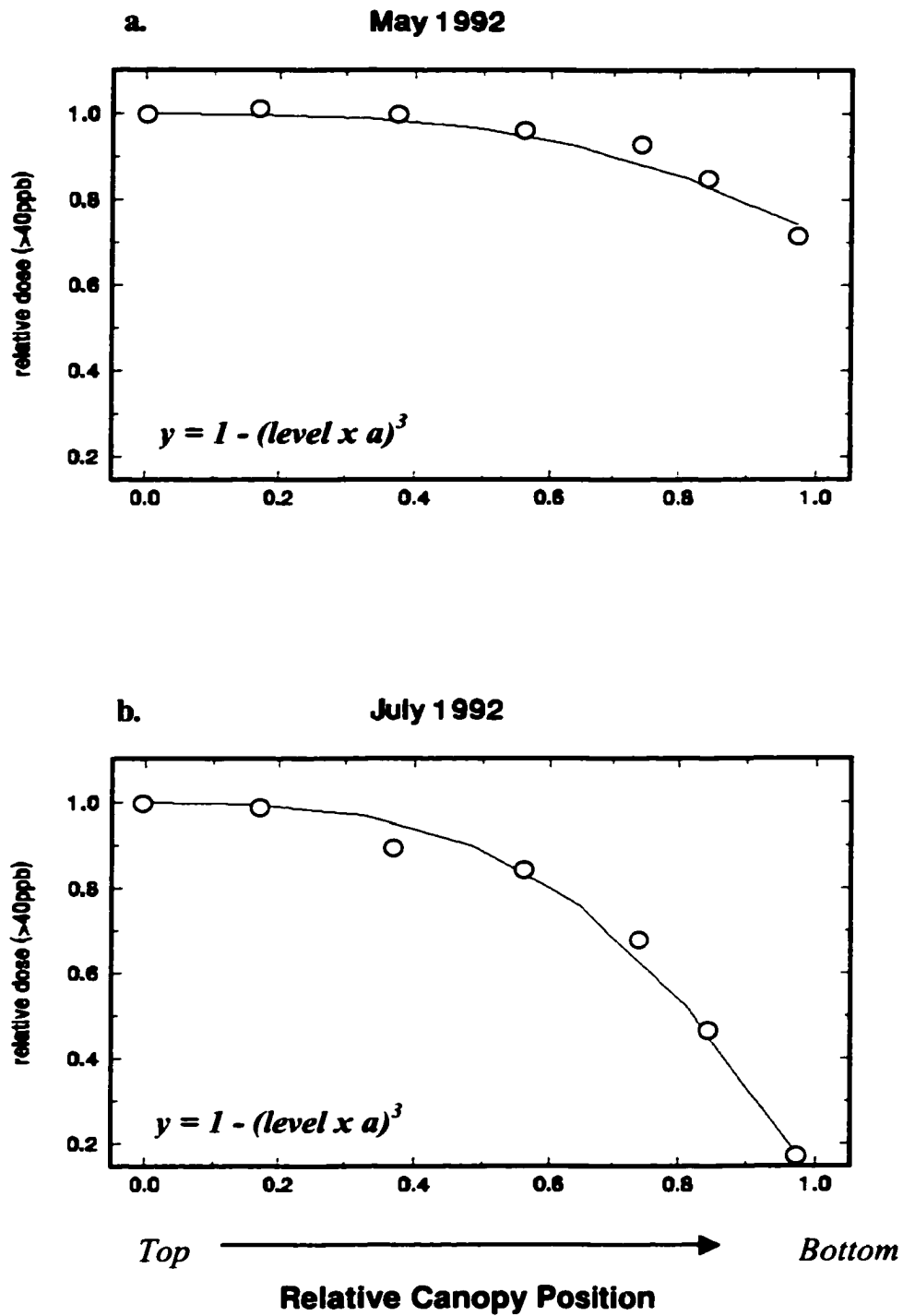


Figure 2.2. Ozone dose > 40ppb in relation to canopy position at the Harvard Forest in Central Massachusetts for May and July of 1992. Both axes have been normalized to a scale of 0 to 1. Data are from Munger et al. (1996).

Table 2.1. Solutions to equation 3, showing canopy gradients of ozone exposure (D40) at Harvard Forest from 1991 to 1993. *a* represents the ozone extinction coefficient from eq. 3, R^2 is the nonlinear least squares coefficient of determination and %red. is the percent reduction in D40 from above to below the canopy. Data were not available for October of 1992.

Month	1991			1992			1993		
	<i>a</i>	R^2	% red	<i>a</i>	R^2	% red.	<i>a</i>	R^2	%red.
May	.67	.98	70	.65	.96	72	.73	.98	64
June	.90	.96	25	.79	.95	49	.83	.98	44
July	1.00	.97	09	.96	.99	18	.81	.98	49
Aug.	.96	.97	17	.90	.95	29	.92	.90	30
Sept.	1.05	.96	01	.92	.98	26	.85	.96	41
Oct.	.87	.98	36	-	-	-	.79	.84	42

years examined, ozone profiles followed seasonal canopy development, becoming established around the time of spring leaf expansion, increasing through mid-summer and declining at the end of the growing season. These trends can be closely approximated by the equation:

$$3) \quad dD40_i = 1 - (i * a)^3$$

where $dD40_i$ is the proportion of the above-canopy D40 at a given canopy level, i is the normalized canopy level from 0 at the top of the canopy to 1 at the ground and a is the ozone extinction coefficient, determined for each month (Figure 2.2). Table 2.1 shows monthly values of a along with the corresponding percent change in D40 from above to

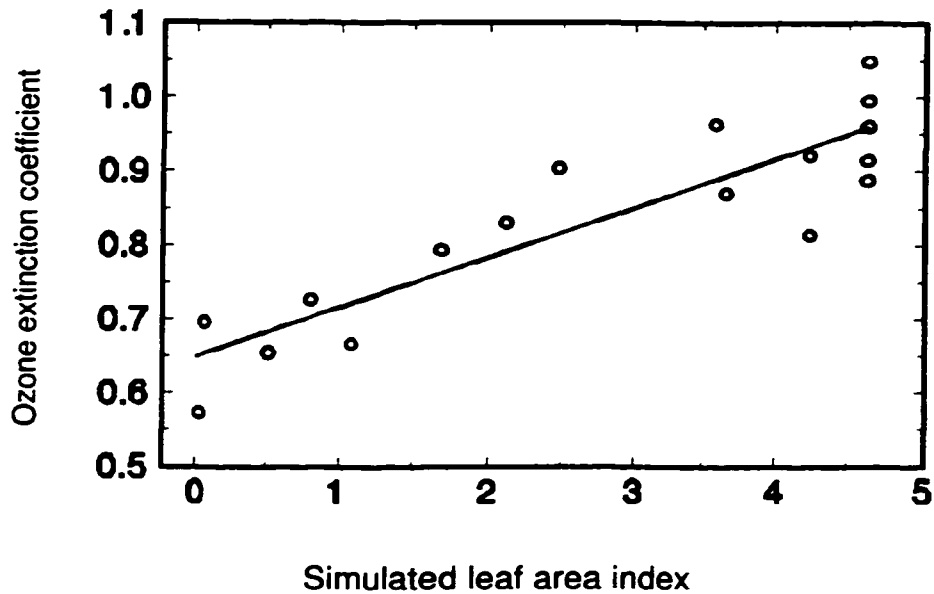


Figure 2.3. Canopy ozone gradient coefficient (a from equation 2) in relation to monthly leaf area index (LAI data are from Aber et al. 1996). Higher values of a correspond to steeper canopy ozone gradients.

below the canopy.

Munger et al. (1996) determined that ozone deposition at Harvard Forest is related to stomatal conductance of water vapor, indicating stomatal uptake as the dominant deposition pathway. Other factors expected to influence canopy ozone gradients are canopy resistance to vertical mixing, ozone deposition directly onto leaf surfaces and scavenging by reactive gases such as VOC's and nitrogen oxides. Because most of these are influenced by canopy leaf area, we compared the observed monthly ozone extinction coefficients with monthly leaf area index. In absence of measured LAI data for this time period, we used values generated by a daily version of PnET, parameterized for the Harvard Forest site using measured canopy biomass and validated against eddy correlation CO₂ flux measurements obtained at the tower (Aber et al. 1996). This

comparison showed LAI to be a strong predictor of vertical ozone depletion ($r^2 = 0.80$, Figure 2.3) suggesting that canopy structure plays an important role in vertical ozone gradients. To include this in the model, predicted monthly LAI is used to calculate the ozone extinction coefficient (*eq. 3*) which then determines the relative D40 for each canopy layer. We cannot presently evaluate the extent to which this relationship might differ in other forests. However, we expect differences to be small for other closed-canopy hardwood forests within the northeast, where canopy structure and atmospheric conditions are similar to those at Harvard Forest. Greater differences may be anticipated in other regions or for other forest types where these factors differ more dramatically.

Interactions between ozone and drought

For each canopy layer, the model calculates photosynthesis with and without ozone in order to determine the potential, integrated ozone effect for the whole canopy. This is necessary in order to allow interaction with drought stress, which is calculated once and applied to the entire canopy rather than being explicitly included in each canopy layer. After the calculation of potential photosynthesis over all canopy layers, the model's water balance routine determines potential transpiration and performs a comparison with the amount of available soil moisture. If soil moisture is not adequate to meet the transpirational demand, water stress ensues and canopy photosynthesis is reduced.

Because the primary physiological response to water limitation is stomatal closure and ozone effects are calculated as a function of stomatal conductance, the potential (pre-drought) whole-canopy ozone effect is reduced each month in proportion to the degree of

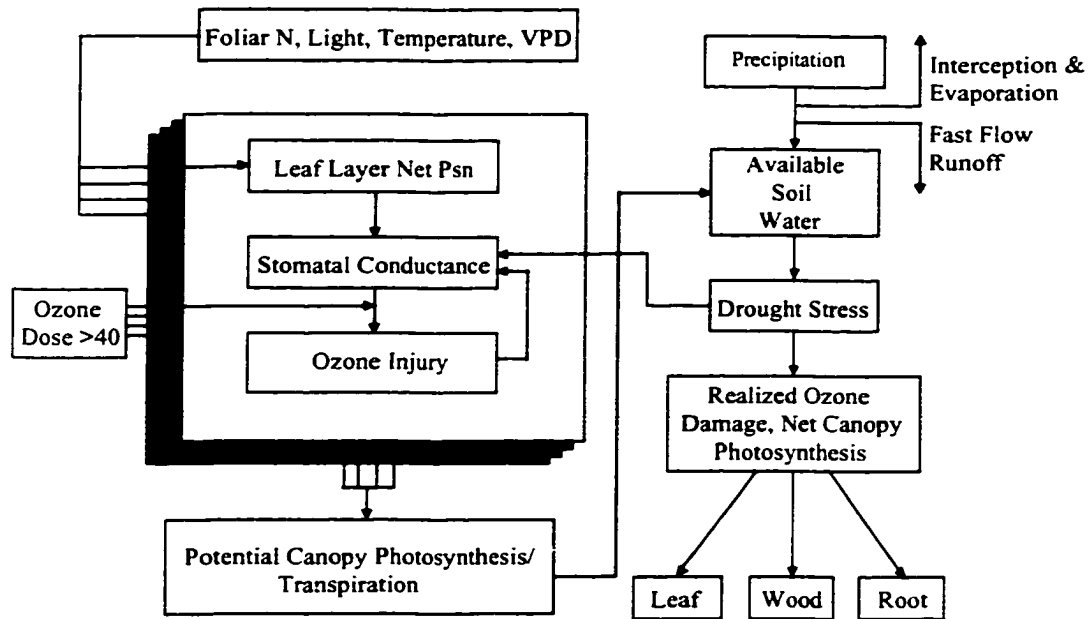


Figure 2.4. Simplified flow diagram of processes included in PnET-O₃.

water stress experienced during that month. For example, if water stress causes a 20% reduction in potential photosynthesis and the potential ozone effect - integrated across all leaf layers - is also a 20% reduction, the final ozone effect is reduced by a factor of 0.8 to 16% ($dO_3 = 0.84$). This assumes that ozone has no negative impact on the ability of stomates to regulate transpiration. As such, the primary water-ozone interaction is for water limitation to reduce ozone uptake, a response which has been observed under experimental conditions (Dobson et al. 1990, Fredericksen et al. 1994) and has been included in model analyses for ponderosa pine seedlings (Chen et al. 1994). Some studies have suggested that under certain conditions, usually after intense and prolonged ozone exposure, stomatal function can become impaired (Reich and Lassoie 1984, Tjoelker et al. 1995). If this occurs, water-ozone interactions would become more

complicated and may include situations where ozone exacerbates drought stress via reductions in water use efficiency. Although this is an area that warrants further investigation, there is presently too little information to include such a feedback in the model.

Model application

A simplified flow diagram of the PnET-O₃ model is shown in Figure 2.4. For the prediction of ozone effects on forest growth, equation 1 was incorporated into the model's photosynthesis routine for each individual canopy layer. For each layer, leaf conductance is determined as a function of net photosynthesis, and is thus affected by available light at that layer, foliar nitrogen content, temperature and vapor pressure deficit. Monthly D40 values are estimated for each layer by combining ambient ozone concentrations with the calculated ozone depletion profiles. Monthly ozone effects are determined from May through October and are based on cumulative exposure over the entire season for each canopy layer.

Ozone data. Ambient ozone data for the northeastern U.S. were obtained from the U.S. Environmental Protection Agency's Aerometric Information Retrieval System for the period of 1987 to 1992. For each collection station, we used raw, hourly concentrations to calculate monthly D40 values and long-term monthly means. We only considered measurements from between 7AM and 7PM to exclude unusually high nighttime concentrations. To minimize error caused by missing data, we imposed a 75% completeness criterion on each month within the data record. For each station, any month containing less than 75% of the expected number of observations was omitted

from the calculation of long-term monthly means. Months with between 75 and 100% data completeness were corrected for missing periods by dividing the measured D40 value by the proportion of data completeness. This assumes that the distribution of concentrations within the missing period was the same as that of the observed data. The majority of sites where this correction was performed had less than 10% missing data. After data screening was complete, we eliminated sites that contained less than a three year record. The resulting data set included 64 sites (from an initial total of approximately 100), each with 3 to 6 years of data from the period of 1987 to 1992 (Figure 2.5). In computing long-term mean D40 values, some bias between sites may result from differences in the years for which data were available.

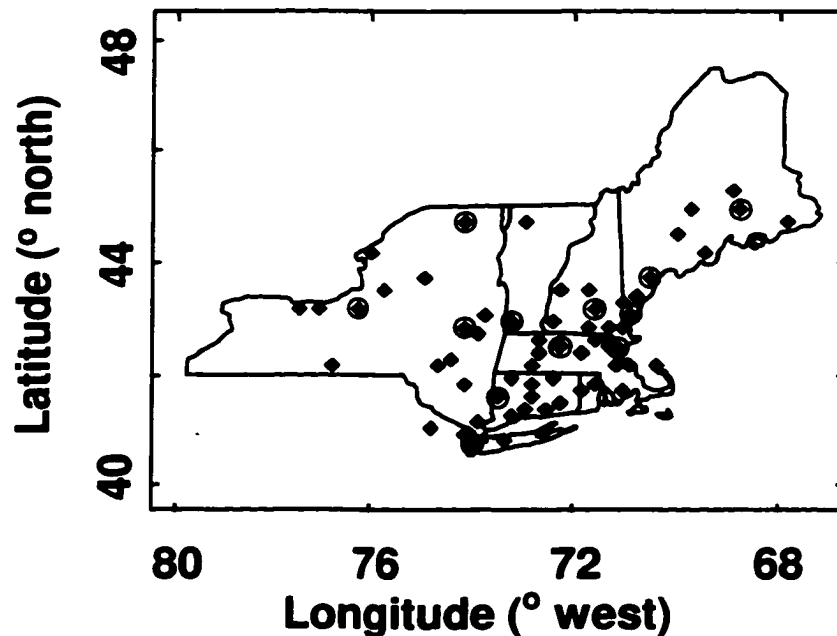


Figure 2.5. Locations of EPA ozone monitoring stations used for this study. Circled stations represent sites where monthly climate and ozone data were used in addition to long-term mean values.

Model application using mean climate and ozone. Climate inputs required to run the model are monthly averages of maximum and minimum daily temperature, solar radiation and vapor pressure deficit along with total monthly precipitation. For model application under average climate and ozone at all 64 ozone monitoring sites, we used long-term mean climate values calculated for each site by a statistical climate model developed for the northeast region (Ollinger et al. 1995). We used a foliar nitrogen concentration of 2.2%, based on values measured among a variety of hardwood species at the Harvard Forest (Martin and Aber 1997). To evaluate the effects of site moisture conditions, we ran the model under a range of soil water holding capacity values (WHC) representing optimal to severely limited soil water retention. We chose this approach instead of using fixed values for each site because soil properties vary over much finer spatial scales than ozone. Hence, ozone levels encountered in the area of each monitoring station may interact with a wide range of soil moisture conditions over the local landscape. The WHC values used ranged from 2 cm, representing a shallow sand with 50% large fragments, to 36 cm, representing a clay loam with no large fragments and 2 m rooting depth. The intermediate value of 12 cm is considered most common for the northeast region, representing a typical glacial till soil with 25% large fragments and 1 m rooting depth (Federer 1982).

We performed an additional set of analyses in order to test the model's sensitivity to canopy ozone gradients (*eq. 3*). For this, the model was re-run at all 64 sites with ozone held constant through all canopy layers. Canopy gradient effects were assessed by comparing declines in annual NPP with intact gradients versus those after gradients were removed.

Table 2.2. Locations of 12 ozone monitoring stations and associated weather stations used for analysis of temporal variation in predicted growth impacts. Stations marked * represent rural sites located near the town or city listed. All stations include data from the entire 1987-1992 period.

<u>Station Name</u>	<u>Latitude</u>	<u>Longitude</u>	<u>Weather Station</u>
New York, NY.	40.68	74.01	New York, NY.
Danbury, CT.	41.42	73.47	Shepaug Dam, CT.
Chelsea, MA.	42.44	71.06	Boston, MA.
Ware, MA.	42.33	72.35	Amherst, MA.
Cape Elizabeth, ME.	43.62	70.25	Portland, ME.
Bangor, ME.*	44.70	68.86	Bangor, ME.
Manchester, NH.	43.03	71.47	Nashua, NH.
Portsmouth, NH.	43.08	71.77	Durham, NH.
Syracuse, NY.*	43.11	76.16	Syracuse, NY.
Lake Placid, NY.*	44.37	73.95	Lake Placid, NY.
Schnectady, NY.	42.81	73.97	Albany, NY,
Bennington, VT.	42.90	73.27	Readsboro, VT.

Model application using monthly climate and ozone. To examine temporal interactions between ozone and climate and to determine year-to-year variability in predicted ozone effects, we selected a subset of 12 sites for analysis using actual monthly ozone and climate values (Figure 2.5, Table 2.2). Site selection was aimed at attaining even distribution across the study region, but was constrained to stations having ozone records for the entire 1987 to 1992 period with minimal missing values. Monthly climate data were obtained from the Northeast Regional Climatic Data Center for weather stations nearest to the ozone monitoring stations (Table 2.2). The weather stations recorded maximum and minimum daily temperature and precipitation, but not solar

radiation. Instead, we used values calculated by the statistical climate model (Ollinger et al. 1995) for each location. Soil WHC was held at 12 cm for all sites. For each site, initial conditions for forest structure and productivity were determined by allowing the model to reach equilibrium under long-term mean climate and ozone as discussed in the previous section. From these initial conditions, predictions were generated using monthly climate and ozone data from 1987 through 1992.

Sensitivity analyses

Sensitivity analyses provide a means of testing the importance of assumptions made in developing and parameterizing a model. Many parameters and algorithms used in PnET-II have been tested previously (Aber and Federer 1992, Aber et al. 1995, 1996) and will not be reexamined here. However, several assumptions used in adding ozone effects to the model warrant further attention as they have potentially important implications on predicted forest response. Those assumptions are: 1) the model's allocation priorities assume that mature trees prioritize foliar production over other plant compartments and that decreases in carbon gain are taken from wood growth over leaf and root growth; 2) in our treatment of interactions between ozone, conductance and water stress, we assume that the ability of stomates to regulate transpiration is not hampered by ozone.

To test the effects of assumption 1, we altered the carbon allocation routine such that ozone effects on photosynthesis were distributed more evenly across all growth compartments. This was done by decreasing allocation of available C to buds for next year's foliage in proportion to the decrease in this year's carbon gain. We labeled this the

BudC effect. Testing assumption 2 required changes at several places in the model. First, if stomatal function becomes impaired, photosynthesis and conductance may gradually become uncoupled such that conductance no longer down-regulates with photosynthesis. Second, an uncoupling of these variables could cause a decrease in plant water use efficiency (WUE). We included these effects in the model based on the results of Tjoelker et al. (1995) in which the relationship between photosynthesis and conductance remained intact through the initial phase of a 2x ozone fumigation experiment, but began to break down during later stages of treatment. Using approximate dose values from Tjoelker et al. (1995), the down-regulation of conductance with photosynthesis is maintained in the model up to a threshold D40 of 11 ppm-h. Between 11 and 41 ppm-h, conductance increases linearly until reaching pre-ozone levels. At the same time, WUE is scaled downward in proportion to ozone effects on total photosynthesis. These changes produce a gradual decline in stomatal function and have the effect of increasing ozone uptake and canopy transpiration. We labeled this the WUE effect.

Previous sensitivity analyses have suggested that foliar nitrogen concentration (FolN) and soil water holding capacity (WHC) are critical parameters in determining rates of photosynthesis and growth in northeastern hardwoods. To examine interactions between these parameters and the above assumptions, we used a randomized, Monte Carlo approach. First, the model was run for the 64 ozone monitoring sites using mean ambient ozone and randomized inputs for FolN and WHC. Values for FolN ranged from 1.8 to 2.6 mg g⁻¹, the approximate range that occurs among northern hardwoods. Soil WHC ranged from 2 to 36 cm. The model was run 10 times for each site for a total of

640 ozone-effect predictions under a range of possible WHC and FolN combinations. This process was then repeated using each scenario of altered model assumptions. The resulting predictions were used to relate regional mean ozone effects to variation in WHC and FolN under each model scenario. This approach was used in order to detect nonlinear interactions that may be missed by single factorial analyses.

Results and Discussion

Mean climate and ozone

Results of model runs using mean climate and ozone indicate decreases in annual net primary production (NPP) of from 3 to 16% as a result of mean ozone levels from 1987 to 1992 (Figure 2.6a) with greatest reductions in southern New York and southern New England where ozone levels and canopy conductance were greatest. The predicted decrease was weakly, but negatively correlated with latitude, following a trend of decreasing ozone from south to north across the region (Figure 2.7). Predictions varied substantially across the range of soil WHC values (2-36 cm), with smaller growth reductions occurring on drier sites where lower rates of conductance limited ozone uptake by foliage.

At WHC = 36 cm, water limitations on NPP and wood production were eliminated for all sites, so these values can be used as a reference in estimating drought effects resulting from other soil moisture conditions (Table 2.3). Under all but the two wettest conditions, water limitation caused greater declines in growth than did ozone. At WHC = 12 cm, representing a typical northeastern glacial till, ozone-induced declines in NPP averaged 81% of those predicted at WHC = 36. At WHC = 2cm, an extreme

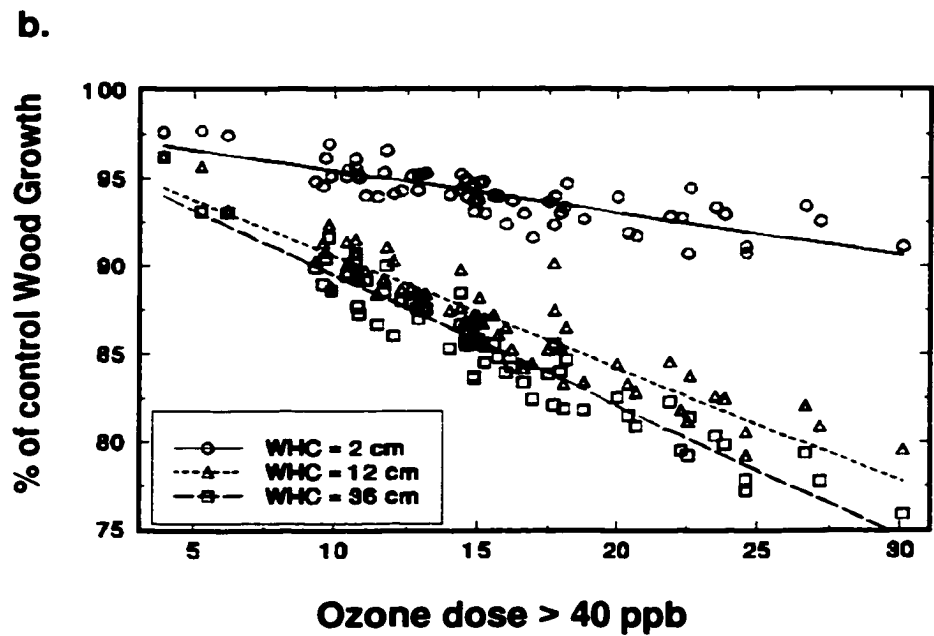
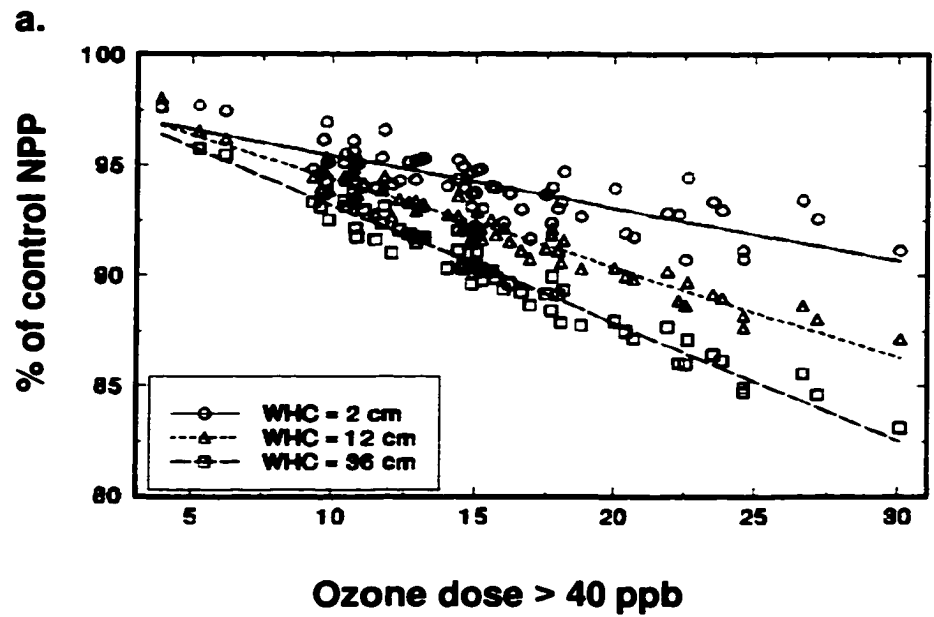


Figure 2.6. Predicted change in a) mean annual NPP and b) mean annual wood production at 64 sites across the study region in response to mean ozone levels from 1987-1992. Predictions are shown for 3 levels of soil water holding capacity to show the change in response from well-watered (WHC = 36) to severely drought-stressed (WHC = 2) conditions

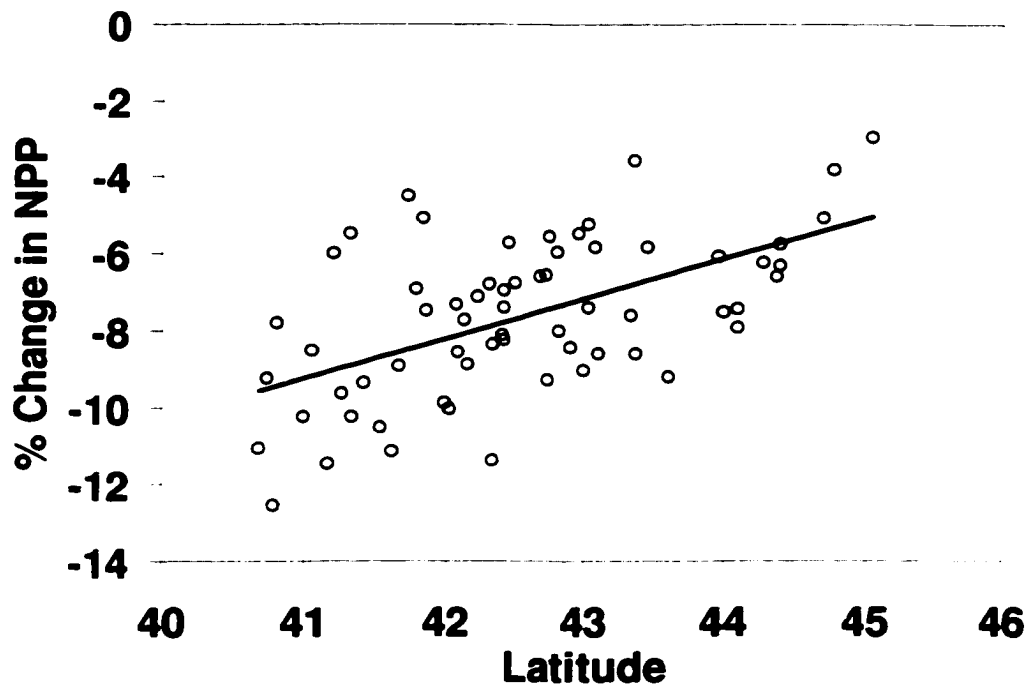


Figure 2.7. Predicted change in NPP due to ozone in relation to latitude.

condition for this region, ozone effects averaged 62% of the drought-free values, despite substantially lower total growth.

Reductions in predicted wood production ranged from 3 to 22% across all ozone and soil moisture conditions (Figure 2.6b). This wider range of variation is a result of the model's carbon allocation priorities which value leaf and root production above wood growth. With high soil moisture (WHC = 24 to 36 cm), ozone effects on total plant growth are taken entirely from wood production, with no declines in canopy leaf area or root growth. This occurs because under these conditions, wood growth is high enough that it can be reduced without reaching the critical ratio of wood to foliage production specified in the model. On progressively drier sites, the ratio of wood to foliar

production decreases until reaching this critical value. Beyond this point, leaf, wood and root growth become more tightly coupled such that further growth declines necessarily affect all three compartments. At WHC = 2 cm, reductions in wood growth accounted for approximately half of the total decline in growth (Table 2.3).

Table 2.3. Predicted net primary production (NPP) and wood growth ($\text{g m}^{-2} \text{ yr}^{-1}$) with and without ozone effects at 5 levels of soil water holding capacity (cm). Values shown are means and standard deviations (in parentheses) from all 64 study sites.

	NPP			WOOD		
	Control	Ozone	%red.	Control	Ozone	%red.
2	723 (37.1)	682 (35.4)	5.7 (1.4)	372 (19.1)	351 (18.2)	5.6 (1.4)
6	1136 (70.9)	1054 (56.2)	7.1 (1.9)	610 (61.1)	546 (34.7)	10.1 (4.4)
12	1354 (80.3)	1254 (66.6)	7.4 (1.8)	792 (89.5)	694 (70.7)	12.2 (3.1)
24	1732 (72.0)	1584 (59.7)	8.5 (2.2)	1124 (77.6)	976 (63.5)	13.1 (3.2)
36	1840 (85.7)	1672 (65.7)	9.1 (2.4)	1228 (93.1)	1060 (71.6)	13.6 (3.4)

Changes in ozone D40 with depth through the canopy had a minimal effect on predicted growth reductions. Canopy gradients did offset declines in NPP, but by an average of only 0.6 percent (max = 1.5%) with respect to results obtained with canopy gradients removed. Although the gradients produced substantial declines in ozone D40 values through the mid and lower canopy (Figure 2.2), ozone in the upper canopy remained high. Because this is where light levels and hence photosynthesis and conductance are greatest, canopy gradients had only a small effect on total canopy ozone uptake. This suggests that unless canopy ozone profiles are substantially different in

other forest types or geographic regions - with concentrations falling off sharply through upper canopy layers - vertical ozone gradients are not an important factor in scaling ozone effects to mature forests. These results are consistent with a similar analysis made previously with a simpler canopy photosynthesis model (Reich et al. 1990).

Interactions between climate and ozone

For the 6 year period from 1987 to 1992, the only unusual year with respect to ozone was 1988 which had significantly higher levels than all other years except 1991

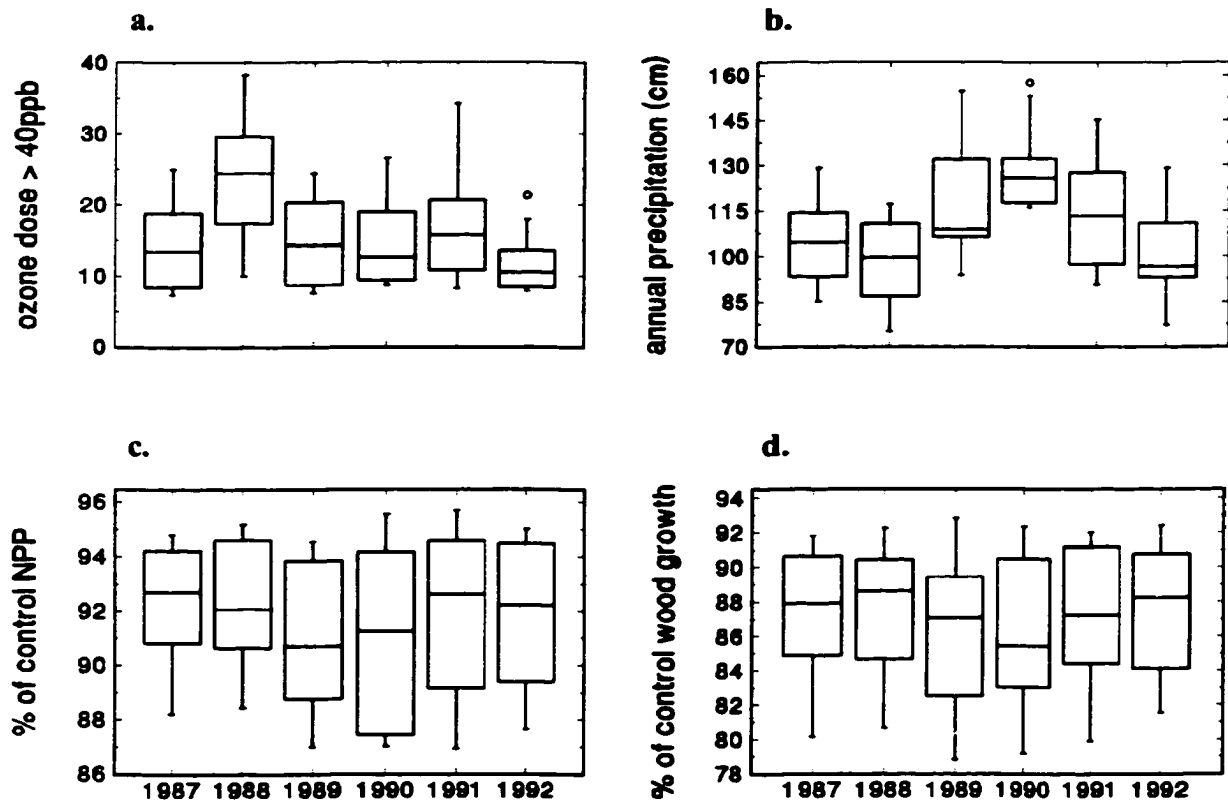


Figure 2.8. Distributions of a) ozone D40, b) annual precipitation, c) percent change in NPP and d) percent change in wood production across the 12 study sites for individual years from 1987 to 1992. Boxes show median values and quartile ranges.

(Figure 2.8a). This was also an anomalous climate year, being one of the warmest on record in the northeast region and having the lowest precipitation of the 6 year period. Precipitation was more variable than ozone, being consistently greater from 1989 to 1991 than during the other three years (Figure 2.8b). Despite these differences in climate and ozone (significant at $p < .05$ using Scheffe's multiple comparison ANOVA), there were no significant year to year differences in predicted growth reductions (Figure 2.8c-d). This largely reflects the tendency for high ozone levels to be associated with hot, high-

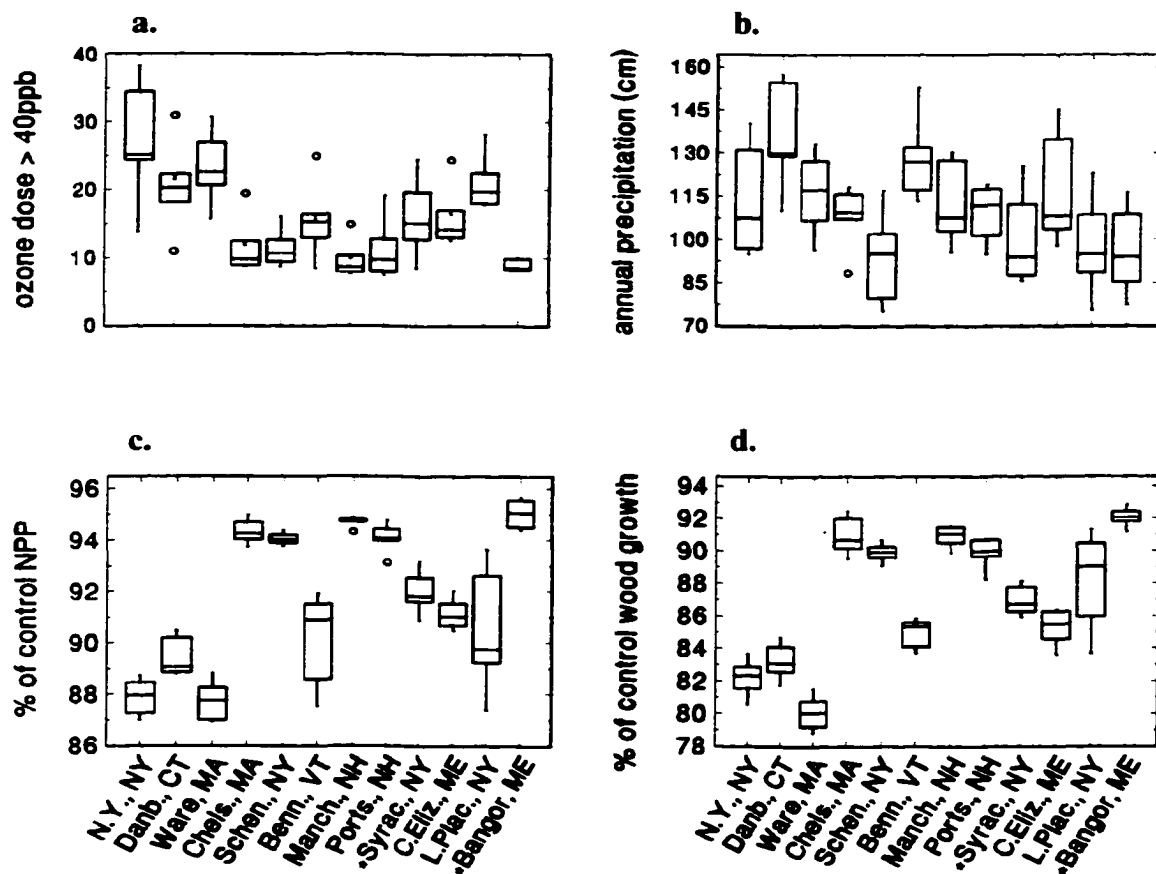


Figure 2.9. Distributions of a) ozone D40, b) annual precipitation, c) percent change in NPP and d) percent change in wood production across the 6 year period from 1987 to 1992 for all 12 study sites.

pressure air masses, which often coincide with increased water limitations. Periods of high ozone (e.g. mid-summer 1988) were commonly offset by co-occurring reductions in conductance, induced by high temperatures and low precipitation.

Whereas temporal variation in predicted growth reductions was minimal, growth reductions across sites were not only variable, but were more variable than either climate or ozone (Figure 2.9, between-site differences determined at $p < 0.05$ using Scheffe's multiple comparison ANOVA). This reflects spatial relationships between conductance and ozone that counter the dominant temporal trends. Although high ozone often coincided with low conductance on a temporal basis, high ozone more often coincided with high conductance on a spatial basis. This is at least partially due to the fact that both ozone production and conductance, in general, decrease from south to north within the study region. For ozone, this is driven by the high density of urban areas along southern portions of the region, whereas patterns of conductance tend to follow latitude gradients in temperature and summer precipitation.

Among the 12 intensive study sites, the greatest growth reductions were predicted for New York City and Ware, Ma., located in central Massachusetts (Figure 2.9), the two sites with the highest ozone levels. Ozone levels were lower in Ware than in New York City, but Ware had higher predicted rates of conductance and thus showed similar growth declines to NYC.

Although there is a general trend of decreasing ozone concentrations with distance from population centers, a clear distinction between urban and rural areas is difficult to make. Urban areas have higher emissions of the nitrogen oxides and volatile organic compounds that lead to ozone production, but ozone concentrations are often

lower in cities than in nearby rural areas because other compounds present in polluted air (e.g. NO) cause a destruction of ozone. Note for example that Chelsea, Ma., an urban area adjacent to Boston, had lower ozone levels than Ware, Ma., Bennington, Vt. and the site near Syracuse, NY., all located in less densely populated areas (Figure 2.9a).

Because ozone and its precursor compounds can be transported considerable distances, rural, down-wind locations can experience unusually high concentrations. This probably explains the relatively high ozone levels and large growth reductions predicted for Cape Elizabeth, Me. and the site near Lake Placid, NY., located at an elevation of approximately 600m. High concentrations are known to occur at coastal and upper elevation sites because of long-range transport of air that has had little contact with ozone-depleting surfaces. High ozone levels at the rural Bennington, Vt. site may reflect its location downwind of the Albany, N.Y. area. Conversely, Schenectady, N.Y., which is adjacent to, but upwind of Albany, experienced lower ozone levels and lower growth impacts.

Sensitivity analyses

Randomized sensitivity analyses indicate nonlinear interactions between model sensitivity to FolN and WHC through their effects on photosynthesis, transpiration, water limitations and ozone uptake. Figure 2.10 shows predicted response surfaces indicating the regional mean ozone effect on NPP at various levels of FolN and WHC under three model scenarios. Figure 2.10a shows standard PnET-O₃ model results and Figures 2.10b and 10c show results from scenarios that include ozone effects on allocation (BudC effect) and water use efficiency (WUE effect) respectively. Each surface was generated

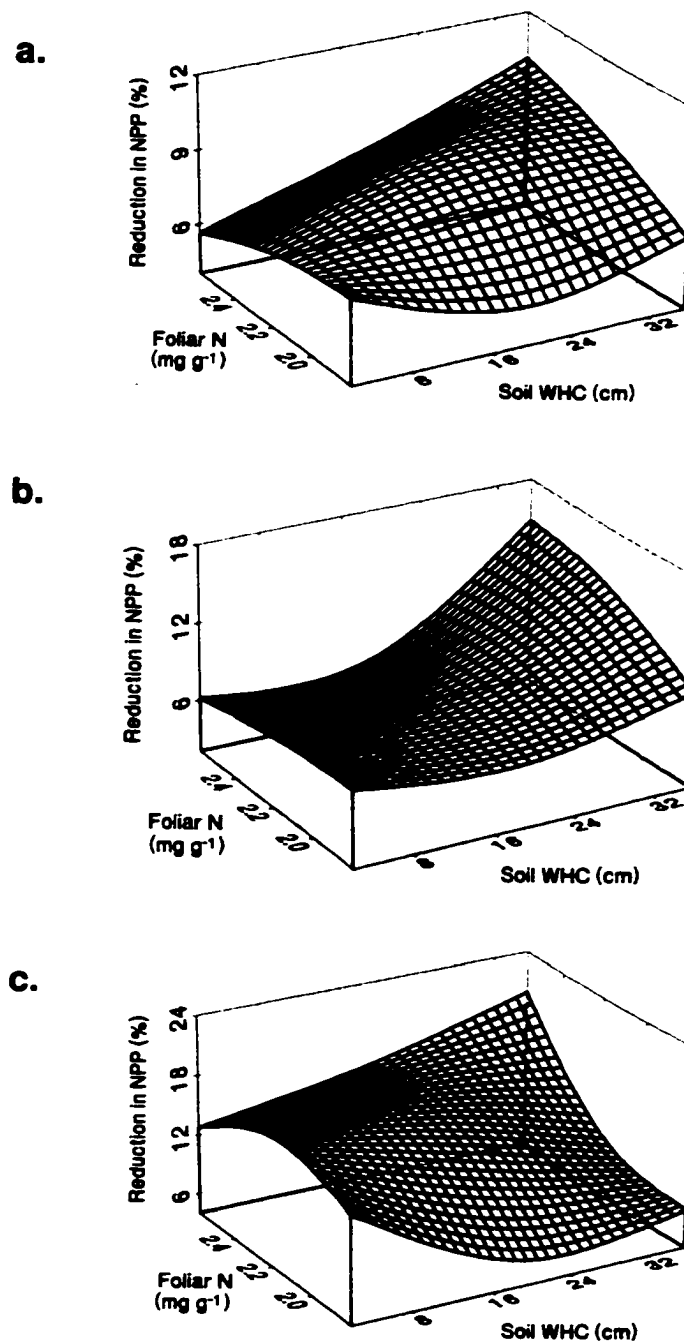


Figure 2.10. Results of Monte Carlo sensitivity analyses showing the regional mean ozone effect on NPP in relation to variation in foliar N and soil WHC. Results are shown for three scenarios indicating model behavior under a) standard PnET-O₃ configuration, b) the BudC effect where allocation to foliage is no longer prioritized above wood and root growth and c) the WUE effect where ozone exposure causes a gradual decline in stomatal function and water use efficiency. See text for thorough description of these scenarios.

from 640 model runs (64 sites x 10 runs each) conducted under ambient ozone, but with randomized inputs for FolN and WHC. Values shown represent regional mean ozone injury from all 64 sites.

Using standard model assumptions, model sensitivity to FolN varied with WHC. On dry sites, FolN had little effect on predicted ozone injury because ozone uptake was controlled largely by water availability. On progressively wetter sites, drought stress was diminished and FolN became an increasingly important regulator of photosynthesis and hence uptake. At WHC = 36 cm, mean ozone injury increased from 6.6 to 10.4 % as FolN increased from 1.8 to 2.6 mg g⁻¹ (Figure 2.10a). Similarly, model sensitivity to WHC tended to be greatest at high FolN where large transpirational demands led to rapid depletion of soil water. At low FolN, water limitations were less common and so WHC had less influence on predicted ozone damage. The mean decline in regional NPP under the full range of FolN and WHC was 7.6% (std. dev. = 1.02), similar to the value obtained using average FolN and WHC values (Table 2.3).

Imposing an ozone effect on allocation to foliage did not change the nature of interactions between FolN and WHC, but did cause an increase in model sensitivity to WHC (Figure 2.10b). Across the lower end of WHC values used (2-16 cm), predicted ozone injury was less than or equal to predictions made under standard assumptions. This was due to a subtle feedback that occurred between ozone and drought stress. At low WHC, the reduction in foliar biomass imposed by the BudC effect caused a small decrease in the transpirational water demand. Where this occurred, the loss of photosynthetically-active leaf area was offset by a decrease in drought stress. At higher WHC, where drought was less common, this tradeoff was not important and ozone-

induced declines in foliar biomass led to greater total injury. The mean decline in regional NPP under this scenario was 8.03% (std. dev. = 4.33).

Imposing an ozone effect on stomatal conductance and water use efficiency caused significant changes in both the location and magnitude of ozone injury (Figure 2.10c). Most noticeable is the fact that ozone injury was no longer greatly offset by water limitations at low WHC. Instead, ozone injury exacerbated water limitations and this had the greatest effect on dry sites. At WHC = 2, ozone injury caused more than a 12% decline in predicted NPP, roughly twice that observed in the previous two scenarios. Lower levels of injury occurred towards the endpoint of low FolN and high WHC where water availability was high and transpirational demands were low. As in the previous two scenarios, the greatest growth declines occurred at high FolN and high WHC where ozone uptake was at its maximum. In this case, uptake was further elevated by the lack of stomatal down-regulation following reductions in photosynthesis. The mean decline in regional NPP under this scenario was 11.43% (std. dev. = 5.0).

Conclusions

In this study, we synthesized information regarding plant response to ozone and applied it in a modeling framework to mature hardwood forests growing under ambient conditions. Our approach was to summarize leaf-level ozone effects on carbon uptake in a forest productivity model that was designed to simulate the growth of mature, closed-canopy forests. Model runs using 6 years of concentration data from 64 sites across the northeastern U.S. indicate reductions in annual dry matter accumulation of between 3 and 16% for the period of 1987 to 1992 (mean = 7.4%). Reductions in predicted wood

production ranged from 3 to 22% (mean = 12.2%).

In general, growth declines were greatest near urban areas in southern portions of the region and in locations where drought stress was absent. Canopy ozone gradients had little effect because ozone depletion was minimal through the upper canopy layers where light levels and stomatal conductance were greatest. Year-to-year variation in predicted growth declines was small because there was a tendency for ozone and stomatal conductance to be inversely correlated on a temporal basis. Periods of high ozone often occurred during hot, dry weather conditions which induced drought stress and limited ozone uptake. Although ozone effects were greatly moderated by variation in climate and soil moisture, growth reductions were substantial even under the driest conditions simulated.

Sensitivity analyses demonstrated how model behavior is influenced by several important assumptions and how predictions might be affected if those assumptions prove wrong. Results of these analyses revealed interactions between foliar nitrogen and soil water holding capacity whereby model sensitivity to one of these parameters depended on the value of the other. Adding an ozone effect on allocation to foliage did not greatly alter the mean regional growth response, but did cause an increase in sensitivity to available soil water. Adding an ozone effect on stomatal function and plant water use efficiency altered both the nature and magnitude of predicted growth declines. In particular, the ozone-water interaction observed under standard model configuration was replaced by a situation in which ozone caused an increase in transpirational water loss and hence drought stress. The mean regional growth decline under this scenario was 11.4%. Although the standard assumptions used in the model may be reasonable given

available data and current ozone levels, these results demonstrate the need for additional field research on mature forest stands. Such work will be necessary for improving our understanding of important processes and assessing the accuracy of model predictions.

CHAPTER III

TROPOSPHERIC OZONE AND LAND USE HISTORY AFFECT REGIONAL FOREST CARBON UPTAKE IN RESPONSE TO CO₂ AND N DEPOSITION

Abstract

To examine potential controls on current forest growth and carbon storage, we analyzed the effects of historical increases in tropospheric ozone, nitrogen deposition and elevated CO₂ on northeastern U.S. forests. We included these factors individually and in combination in a forest ecosystem model which was run from 1700 to 2000 under different scenarios of land use history. The analyses suggest that historical increases in CO₂ and N deposition have stimulated forest growth and carbon uptake, but to different degrees following agriculture and timber harvesting. Further, inclusion of tropospheric ozone offset a substantial portion of the predicted increases caused by CO₂ and N deposition. This result is particularly relevant given that ozone pollution is widespread across much of the world and is spatially correlated with nitrogen deposition.

Introduction

Eastern U.S. forests have been subjected to a number of environmental changes that stem from human industrial and agricultural activities. Although recent studies suggest an important role for these systems as carbon sinks (Turner et al. 1995, Fan et al. 1998, Houghton et al. 1999), carbon budget estimates vary widely and our understanding

of underlying mechanisms remains incomplete. To date, attention to environmental factors that alter rates of forest carbon uptake has focused on interactions between elevated CO₂ and nitrogen deposition. Elevated CO₂ stimulates photosynthesis and tree growth in both seedlings and mature forests (Curtis and Wang 1998, Ellsworth 1999), but the degree to which this leads to increased carbon storage depends on feedbacks with plant C:N ratios, litter decomposition and soil N availability (Comins and McMurtrie 1993, Lloyd 1999). Elevated N deposition can increase growth in N-limited systems (Vitousek and Howarth 1991), but its effect on long-term carbon storage may be limited if increased growth occurs in the form of low C:N ratio tissues with fast turnover rates (Townsend et al. 1996, Nadelhoffer et al. 1999).

Model analyses that include C and N feedbacks have estimated large terrestrial carbon sinks resulting from the widespread occurrence of N deposition (Lloyd 1999, Townsend et al. 1996, Holland et al. 1997). Although models differ in the magnitude of predicted carbon sequestration, most agree that the current spatial distribution of N deposition combined with a relatively young age distribution make eastern North American forests an important regional sink. However, the effects of disturbance and land use history were not included in these analyses, yet these have significant effects on current forest growth and response to N deposition via their long-term effects on soil C and N pools (Aber and Driscoll 1997).

An additional factor that has important implications for forest carbon storage, but has received surprisingly little attention, is tropospheric ozone. Among common air pollutants, ozone is probably the most damaging to terrestrial vegetation and frequently occurs at high concentrations over large portions of the world (Chamides et al. 1994).

Ozone concentrations that are common in industrialized regions are known to cause large reductions in carbon fixation and biomass production in native plants as well as agricultural crops (Chamedes et al. 1994, Reich 1987, McLaughlin and Downing 1995, Chapelka and Samulson 1998) and to alter patterns of plant carbon allocation (Laurence et al. 1994). All of these suggest a strong potential for ozone to alter rates of carbon storage in native ecosystems, perhaps offsetting the effects of elevated CO₂ and N deposition (Volin et al. 1998).

Although ozone continues to receive attention for its harmful effects on human health, food production and plant growth, it has never been included in analyses of broad-scale carbon fluxes. This stems in part from the inherent variability of ozone concentrations and observed plant responses (Chapelka and Samulson 1998), but also reflects a gap between the scientific communities studying ecological ozone effects and those concerned with terrestrial carbon fluxes.

Methods

In this analysis, we examine potential effects of tropospheric ozone, elevated CO₂ and N deposition under two land use history scenarios in order to determine the relative importance of each factor on predicted forest growth and carbon storage. We combined response algorithms for all factors in the PnET-CN forest ecosystem model, a model of carbon, nitrogen and water balances that has been previously applied and tested across the northeast study region (Aber et al. 1995, 1997, Ollinger et al. 1998). Algorithms for canopy physiology, carbon allocation, N cycling and water balances have been described previously (Aber et al. 1997, Ollinger et al. 1998) as have algorithms for the individual effects of tropospheric ozone and N deposition (Aber and Driscoll 1997, Ollinger et al.

1997). Here we add new equations for the photosynthetic response to atmospheric CO₂ and integrate all factors under different scenarios of land use history. As our treatment of each factor is necessarily limited, our goal is not to conduct an exhaustive analysis of all possible multiple stress outcomes, but rather to examine how interactions among a number of important responses might be affecting present-day forest carbon fluxes.

Ozone

Physiological ozone response algorithms were derived from a number of controlled exposure studies and are based on cumulative ozone uptake to internal leaf surfaces (Reich 1987). Ozone effects on photosynthesis are based on the equation:

$$1) \ dO_3 = 1 - (k \ g \ D40)$$

where dO_3 is the ratio of ozone-exposed to control photosynthesis, k is an empirically derived ozone response coefficient with a value of 2.6×10^{-6} for hardwood forests, g is mean stomatal conductance (mm s^{-1}) and $D40$ is the cumulative ozone dose above a threshold concentration of 40 ppb. Vertical ozone concentration gradients are calculated from canopy leaf area index, which influences resistance to vertical mixing and ozone depletion on leaf surfaces (Ollinger et al. 1997). Because ozone uptake is dependent on stomatal conductance, factors that affect conductance (e.g. foliar N concentrations and drought stress) are important regulators of ozone damage.

Nitrogen Deposition

N deposition and land use history act through their effects on soil carbon and nitrogen pools, plant and soil C:N ratios, rates of N supply to vegetation and losses to

drainage water (Aber et al. 1997). Nitrogen fluxes are determined for all plant pools based on rates of supply versus plant demand. The C:N ratio of plant tissues are reflected in litter which decomposes into a single soil organic matter pool. Nitrogen mineralization is affected by soil C:N ratios, with high C:N ratio material increasing immobilization and decreasing N supply to vegetation. Prior analyses of these interactions indicate that historical disturbance effects on soil C and N dynamics can persist for several hundred years, depending on disturbance severity and rates of atmospheric N deposition (Aber and Driscoll 1997).

CO₂

Leaf photosynthetic rates are driven by foliar N concentrations and atmospheric CO₂ levels. The photosynthetic response to CO₂ algorithm derived for the present study uses a Michalis-Menton equation, fit to normalized A-Ci curves (scaled from 0 to 1, where 1 is CO₂-saturated carbon fixation) taken from a number of eastern tree species grown in CO₂ exposure studies (Pettersson and McDonald 1992, Curtis et al. 1995, Ellsworth et al 1995, Lewis et al. 1996, Figure 3.1). The CO₂ response is described by the equation

$$2) R_{Ca} = 1.22 * (C_i - 68) / (C_i + 136)$$

where R_{Ca} is the proportional difference in photosynthesis between that which occurs at current CO₂ and the CO₂ concentration simulated in the model (C_a) for a given year. For this purpose, ambient CO₂ is assumed to be 350 μmol/mol. Although atmospheric CO₂ concentrations are presently higher and continuing to rise, 350 μmol/mol more closely

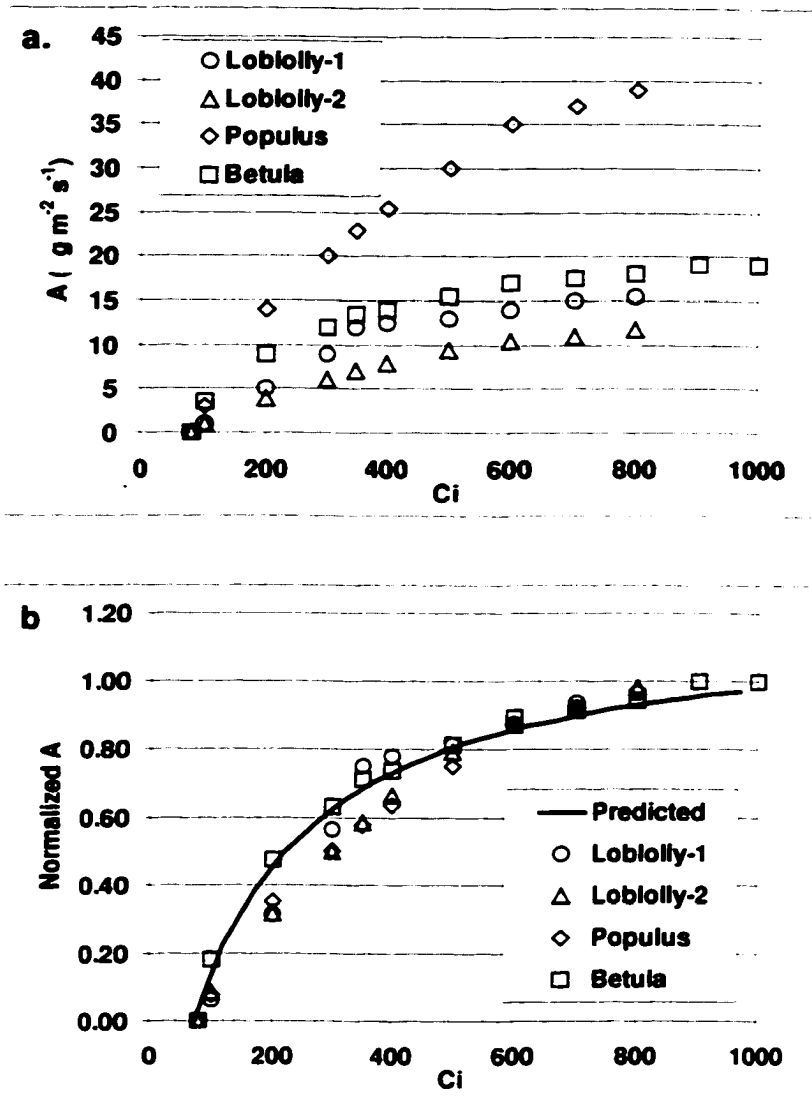


Figure 3.1. a) Photosynthesis in relation to internal leaf CO_2 concentrations (C_i) for conifer (*Pinus taeda*) and hardwood (*Betula pendula* and *Populus euroamericana*) species taken from the literature. b) Data from Figure 3.1a with photosynthetic rates normalized to CO_2 -saturating rates. The line represents the Michaelis-Menton function (eqn. 2) incorporated into the PnET-CN model.

represents the majority of ambient CO_2 photosynthetic rates reported in the literature over the past decade and thus made a reasonable baseline for use in the model. C_i is the internal leaf CO_2 concentration that occurs at the ambient concentration C_a , which varies

over time in accordance with the Mauna Loa CO₂ record and data from ice cores. The constant 68 represents the photosynthetic CO₂ compensation point, 136 is the half saturation concentration and 1.22 is an empirically-derived constant. The equation takes a similar form to that used in other models of leaf photosynthesis (e.g. McMurtrie and Wang 1993), but here is fit to data for eastern U.S. hardwood and conifer tree species (using data from Pettersson and McDonald 1992, Curtis et al. 1995, Ellsworth et al. 1995 and Lewis et al. 1996).

Internal leaf CO₂ concentrations (C_i) are predicted from an inverse relationship between the C_i/C_a ratio and foliar nitrogen concentrations (Farquhar and Wong 1982). This ratio varies from 0.8 to 0.65 as foliar N increases from 1 to 3 %, reflecting greater internal CO₂ fixation in foliage with higher N concentrations. Photosynthetic capacity at ambient CO₂ and response to variation in foliar nitrogen concentrations are described by equations from Reich et al. (1995).

Although there has been considerable discussion surrounding the effects of elevated CO₂ on stomatal conductance (e.g. Field et al. 1995), recent evidence from a comprehensive meta-analysis (Curtis and Wang 1998) and a mature-forest CO₂ exposure experiment (Ellsworth 1999) suggests that this may not be as important as previously anticipated. Our model includes an optional conductance response, driven by CO₂ gradients across the stomatal boundary, but we did not invoke this response for the present analysis in light of these recent findings.

Using a purely conceptual approach, stomatal response to CO₂ can be characterized as follows: if conductance and photosynthesis are treated as coupled processes (Jarvis and Davies 1998) and C_i/C_a ratios remain unaffected by altered CO₂ (as

shown by Drake and González-Meler 1996), then CO₂-induced increases in photosynthesis should cause proportional reductions in conductance as the absolute CO₂ gradient across the leaf surface increases. Such a response has been used by other models (McMurtrie and Wang 1993), and has been included as an optional response in our model causing an inverse interaction between CO₂ concentration and ozone uptake. However, experimental evidence for this effect has been inconsistent. A negative interaction between CO₂ and ozone uptake has been observed in some seedling studies (Volin et al 1998), but has not occurred others (Kull et al. 1996). These inconsistencies point to a lack of basic understanding regarding factors that determine stomatal conductance, particularly when examined over a wide range of time scales.

Model Analyses

Multiple factor interactions occur through a series of feedbacks involving leaf physiology, moisture availability, foliar N concentrations, carbon allocation and biomass production, litterfall and litter C:N ratios, decomposition, soil N supply and plant N demand. Acclimation to any environmental change occurs through source-sink interactions between soil nitrogen availability and plant demand. For instance, an increase in photosynthesis due to elevated CO₂ creates increased plant demand for N and reduced foliar N concentrations, which affects subsequent rates of photosynthesis, litter C:N ratios and decomposition.

We applied the model to 64 sites across the northeastern United States where ground-level ozone data were available for the period of 1987-1992 from U.S. EPA monitoring stations (Ollinger et al. 1997, Figure 3.2). Ozone data used in the model

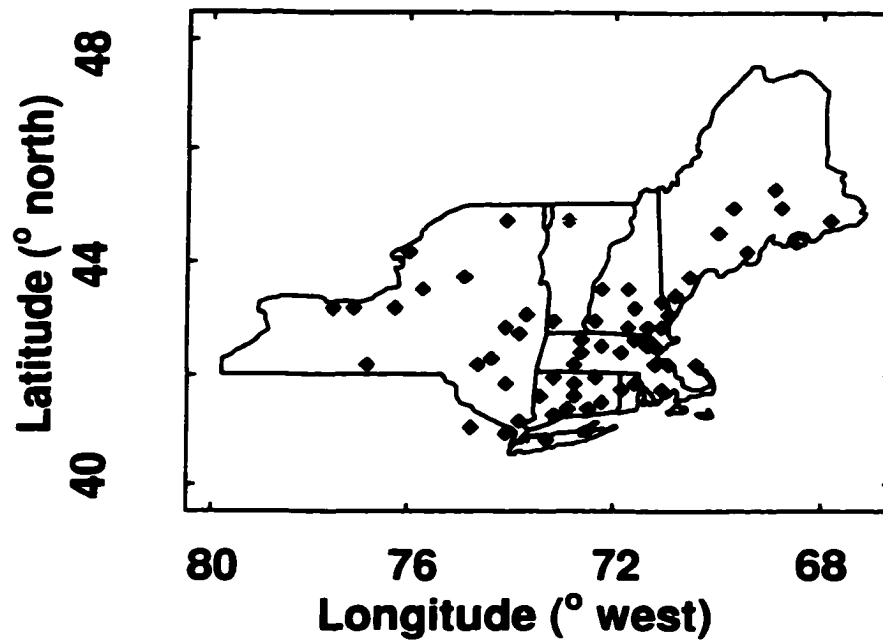


Figure 3.2. Locations of 64 ozone monitoring sites in northeastern US where model simulations were performed.

represent long-term mean monthly values measured at each site. Annual rates of wet + dry N deposition were determined for each site using a regional deposition gradient analysis (Ollinger et al. 1993). Deposition rates declined along a SW to NE gradient from a high of 12 Kg ha⁻¹ yr⁻¹ to a low of 4 Kg ha⁻¹ yr⁻¹. Monthly climate data (maximum and minimum temperature, precipitation and solar radiation) were calculated by a statistical climate model, derived from over 300 weather stations within the region (Ollinger et al. 1995). We used mean rather than historical climate data in order to more clearly identify effects of the environmental factors this study was intended to examine. The model was parameterized for northern hardwoods and run for each site under historical scenarios of agriculture and timber harvesting. We ran all sites with both disturbance regimes to allow clear identification of site history effects and because detailed site history data were not available for each location.

The timber harvest scenario was based on the site history of the Hubbard Brook Experimental Forest in New Hampshire as described by Whittaker et al. (1974). We simulated the following treatments: a 50% harvest in 1850, a 20% thinning treatment in 1909, and an 80% harvest in 1917. In each case, 80% of harvested biomass was removed and 20% was assumed to remain as slash. We also included a 20% mortality event in 1938, with 40% of dead biomass removed. This follows damage caused by a major hurricane and a subsequent salvage logging operation. We view this scenario as representative of many northeastern forests that have a history of timber harvesting.

The agriculture scenario was based on the site history records for the Harvard Forest in Central Massachusetts. Although precise removal rates for carbon and nitrogen are unknown, the land within Harvard Forest was farmed from approximately 1750 to 1850 and so a significant fraction of production would have been removed annually. Following forest regrowth, a large portion of the area was also harvested around 1945. We simulated these patterns in the model with the following treatments: agricultural cultivation between 1750 and 1850 with continuous removal of 5% of biomass production, and an 80% timber harvest in 1945, 20% of which was left as slash.

The model was run at monthly intervals from 1700 to the year 2000 with and without transient increases in CO₂, O₃ and N deposition. Atmospheric CO₂ concentrations were determined using an algorithm that follows ice core CO₂ data and the Mauna Loa CO₂ record. CO₂ concentrations are held at 280 ppb for all years prior to 1800 and then increase nonlinearly to the present day level of 363 ppb (Houghton et al. 1995). The CO₂ ramp is described by:

$$3) \text{ CO}_2 = 280 + [0.0188 * (\text{year} - 1800)]^{3.35}$$

where CO₂ concentrations are in ppm and *year* refers to the year simulated beyond the year 1800. The equation projects exponential increases in CO₂ concentrations into the future, reaching a level of 600 ppb by 2100. Although this is within the range of current predictions for the future, CO₂ concentrations beyond 2100 are expected to eventually level out (Houghton et al 1995) and so this ramp should not be used for longer-range projections.

After Aber and Driscoll (1997), N deposition was held at 25% of its current levels prior to 1930 and then increased linearly to the present. Because ozone results from similar forms of industrial activity as N deposition, this same ramp was used for ozone.

Results and Discussion

Running all sites with an agricultural site history and background (pre-industrial) levels of CO₂, O₃ and N deposition produced year-2000 NPP values of from 863 to 1021 g m⁻² yr⁻¹ (dry biomass) with a mean of 944 g m⁻² yr⁻¹. Total annual carbon accumulation, or net ecosystem production (NEP) ranged from 86 to 123 gC m⁻² yr⁻¹ with a mean of 105 gC m⁻² yr⁻¹. This positive carbon balance reflects the long-term effects of 18th and 19th century agriculture on soil carbon pools, soil respiration and biomass accumulation. Simulating the historical increase in atmospheric CO₂ caused a 17.2% increase in NPP and a 52.3% increase in NEP (Fig. 3a, b). The greater increase in NEP than NPP occurred because of the slow turnover rates for woody biomass and soil organic matter, which create long lag times between increased growth and increased soil

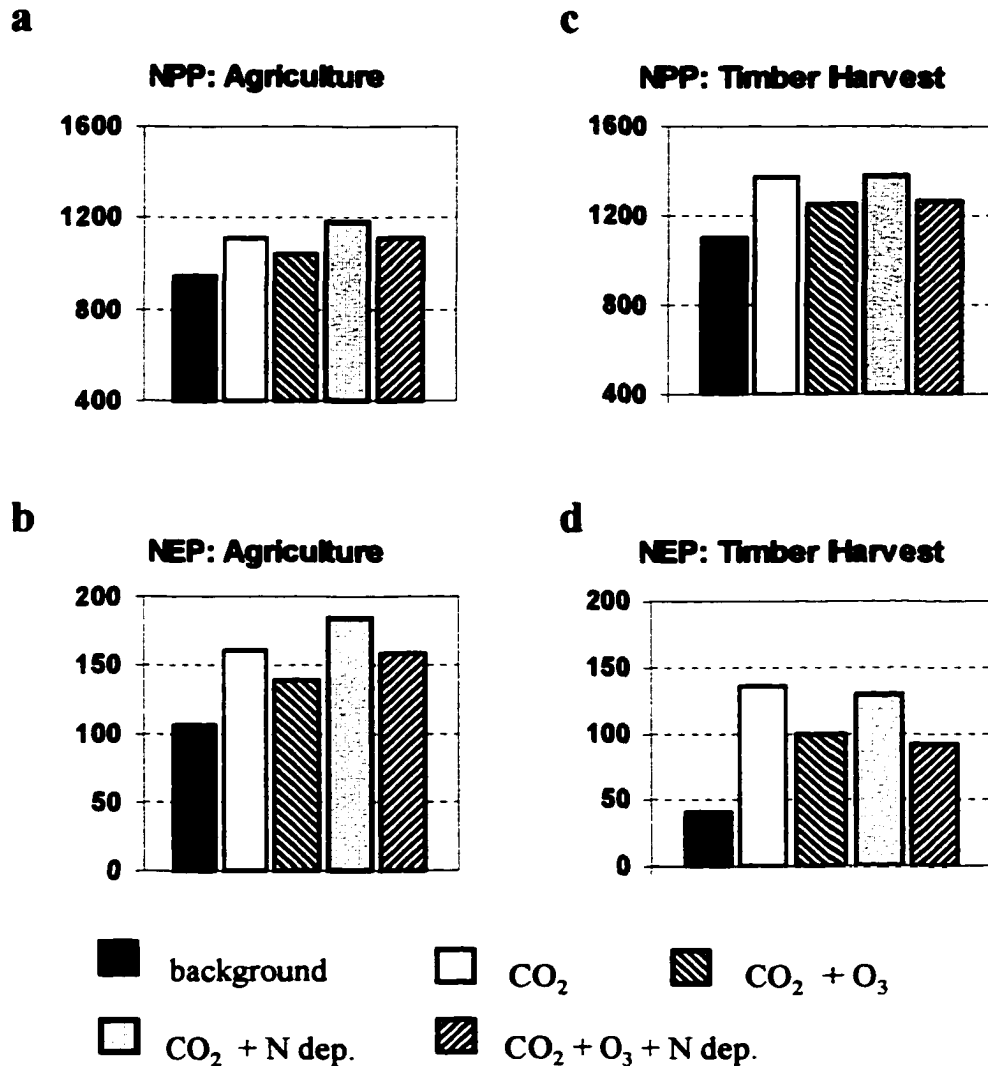


Figure 3.3. Predicted mean net primary production (NPP, g m⁻² yr⁻¹) and net ecosystem production (NEP, gC m⁻² yr⁻¹) under different combinations of CO₂, O₃ and N deposition and two land use history scenarios. Values shown are means (n = 64) of predictions for the year 2000, at the end of 300-year simulations (1701-2000).

respiration. Including the historical increase in ozone offset much (41 %) of the growth increase caused by elevated CO₂ and resulted in a regional mean NPP of 1040 g m⁻² yr⁻¹. NEP remained elevated with respect to the control run, but was 14% lower than under elevated CO₂ and no ozone.

The combination of rising N deposition and CO₂ (with no ozone) caused large gains in both NPP and NEP, which averaged 1185 g m⁻² yr⁻¹ and 184 gC m⁻² yr⁻¹ respectively, increases of 25 and 75% over pre-industrial conditions. Simulating increases in all factors simultaneously, which represents the most complete of all scenarios, produced NPP estimates ranging from 1037 to 1207 g m⁻² yr⁻¹ (mean = 1109 g m⁻² yr⁻¹) and NEP values of 137 to 185 gC m⁻² yr⁻¹ (mean = 158 gC m⁻² yr⁻¹), increases of 17 and 50% with respect to the control scenario. These values are similar to those observed under rising CO₂ alone, indicating that the effect of N deposition on carbon sequestration across the region was largely offset by ozone-induced declines in photosynthesis. Ozone effects on photosynthesis were slightly greater in the presence of elevated N deposition because the added N caused increases in foliar N concentrations, leaf gas exchange and ozone uptake. When compared to the scenario of elevated CO₂ and N deposition, (but no ozone) the combined scenario indicated ozone effects on NEP of from -6 to -22 % with a regional mean of -14% (Fig. 3b).

As discussed earlier, these simulations did not include a CO₂ effect on stomatal conductance, the implications of which are that conductance would have been higher in the past, under lower CO₂ concentrations, and would have produced higher rates of historical ozone uptake. Including this effect in trial simulations (results not shown) had a minimal effect, however, because the increase in conductance occurred at times of low ozone concentrations. This will become a more important issue for extrapolation into the future, given that CO₂ and O₃ are both expected to continue increasing.

When all sites were simulated with a history of timber harvesting instead of agriculture, NPP averaged 1096 g m⁻² yr⁻¹ and NEP averaged 41 gC m⁻² yr⁻¹ under control

conditions. The higher rate of NPP and lower rate of NEP relative to simulations with an agricultural history reflects the lower intensity of disturbance to soil C and N pools imposed by timber harvesting than by agriculture. The simulated agricultural disturbance included continuous biomass removals for the 100 year period from 1750 to 1850. This caused depletion of soil C and N pools which had not recovered after 150 years of regrowth, even when the last half of that period experienced rising N deposition. Following the less severe effects of timber harvesting (as simulated in our analysis), faster recovery of N cycling and higher foliar N concentrations led to higher rates of productivity. Because soil pools were disturbed to a lesser degree, soil respiration remained higher, keeping total carbon fluxes more tightly balanced than were observed following agriculture.

Interactions among CO₂, O₃ and N deposition were qualitatively similar following timber harvesting to those observed following agriculture (Fig. 3 c, d). However, because N limitations were weaker in the timber harvest simulations, plant C:N ratios were lower, causing plant growth to become more responsive to CO₂ and less responsive to N deposition. The historical rise in CO₂ produced increases in NPP and NEP of 25 and 232 % (reaching values of 1370 g C m⁻² yr⁻¹ and 136 gC m⁻² yr⁻¹ respectively) while N deposition had a minimal effect. Declines in growth due to ozone in the CO₂ + O₃ and combined scenarios were greater than those observed following agriculture because of higher foliar N concentrations and greater ozone uptake by foliage. Compared to the scenario of increased CO₂ and N deposition, the combined scenario produced a mean ozone effect on NEP of -37.6 gC m⁻² yr⁻¹ or -29 % (Figure 3.3 d).

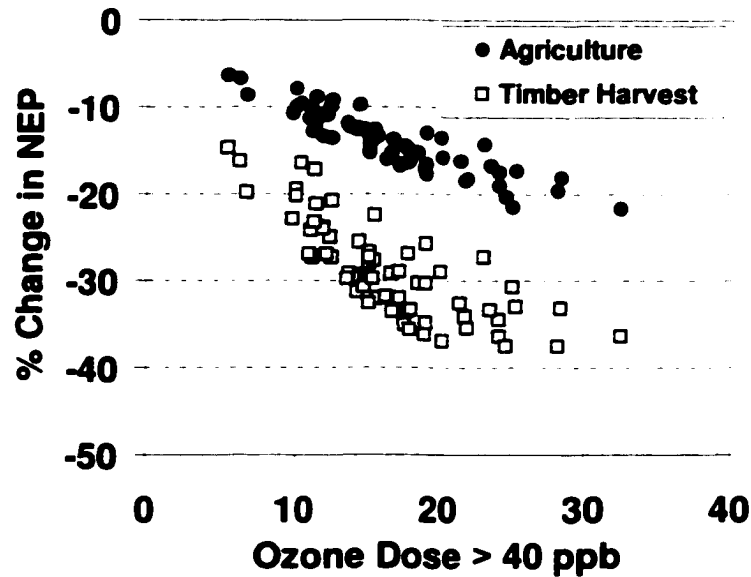


Figure 3.4. Predicted change in current annual net ecosystem production (NEP) in response to ambient ozone concentrations across the northeastern U.S. under two land use history scenarios. Reductions in NEP represent the difference between predictions generated with rising in $CO_2 + O_3 + N$ deposition and those with rising $CO_2 + N$ deposition, but no ozone. Ozone Dose > 40 ppb is the sum of hourly daytime concentrations above a threshold concentration of 40 ppb, accumulated over one growing season. Ozone data shown are mean values over the period of 1987 and 1992.

The predicted rate of carbon accumulation under the combined scenario following agriculture ($158 \text{ gC m}^{-2} \text{ yr}^{-1}$) is within the measured range of $140 - 280 \text{ gC m}^{-2} \text{ yr}^{-1}$ from eddy flux tower measurements at the Harvard Forest in central Massachusetts (Wofsy et al. 1993) and also agrees reasonably well with an estimate for the northeast region of approximately $175 \text{ gC m}^{-2} \text{ yr}^{-1}$ from forest inventory data (Turner et al. 1995). However, predictions following a history of timber harvesting (regional mean = $92 \text{ gC m}^{-2} \text{ yr}^{-1}$) fell below these estimates, possibly indicating the predominance of more intensive disturbance histories within the region.

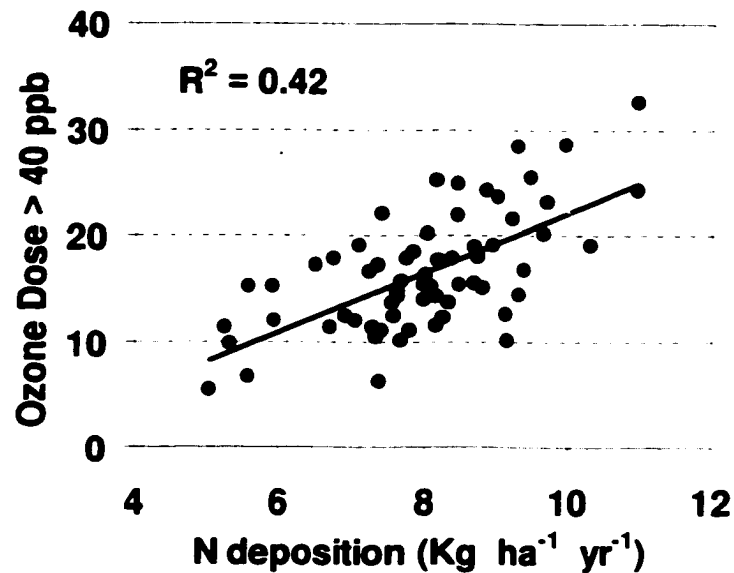


Figure 3.5. Mean ozone Dose > 40 ppb in relation to annual wet + dry nitrogen deposition (kg ha⁻¹ yr⁻¹) for the 64 study sites across the northeastern U.S. region.

Our simulations suggest that over the past several decades, increases in atmospheric CO₂ and N deposition have caused substantial increases in current rates of growth and carbon accumulation across northeastern forests, but that the magnitude of these gains has been considerably reduced by concurrent increases in ozone (Figure 3.4). The larger relative declines in NEP than NPP stems from the fact that ozone has a proportionately greater effect on predicted wood growth than on leaf or root growth. Hence, relatively small reductions in biomass production can translate to greater reductions in ecosystem carbon gain because of the decades to centuries required before reductions in wood growth translate to reduced soil respiration.

These results have implications for areas beyond the northeastern U.S. because many regions experience higher-than-background ozone levels and because the spatial distributions of nitrogen deposition and ozone are not independent. Whereas cycles of C

and N are coupled within the biosphere, patterns of N deposition and surface ozone concentrations are linked in the atmosphere due to the dependence of ozone formation on nitrogen oxide emissions. This is demonstrated by a correlation across the northeast region between rates of N deposition and ozone exposure (Fig. 5), a relationship that has been predicted to occur globally (Chamides et al. 1994, Holland et al. 1997). Variation in this trend should result from differences in N sources (e.g. ozone should follow N deposition to a lesser extent in areas where N deposition results primarily from agricultural ammonium emissions instead of industrial NO_x emissions) and from climate variables that affect ozone formation and uptake independently of N emissions. Nevertheless it seems reasonable to suggest that the reduction of N-induced carbon sinks by ozone may be a general phenomenon across broad spatial scales. Further, as forests mature and recover from past disturbance, the response to N additions will decrease as N limitations are alleviated, but the damaging effects of ozone will remain.

At present, experimental evidence for the results of this analysis are lacking, and so they should be treated as hypotheses that stem from the interactions explicitly included in the model. Although the processes included have all been identified as important responses to the environmental factors addressed, other processes that are either beyond the scope of the model (e.g. ozone effects on tree survival or forest composition) or for which little information is presently available (e.g. long-term acclimation to elevated CO₂) may be of equal or even greater importance. While we view the synthesis of existing information and advancement of new hypotheses as a useful step, efforts to verify predicted ozone - CO₂ - N deposition - land use history interactions are greatly needed before the results of simulation models can be confidently accepted.

CHAPTER IV

FOLIAR CHEMISTRY IN RELATION TO NITROGEN CYCLING AND NITRATE PRODUCTION ACROSS A TEMPERATE FOREST LANDSCAPE: INFLUENCE OF DISTURBANCE HISTORY AND SPECIES COMPOSITION

ABSTRACT

Although understanding of nitrogen cycling and nitrification in forest ecosystems has improved greatly over the past several decades, our ability to characterize spatial patterns is still quite limited. A number of studies have shown linkages between canopy chemistry and N cycling, but few have considered the degree to which these trends can provide an indicator of forest N status across large, heterogeneous landscapes. In this study, we examined relationships among canopy chemistry, nitrogen cycling and soil carbon to nitrogen ratios across 30 forested stands in the White Mountains of New Hampshire. Plots included a wide range of species (sugar maple, red maple, American beech, yellow birch, paper birch, red spruce, balsam fir, eastern hemlock) and were broadly grouped into two disturbance categories; those that were historically affected by intensive logging and/or fire and those that have experienced minimal human disturbance.

Across all plots, rates of net N mineralization and nitrification were correlated with canopy nitrogen concentrations, but the relationships differed between disturbance treatments. In deciduous forests, historically undisturbed stands had significantly higher

rates of N mineralization and nitrification than previously disturbed stands, but these differences were not clearly reflected in patterns of stand-level canopy chemistry. Although soil C:N ratios also differed between disturbed and undisturbed stands, a relationship between soil C:N ratios and canopy lignin:N ratios did not appear to vary with either forest type or disturbance, suggesting that this trend can provide a robust indicator across diverse conditions.

Relationships between foliar chemistry and N cycling within individual species revealed interesting differences between species and functional groups. For 4 out of 5 deciduous species, foliar N increased with increasing N mineralization, indicating that species were responsive to changes in N availability and suggesting a positive feedback between foliar chemistry and soil N status. These patterns led to significant differences in foliar N between disturbance treatments for some species, but these differences were masked at the stand level by successional changes in species composition. Among coniferous species, foliar N showed no variation across wide N cycling gradients suggesting a fundamentally different plant-soil interaction.

We also examined the potential for extending observed field relationships to the entire region using a high-quality data set of high spectral resolution remote sensing, obtained from NASA's AVIRIS instrument (Airborne Visible and InfraRed Imaging Spectrometer). Cloud-free AVIRIS data from 56 scenes covering the White Mountain National Forest were successfully calibrated to canopy lignin:N ratios and applied to prediction of C:N ratios in soils. Validation at 10 independent plots showed a reasonable prediction accuracy, but suggest some overprediction at the low end of the range. Preliminary regional estimates of soil C:N ratios indicate that 63% of the region's land

area falls below a value of 22. This value is significant because our field data, as well as data from other studies, have identified this as a threshold for the onset of nitrification. Below 22, we expect increasing, but variable rates of nitrification, depending on other factors such as disturbance and species composition.

Introduction

The production of nitrate in forest soils represents a key ecological process that can affect the chemistry and nutrient capital of soils and drainage waters and can alter the dynamics of plant communities. Following disturbances that reduce plant demand for available N, production and leaching of nitrate can lead to depletion of soil N pools and elevated NO_3^- concentrations in streams (Bormann and Likens 1979, Vitousek et al. 1979, Aber et al. 1997). In intact ecosystems, nitrate production is often associated with reduced plant demand relative to N supply, for example, as biomass accumulation declines (Bormann and Likens 1979, Vitousek and Reiners 1975 Aber et al. 1997), or as excess N accumulates from high levels of atmospheric N deposition (e.g. Aber et al. 1989, Gunderson et al. 1998). In all cases, NO_3^- production is considered an important issue because of the potential for elevated NO_3^- concentrations and acidity in surface waters and concurrent removal of base cations from soils (e.g. Aber et al. 1989, Murdoch and Stoddard 1992, Bailey et al. 1996, Peterjohn et al. 1996, Likens et al. 1996).

Despite considerable attention given to studying patterns of nitrogen cycling and nitrate production during forest development, our understanding of environmental controls remains incomplete and our ability to predict and/or detect spatial patterns across forested landscapes is presently very limited. The identification of simple and observable

indicators of forest nitrogen status would greatly enhance our ability to characterize spatial patterns and would help resolve relationships with possible environmental drivers. A large and growing body of literature has documented linkages among foliar chemistry, decomposition, N cycling and productivity in forest ecosystems (e.g. Fogel and Cromack 1977, Melillo et al. 1982, Pastor et al. 1984, McClaugherty and Berg 1987, Aber et al. 1990, Stump and Binkley 1993, Scott and Binkley 1997), which raises the question of whether foliar chemistry might serve as such an indicator.

At local to continental scales, N mineralization has been related to foliar and litterfall N (Yin 1992, Nadelhoffer et al. 1985), lignin (Wessman et al. 1988) and the ratio of lignin to N (Stump and Binkley 1993, Scott and Binkley 1997). Aboveground production has been related to litterfall N (Pastor et al. 1984, Nadelhoffer et al. 1985), foliar N content or concentration (Pastor et al. 1984, Smith 2000) and N mineralization (Pastor et al. 1984, Reich et al. 1997). Experimental N additions in the United States and Europe have shown that forest response to N amendments consists of simultaneous changes in N mineralization, soil C:N ratios, nitrification potential, productivity and foliar N concentrations (Magill et al. 1996, 1997, Gunderson et al. 1998). Concurrent with these changes are increased potential for NO_3^- losses to ground and streamwater, a response that has been related to both soil C:N ratios (Dise and Wright 1995, Gunderson et al. 1998) and foliar N concentrations (Tietema and Beier 1995).

Although foliar chemistry is not an easily observable property across broad spatial scales, the capacity for detection with high spectral resolution remote sensing has been recognized for some time (Wessman et al. 1988) and this ability has been identified as a useful approach to studying terrestrial biogeochemical cycles (Schimel 1995). Further,

recent advances with hyperspectral remote sensing capabilities (ACCP 1994, Martin and Aber 1997) and development and launch of space-borne sensors (e.g. NASA's Hyperion instrument on the EO-1 platform) make this a reasonable avenue for further investigation.

In this study, we use spatially extensive field measurements to examine relationships among canopy chemistry, soil C and N ratios and soil N transformations across the White Mountain National Forest in New Hampshire, USA. Results are presented with respect to variation in species composition and disturbance history. We also present estimates of soil C:N ratios for the White Mountain region, derived by combining observed field relationships with image data collected by an airborne high spectral resolution remote sensing instrument.

Methods

Study Area

The White Mountain National Forest covers 3650 km² in central New Hampshire and includes areas of low, rolling hills as well as large mountains that extend above treeline. Forests range from 200 to 1400m in elevation. The White Mountain region includes a wide variety of vegetation and site types, representative of those present across most of the northeastern U.S. These types range from oak-pine valley bottoms on lacustrine and glacio-fluvial substrates, to northern hardwood mid-slopes on basal and ablation glacial tills, to spruce-fir on upper mountain slopes and alpine tundra mountain tops. Soils are coarse-textured spodosols and inceptisols formed on glacially-deposited tills or sandy outwash with shallow bedrock histosols on upper slopes. Soils have high stone contents and this property often exerts equal or greater influence on water holding

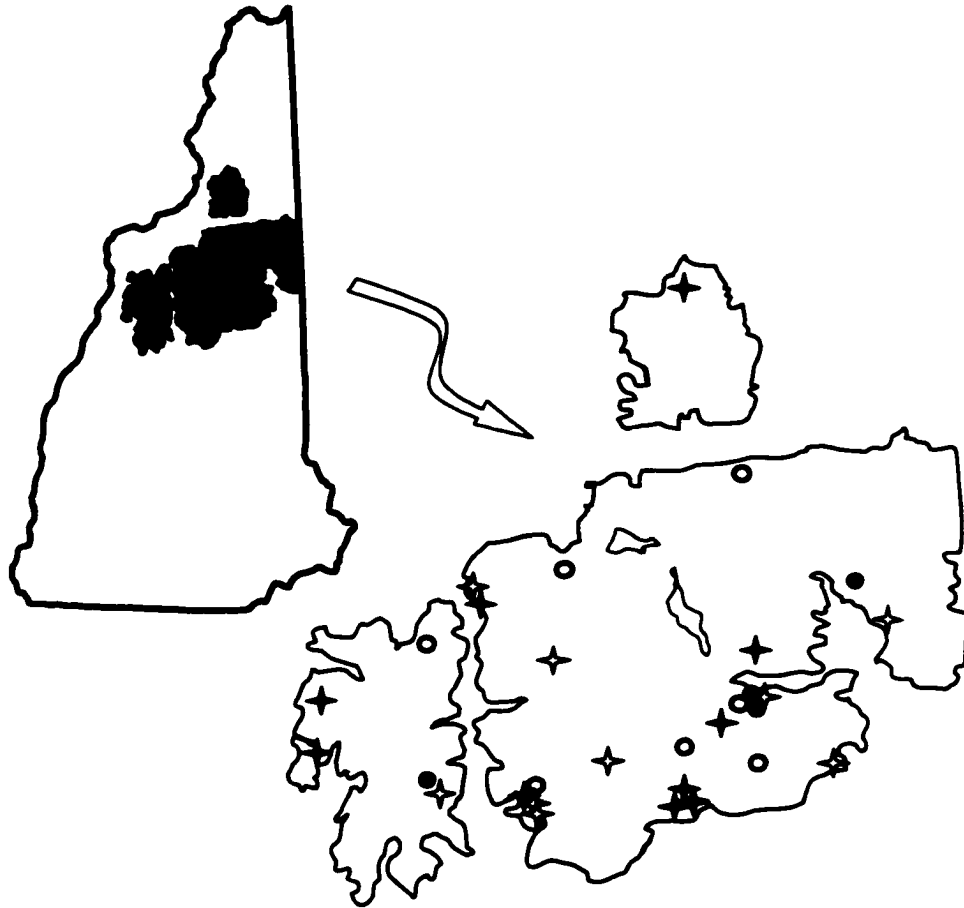


Figure 4.1. Map of the White Mountain National Forest showing locations of sample sites. Stars = hardwood stands, circles = conifers; closed symbols are stands that were historically affected by logging or fire, open symbols are undisturbed.

capacity than texture.

For the current analysis, a network of 30 plots were established for sampling of foliar chemistry and soil nitrogen fluxes (Figure 4.1). Plot selection was aimed at capturing a range of forest communities and disturbance histories, although these factors are often interdependent. Plot elevations ranged from approximately 300 to 800 meters. Major tree species represented include paper birch (*Betula papyrifera* Marsh.), yellow birch (*Betula alleghaniensis* Britt.), red maple (*Acer rubrum* L.), white ash (*Fraxinus americana* L.), sugar maple (*Acer saccharum* L.), American beech (*Fagus grandifolia*

Ehrn.), eastern hemlock (*Tsuga canadensis* L. Carr.), red spruce (*Picea rubens* Sarg.) and balsam fir (*Abies balsamea* (L.) Mill.). Most plots contained mixtures of two or more species.

Prior to European settlement, the most common natural disturbances in the region were wind and fire, which occurred at intervals of hundreds to thousands of years (Lorimer 1977, Fahey and Reiners 1981). Between approximately 1850 and 1920, large tracts of forest were intensively logged and severe slash fires followed by heavy soil erosion were common (Chittenden 1905). Public concern led to the Weeks Act in 1911 which allowed federal purchase of the White Mountain National Forest, largely as a means of reducing soil erosion and river sedimentation. At present, most of the region has returned to forest, but many areas continue to be harvested as successional forests mature.

When land was purchased for the National Forest, forest surveyors mapped forest type (hardwood, spruce-fir, or subalpine) and condition, making reference to the locations of major disturbances that had occurred. Major categories of forest condition included undisturbed forest, lightly culled, second growth and cutover (both of which indicate large areas of clearcut forest) and burned (which often indicate slash fires that occurred after major cutting activities). Following Goodale and Aber (2000), who found differences in nitrification and soil C:N ratios between old growth and disturbed sites, but not between areas that had been burned versus those that had been logged, we grouped logged and burned sites into a single class. For stands with minimal human disturbance, we grouped sites determined to be old growth, of which there were relatively few, with plots that were mapped as lightly culled, which represent areas where low-intensity

selective cutting occurred. Today, these areas share many structural characteristics with old growth stands, suggesting that disturbance was either absent or relatively minor compared to the large scale clear cuts and fires that occurred elsewhere. We refer to this group as “undisturbed” for simplicity, although “undisturbed and minimally disturbed” would be more accurate. In all, 14 plots were determined to be undisturbed or minimally disturbed (10 hardwood and 4 conifer) and 16 plots had been heavily disturbed by logging and/or fire (9 hardwood and 7 conifer).

Field Sample Collection and Analysis

Soils. Rates of N mineralization and nitrification were measured using the polyethylene bag method (Nadelhoffer et al. 1983, Pastor et al. 1984) and a combination of field and laboratory incubations (Zak et al. 1989). The widespread distribution of plots in remote locations prevented us from conducting repeat *in situ* incubations on all plots. As an alternative, we used 4-week laboratory incubations, and on a subset of ten plots, we conducted annual measurements using successive field incubations.

Following the results of Zak et al. (1989) and Carlyle et al. (1998), we anticipated that within plots where both lab and annual field incubations were performed, a correlation between the two would provide confidence that the laboratory method adequately captured spatial variability and would allow estimation of annual cycling rates on all 30 plots. A similar data set collected for a related study at the Bartlett Experimental Forest in the central White Mountains allowed us to expand this comparison from 10 to 24 plots (Ollinger unpublished data, Goodale and Aber 2000). All

groups of plots (Bartlett, WMNF field and WMNF lab) contain all major forest types included in this study.

For plots where annual N cycling measurements were made, soils were incubated in situ for 5-6 week periods throughout the 1998 growing season, with one over-winter incubation from October 1998 to May 1999. Two plots were sampled during the 1997 growing season through May of 1998. Two other plots that were sampled in both years (1997 and 1998) revealed little between-year variation, so we included the 1997 plots in the present analysis. For each incubation, net N mineralization and net nitrification were determined as the increase in $\text{NH}_4\text{-N}$ plus $\text{NO}_3\text{-N}$ (mineralization) or $\text{NO}_3\text{-N}$ (nitrification) relative to an initial soil core, taken from alongside the incubated core. Soil cores were 6 cm in diameter and included the organic horizon plus the top 10 cm of mineral soil, unless restricted by impenetrable soil material or bedrock. Within each 0.1 ha plot, five subplots were established and, for each sample period, three cores were incubated at each subplot making a total of 15 soil cores per plot.

For laboratory incubations, samples were collected during mid July using the same plot design and sampling methods as used for annual measurements, but soil cores were incubated for 4 weeks in the laboratory at approximately 22°C before KCl extraction and chemical analysis. A limitation of the buried bag method is that core moisture contents remain constant throughout the incubation period, whereas moisture levels in natural soils typically fluctuate. We attempted to avoid the potential bias of extreme conditions by sampling when soils were moist, but not saturated (not within 2 days of a hard rainfall event).

After collection (initial samples) or incubation (field and lab incubated samples), samples were separated into organic and mineral horizons, homogenized and composited by subplot. Approximately 10 g of each sample were then extracted in 1 mol/L KCl for 48 hours. A subsample was oven dried at 105°C for determination of soil moisture contents. Soil extracts were filtered and analyzed for NH_4^+ and NO_3^- on a Bran & Leubbe TrAAcs 800 autoanalyzer (Bran & Leubbe, Buffalo Grove, Illinois, USA). Net N mineralization was calculated as the difference between extractable NH_4^+ -N plus NO_3^- -N in the incubated versus initial samples. Net nitrification was determined similarly, but using extractable NO_3^- -N only. Total carbon and nitrogen contents were determined for both organic and mineral soils using a Fisons CHN Elemental Analyzer (Fisons Instruments, Beverly Massachusetts, USA). Organic and mineral soil samples were also analyzed for pH in 0.01N CaCl_2 .

Values presented for all soil variables are plot-level averages. Values presented for N mineralization and nitrification are totals for organic plus mineral soil unless otherwise noted.

Foliar Chemistry. Shotguns were used to obtain upper and mid canopy foliage from three to five trees each of all dominant and co-dominant species on a plot. Green foliage samples were obtained in late July to coincide with the peak of the growing season and with overflights of an airborne remote sensing instrument. Samples were dried (70°C) and ground through a 1 mm mesh sieve and analyzed for nitrogen, lignin and cellulose using previously tested methods of near-infrared spectroscopy (McLellan et al. 1991, Bolster et al. 1996).

The relative abundance of each species by fraction of leaf area in the canopy was determined using a camera point sampling technique developed by Aber (1979). Vertical transects were sampled by varying the focal plane of a 35 mm camera and recording the presence of foliage by species from the bottom to the top of the canopy. The method weights detection of foliage in the upper canopy more heavily than in the lower canopy to account for the higher probability that upper canopy foliage will be obscured. Species abundance values determined in this way were used to weight species-specific foliar chemistry measurements in calculating whole-plot canopy chemistry. Plot-level canopy chemical concentrations were calculated as the mean of foliar concentrations for individual species, weighted by fraction of canopy foliar mass per species. Fraction of species by leaf area was converted to fraction by weight using measured specific leaf weights for each species.

We used this method of quantifying canopy composition instead of a simpler approach based on basal area, because the latter approach was found to yield less accurate results, particularly in stands of mixed species composition. The accuracy of the camera point method was validated against canopy composition measurements obtained directly from leaf litter collections (Smith 2000).

Remote Sensing. High spectral resolution remote sensing image data were obtained for the White Mountain region using NASA's Airborne Visible/Infrared Imaging Spectrometer (AVIRIS). The AVIRIS instrument is flown aboard an ER-2 aircraft at an altitude of 20,000 m and measures upwelling radiance from the solar reflected spectrum in 224 contiguous channels from 0.4 to 2.5 μm with a spectral resolution of 0.01 μm (Green et al. 1998). On August 12, 1997, we obtained fifty-six

contiguous 10x10 km scenes with a spatial resolution of approximately 17 m covering the entire White Mountain region under cloud-free conditions. On the ground, foliar chemistry data were collected at 81 plots (using the same methods described in the preceding section) within 3 days of the AVIRIS overflight. Although image data from the same year as our soil analyses would be ideal, complete coverage could not be obtained in 1998 due to cloud cover. Multi-year foliar chemistry data for a number of plots indicated that between year differences were minimal, particularly with respect to the degree of spatial variation encountered over the region (Smith 2000).

AVIRIS at-sensor radiance data were transformed to apparent surface reflectance using the ATREM model (Gao et al. 1992). After geometric registration, AVIRIS reflectance spectra for 2x2 pixel areas covering each sample plot were extracted. Reflectance spectra were converted to absorbance prior to calibration in order to linearize spectral response to chemical constituent concentration. A first-order derivative transformation was then applied to each absorbance spectrum in order to resolve overlapping spectral peaks and to remove baseline offsets, caused by varying sun-sensor-target geometry over the study area (Hruschka 1987).

Partial least squares (PLS) regression was used to relate AVIRIS spectral response to canopy chemistry data for each sample stand. PLS regression methods reduce the full spectrum data to a smaller set of independent latent variables, or factors, with the constituent concentration data used directly during the spectral decomposition process (Shenk and Westerhaus 1991). As a result, full spectrum wavelength loadings for significant PLS factors, from which regression coefficients are derived, are directly

related to constituent concentration and thus describe the spectral variation most relevant to the modeling of variation in the chemical data.

Results

Soil N transformations

At plots where mineralization and nitrification rates were measured using both lab incubations and successive field incubations, there was a strong correlation between the two methods (Figure 4.2). Similar results were obtained from a related study at the Bartlett Experimental Forest located in the central White Mountains (Ollinger unpublished data, Goodale and Aber 2000). Together, these relationships indicate that lab incubations were a good measure of relative N cycling across the study area and can be reliably used to estimate annual rates. Because annual rates are more easily compared to results published elsewhere, we used these trends to extrapolate lab incubation data to annual N transformation rates and will refer to these values throughout the remainder of this paper. Relationships reported between soils and other variables (e.g. foliage) are qualitatively similar using either lab or field N cycling data given the linear relation between the two.

Across all plots, mean annual N mineralization ranged from 32.0 to 162.2 kg ha⁻¹ yr⁻¹ (Table 4.1). In general, mineralization was lowest on plots dominated by red spruce or hemlock and highest in northern hardwood-dominated plots, although considerable variation was observed in both groups. Nitrification ranged from near zero to 135.9 kg ha⁻¹ yr⁻¹, or from 0 to 84 percent of N mineralized, and was strongly related to N

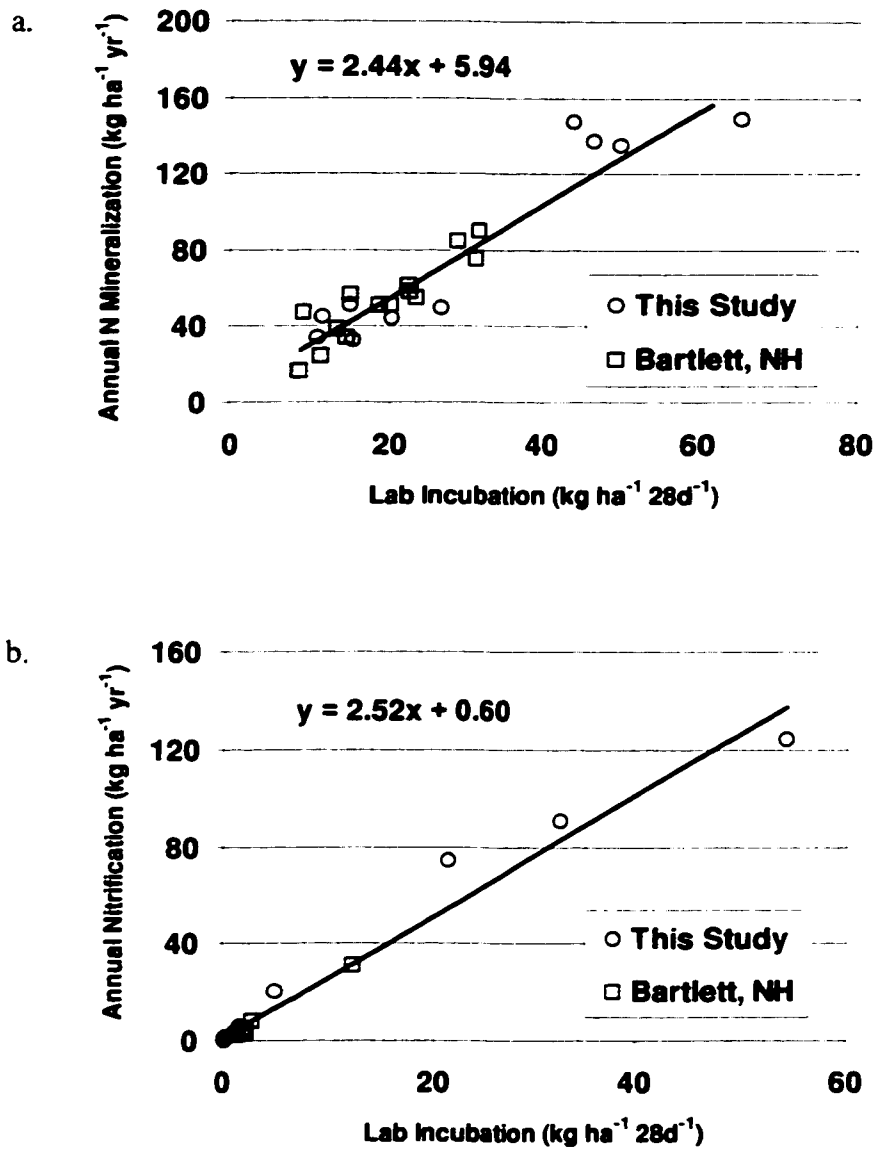


Figure 4.2. Comparison of lab incubated ($\text{kg N ha}^{-1} 28\text{d}^{-1}$) and annual field measured ($\text{kg N ha}^{-1} \text{yr}^{-1}$) rates of a) net N mineralization and b) net nitrification. The mineralization relationship is described by $N_{\text{min}}(\text{annual}) = 2.44 \times N_{\text{min}}(\text{lab}) - 5.94$ ($R^2 = 0.88$). The nitrification relationship is $\text{Nitr}(\text{annual}) = 2.52 \times \text{Nitr}(\text{lab}) + 0.60$ ($R^2 = 0.96$).

Table 4.1. *Plot characteristics and plot-level mean concentrations of foliar nitrogen and lignin.*

Site	Community Type	Disturbance History	Foliar Chemistry	
			%N	%Lignin
10	Sugar Maple	Select Cut	2.35	19.09
14	Sugar Maple	Select Cut	2.13	18.69
7	Sugar Maple	Uncut	2.27	19.28
6	Sugar Maple/Beech	Select Cut	2.13	21.13
5	Sugar Maple/Beech	Select Cut	1.87	20.42
13	Beech/Maple/Birch	Uncut	n.a.	n.a.
12	Beech/Sugar Maple	Uncut	n.a.	n.a.
9	Beech/Yellow Birch	Uncut	2.13	23.82
11	Beech/Maple/Birch	Uncut	n.a.	n.a.
8	Beech	Select Cut	2.36	23.02
29	Sugar Maple	Heavy Logging	2.10	17.9
26	Beech/Yellow Birch	Logged/Burned	2.21	25.37
24	Sugar Maple/Birch	Heavy Logging	2.28	18.41
21	Sugar Maple/Beech	Logged/Burned	1.77	17.82
23	Paper Birch/Beech	Burned	2.28	21.12
25	Red Maple/Beech	Heavy Logging	2.27	21.59
20	Red Maple/Beech/Birch	Heavy Logging	1.61	20.14
22	Sugar Maple/Yellow Birch	Heavy Logging	2.01	21.93
27	Beech/Red Maple	Logged/Burned	1.72	22.79
3	Red Spruce	Select Cut	1.38	23.18
2	Hemlock	Uncut	1.22	15.97
4	Red Spruce	Select Cut	1.49	25.75
1	Red Spruce	Select Cut	1.17	23.96
30	Balsam Fir	Heavy Logging	1.75	23.62
19	Balsam Fir/Red Spruce	Heavy Logging	1.54	23.59
28	Balsam Fir/Red Spruce	Heavy Logging	1.54	24.07
15	Red Spruce/Hemlock	Heavy Logging	0.98	22.03
16	Hemlock/Red Spruce	Logged/Burned	1.05	19.87
18	Red Spruce	Burned	1.33	24.07
17	Red Spruce/Hemlock	Logged/Burned	1.1	22.65

n.a. = data not available

Table 4.1, continued. Soil C:N ratios of the forest floor, top 10 cm of mineral soil and total for organic plus mineral soil. Values are plot-level means and standard errors.

Site	C:N Ratio					
	Forest Floor		Mineral		Total	
	Mean	S.E.	Mean	S.E.	Mean	S.E.
10	16.5	1.16	13.4	0.31	13.6	0.32
14	17.2	1.52	15.6	1.87	16.3	1.66
7	18.1	0.70	16.0	0.78	16.5	0.57
6	18.7	0.90	15.6	0.70	16.5	0.40
5	18.6	0.18	17.7	0.11	17.9	0.12
13	21.2	0.89	18.2	0.70	18.6	0.61
12	20.4	0.79	17.5	0.93	18.9	0.85
9	17.9	0.05	19.6	0.38	19.2	0.25
11	19.3	0.39	19.3	0.53	19.3	0.39
8	23.3	0.74	20.2	1.28	21.4	1.21
29	15.9	0.31	13.1	0.41	13.5	0.37
26	20.0	0.77	16.5	0.30	18.2	0.56
24	20.7	0.50	18.6	0.99	19.1	0.86
21	21.2	0.37	19.1	0.98	19.9	0.69
23	20.6	0.37	19.8	0.79	20.2	0.50
25	21.4	1.07	20.4	0.85	21.1	0.86
20	23.4	0.71	20.1	0.49	21.8	0.58
22	22.7	1.28	21.4	1.16	22.0	0.99
27	25.1	1.04	23.9	1.70	24.2	0.78
3	23.1	0.96	22.6	0.58	22.9	0.74
2	28.8	1.09	26.6	1.36	28.2	1.09
4	31.9	1.00	27.0	1.52	30.2	0.39
1	34.6	1.25	35.3	1.93	33.0	1.26
30	20.7	1.78	21.0	0.97	21.0	1.63
19	22.6	1.61	20.5	0.83	22.1	1.35
28	23.2	1.81	22.9	1.25	23.0	1.56
15	28.9	2.24	22.5	1.93	26.1	1.96
16	33.2	0.91	29.1	1.85	31.8	1.39
18	35.8	1.54	30.7	1.29	34.8	1.40
17	41.1	0.82	31.9	1.53	36.0	0.96

Table 4.1, continued. Net N mineralization and net nitrification, calculated by combining measured data from 28 day laboratory incubations with the relationship between lab and annual values shown in Figure 4.2. Standard errors were calculated as proportions from laboratory incubations applied to estimated annual values and do not reflect any additional error introduced by the relationship in figure 4.2.

Site	N Cycling (kg ha ⁻¹ yr ⁻¹)			
	N Mineralization		Nitrification	
	Mean	S.E.	Mean	S.E.
10	162.2	21.8	135.9	15.2
14	111.6	14.0	34.0	7.6
7	126.1	22.3	82.2	5.2
6	143.1	42.3	78.8	25.8
5	101.7	13.3	34.8	11.0
13	122.2	23.8	20.7	4.2
12	122.0	11.9	31.9	6.5
9	111.2	8.8	54.1	6.7
11	110.8	6.8	36.8	7.3
8	102.2	9.5	27.1	9.7
29	74.8	11.0	29.1	2.1
26	51.3	15.1	16.5	5.6
24	69.6	11.7	13.7	1.6
21	69.5	10.9	6.2	3.5
23	117.4	9.6	13.3	3.9
25	117.1	11.5	41.2	16.5
20	33.4	7.3	1.9	16.8
22	92.9	7.3	30.7	6.7
27	68.7	11.8	3.4	2.4
3	41.5	9.0	9.1	3.0
2	47.3	14.4	3.4	0.2
4	54.5	14.2	1.5	0.9
1	47.7	13.4	0.2	0.4
30	114.7	8.2	48.2	2.1
19	117.0	16.5	20.3	7.9
28	82.2	17.3	2.9	2.1
15	42.6	10.1	1.6	2.1
16	42.4	6.9	1.5	60.7
18	47.9	9.1	1.1	1.7
17	32.0	7.9	1.4	1.1

Table 4.1, continued. Soil pH for organic and mineral horizons. Values are plot-level means and standard errors.

Site	Soil pH			
	<u>organic</u>		<u>mineral</u>	
	Mean	S.E.	Mean	S.E.
10	3.86	0.03	3.62	0.04
14	4.64	0.08	4.46	0.07
7	3.72	0.11	3.78	0.16
6	4.03	0.28	4.08	0.12
5	3.65	0.07	3.65	0.06
13	3.36	0.04	3.71	0.12
12	3.31	0.06	3.64	0.06
9	3.21	0.04	3.51	0.11
11	3.37	0.04	3.60	0.08
8	3.44	0.10	3.46	0.07
29	4.75	0.13	4.64	0.13
26	3.81	0.09	3.78	0.05
24	3.56	0.05	3.93	0.05
21	3.41	0.06	3.72	0.17
23	3.28	0.06	3.32	0.10
25	3.56	0.04	3.93	0.08
20	3.68	0.18	3.85	0.18
22	3.35	0.07	3.51	0.11
27	3.68	0.14	4.04	0.15
3	3.22	0.09	3.05	0.05
2	n.a.	n.a.	n.a.	n.a.
4	3.03	0.04	3.40	0.11
1	n.a.	n.a.	n.a.	n.a.
30	3.37	0.05	3.39	0.10
19	3.22	0.12	3.54	0.19
28	3.33	0.07	3.09	0.04
15	3.22	0.03	3.34	0.03
16	3.14	0.05	3.50	0.12
18	2.75	0.04	3.27	0.18
17	2.64	0.04	3.40	0.21

n.a. = data not available

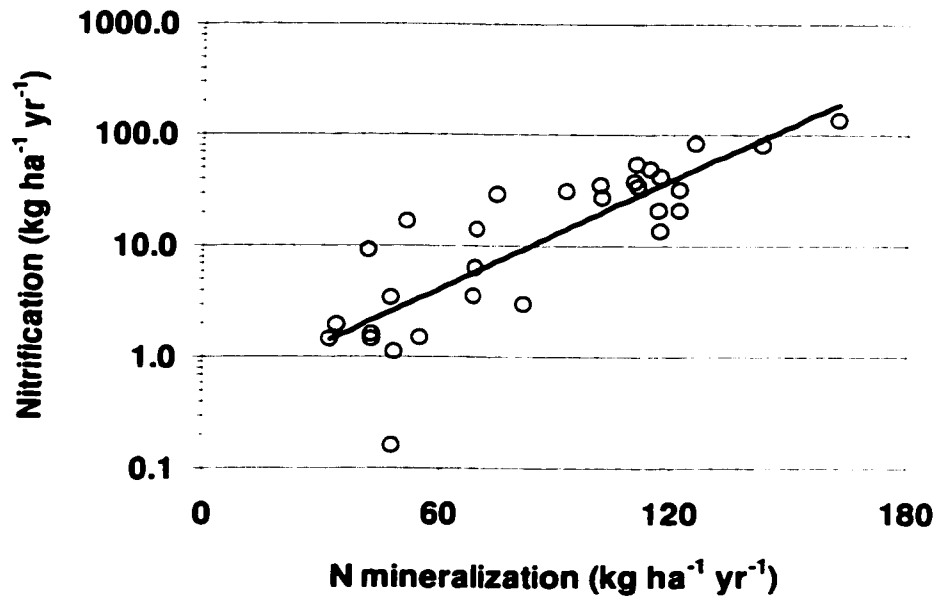


Figure 4.3. Net nitrification (shown on a log scale) in relation to net N mineralization ($R^2 = 0.77$, $p < 0.001$).

mineralization ($R^2 = 0.77$, $p < 0.001$ for log-transformed nitrification versus N mineralization, Figure 4.3).

Within soils, N mineralization and nitrification were related to soil C:N ratios (calculated as total soil N to total soil C across organic and mineral horizons, Figure 4.4), but the relationship was stronger for nitrification than for mineralization. For both mineralization and nitrification, the observed trends were fitted with exponential functions (N mineralization = $277 \times e^{[-0.0057 \times \text{soil C:N}]}$, $R^2 = 0.51$, $p < 0.001$; nitrification = $1996 \times e^{[-0.2343 \times \text{soil C:N}]}$, $R^2 = 0.73$, $p < 0.001$), but both could also be described as linear below a threshold C:N ratio of approximately 22. Above this threshold, nitrification rates remained at or close to zero. These trends were observed within individual soil horizons, but were stronger in mineral than organic soils (Table 4.2). Soil C:N ratios were linearly related to pH, although the relationship was stronger in organic than mineral horizons

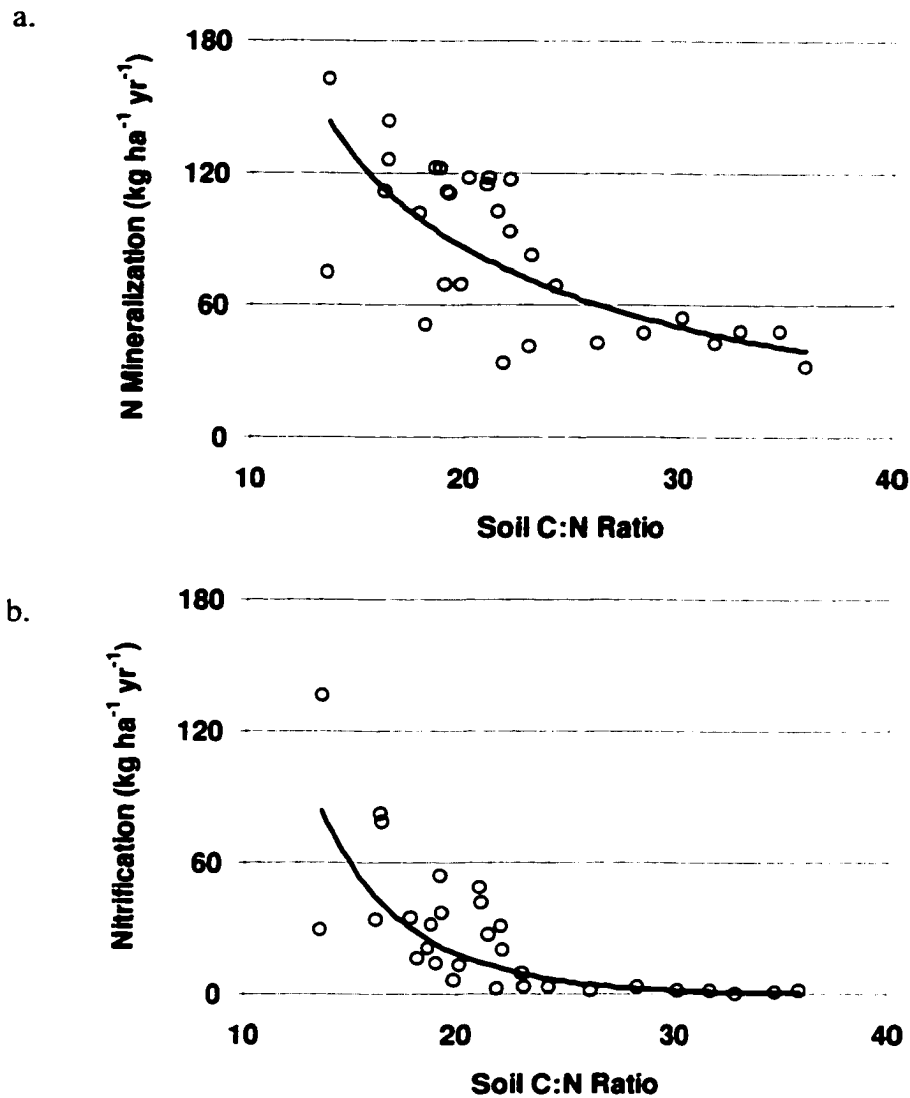


Figure 4.4. Soil C:N ratios (forest floor + top 10 cm mineral soil) in relation to a) net N mineralization and b) net nitrification.

(Table 4.2). Soil pH was not related to N mineralization in either organic or mineral horizons, and was only weakly related to nitrification in the organic horizon.

Within hardwood-dominated plots, there were significant differences in N cycling rates between plots with different disturbance histories (Figure 4.5a, differences in mean values tested with one-way analysis of variance at $p < 0.05$). Plots that were undisturbed had significantly higher rates of N mineralization and nitrification and slightly but

Table 4.2. Correlation matrix for relationships within and between soils horizons (*O* = organic, *M* = mineral) among *N* mineralization (*Nmin*), nitrification (*Nitr.*), soil C:*N* ratios and soil pH. Regression R^2 values are shown with *P* values in parentheses. *n.s.* = not significant at $p < 0.05$).

Variable	<i>Nmin-M</i>	<i>Nmin-O</i>	<i>Nitr.-M</i>	<i>Nitr.-O</i>	<i>CN-M</i>	<i>CN-O</i>	pH-M
<i>Nmin-O</i>	n.s.						
<i>Nitr.-M</i>	0.8 (<0.001)	n.s.					
<i>Nitr.-O</i>	0.35 (0.001)	0.3 (0.003)	0.60 (<0.001)				
<i>CN-M</i>	0.45 (<0.001)	n.s.	0.53 (<0.001)	0.28 (0.004)			
<i>CN-O</i>	0.72 (<0.001)	0.11 (0.05)	0.69 (<0.001)	0.035 (0.001)	0.89 (<0.001)		
pH-M	n.s.	n.s.	n.s.	n.s.	0.33 (0.002)	0.22 (0.015)	
pH-O	n.s.	ns	0.13	0.15	0.62	0.51	0.73

significantly lower soil C:*N* ratios than heavily disturbed sites. For undisturbed sites, *N* mineralization and nitrification averaged 121.3 and 58.6 kg ha⁻¹ yr⁻¹, respectively, while soil C:*N* ratios averaged 17.82. For disturbed sites, *N* mineralization and nitrification averaged 77.18 and 17.35 kg ha⁻¹ yr⁻¹, respectively, while soil C:*N* ratios averaged 20.00. It should be noted that we did not attempt to control for differences between sites other than disturbance history and forest type, and factors such as soil texture could explain some of the observed differences in *N* cycling. However, it is noteworthy that *N* mineralization rates on undisturbed plots showed relatively little variation, while disturbed plots had consistently lower values and exhibited much greater variability.

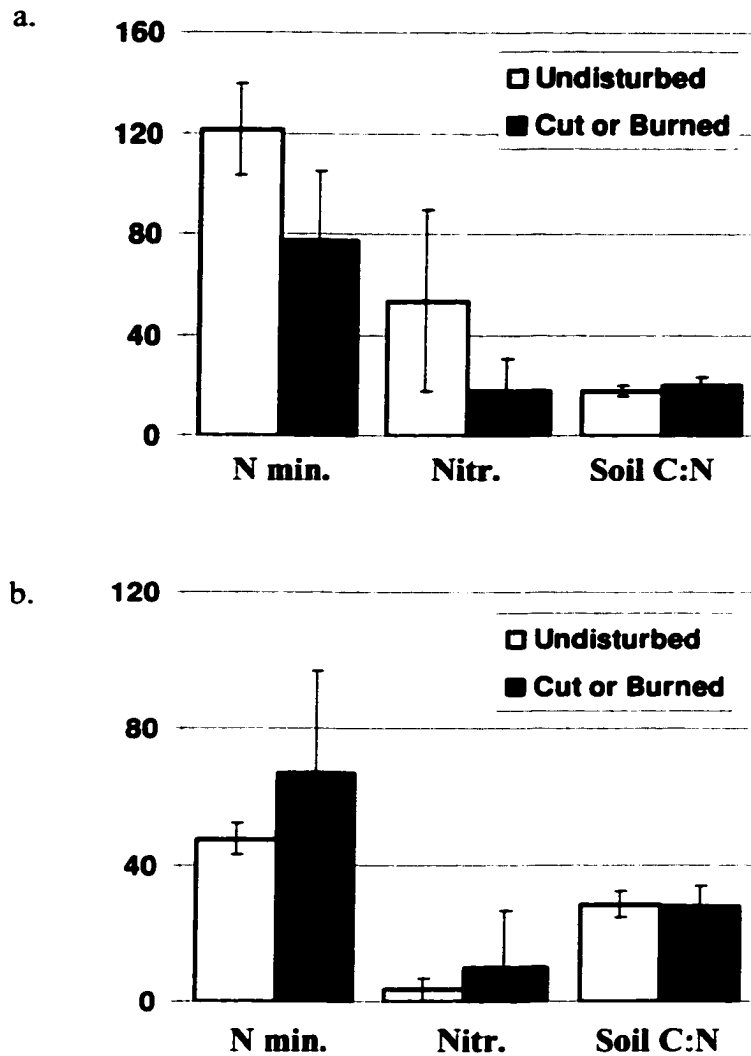


Figure 4.5. Comparison of mean N mineralization and nitrification ($\text{kg ha}^{-1} \text{ yr}^{-1}$) and soil C:N ratios between undisturbed (old growth or lightly culled) and disturbed (heavily logged and/or burned) stands for a) deciduous and b) coniferous forests. Error bars show standard deviations.

Within conifer-dominated stands, disturbance effects were the reverse of those observed in hardwoods; N mineralization and nitrification rates were higher in stands that had been disturbed than in those that had not (Figure 4.5b). However, our sample size for undisturbed conifers was small ($n = 4$) and these differences were not significant. Soil

C:N ratios were nearly identical between the two groups, averaging 28.58 and 28.12 in undisturbed and disturbed sites, respectively.

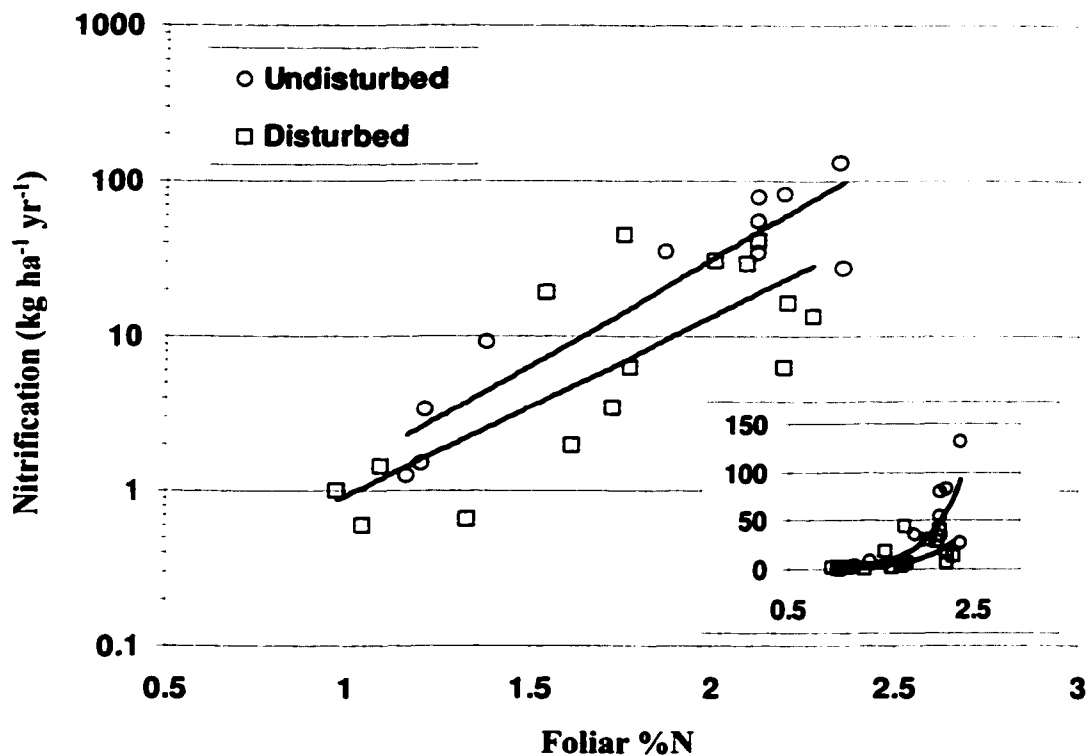


Figure 4.6. Net nitrification in relation to mass-based foliar N concentrations for disturbed and undisturbed stands. The relationship is shown on a log scale due to the nonlinear response of nitrification (see inset). The trends are described by $\text{Log}(\text{NO}_3) = 2.75(\text{folN}) - 2.96$ ($R^2 = 0.81$, $P < 0.001$) for undisturbed stands and $\text{Log}(\text{NO}_3) = 2.94(\text{folN}) - 4.28$ ($R^2 = 0.63$, $p < 0.001$) for disturbed stands.

Foliar chemistry and soil N status

Mass-based canopy nitrogen concentration ranged from 1.61 to 2.36 % in hardwood-dominated stands and from 0.98 to 1.75 % in conifer-dominated stands (Table 4.1).

Lignin concentrations ranged from 17.82 to 25.38 % in hardwood stands and from 15.97 to 25.75 % in conifer stands. Conifer stands typically had higher lignin than deciduous

Table 4.3. Stepwise regression results showing best-fit predictions of soil N variables against foliar chemistry along with slope and intercept dummy variables for disturbance history and forest type. Data shown are coefficients for each variable (*p* values in parentheses) and overall regression R^2 .

	<u>Foliar Chemistry</u>		<u>Disturbance</u>		<u>Forest Type</u>		R^2 (P)
	% N	Lignin/N	slope	intercept	slope	intercept	
<u>ALL PLOTS:</u>							
Soil C:N Ratio		1.212 (<0.001)					0.71 (<0.001)
N Mineralization	86.760 (<0.001)		-11.421 (0.026)		21.053 (0.044)		0.68 (<0.001)
Nitrification (log)	2.372 (<0.001)			-1.003 (0.016)			0.73 (<0.001)
<u>HARDWOODS:</u>							
Soil C:N Ratio		1.320 (0.040)					0.47 (0.040)
N Mineralization	64.667 (0.029)			-35.381 (0.02)			0.63 (0.002)
Nitrification (log)	2.556 (0.008)		-1.220 (0.01)				0.70 (<0.001)
<u>CONIFERS:</u>							
Soil C:N Ratio	-14.52 (0.040)						0.40 (0.040)
N Mineralization	96.392 (0.003)						0.63 (0.003)
Nitrification (log)	3.700 (0.021)						0.52 (0.021)

stands, with the exception of a plot dominated by eastern hemlock, a species that has much lower foliar lignin concentrations than most other conifers. Canopy N concentrations showed a strong linear correlation with soil C:N ratios ($R^2 = 0.65$, $p < 0.001$) and were also related with both N mineralization and nitrification. For N mineralization, the trend was best fit with a linear regression ($R^2 = 0.54$, $p < 0.001$). For nitrification the trend was nonlinear and was best fit with regression of log-transformed nitrification rates against foliar %N ($R^2 = 0.67$, $p < 0.001$).

Further, relationships between foliar chemistry and nitrification showed different patterns between disturbed and undisturbed sites, with undisturbed sites having higher nitrification per unit foliar N than previously disturbed sites (Figure 4.6). Differences in these trends were significant at $p < 0.05$ using regression of log-transformed nitrification rates on foliar N concentrations with inclusion of slope and intercept dummy variables for disturbance history (Table 4.3). If only hardwood stands were considered, the disturbance interaction increased the regression R^2 from 0.51 to 0.70 over using foliar nitrogen alone, indicating that differences in nitrification between disturbance treatments were not clearly reflected in foliar N concentrations. Foliar nitrogen was the best predictor of nitrification among conifers, although our sample set for conifer stands was limited and nitrification rates were generally much lower than in hardwood stands.

Relationships between foliar chemistry and N mineralization showed similar differences across disturbance treatments and also differed between coniferous and deciduous forests, with conifers having lower foliar N concentrations at a given N mineralization rate than hardwoods (Table 4.3). Foliar lignin was not related to N mineralization, but was weakly correlated with soil C:N ratios ($R^2 = 0.13$, $p = 0.06$) and the ratio of lignin to N improved the fit slightly over using foliar N alone (R^2 increased from 0.65 to 0.72, Figure 4.7). Although soil C:N ratios differed between undisturbed and disturbed stands, there were no differences in the relationships with foliar nitrogen or lignin to N ratios suggesting that disturbance effects on C:N ratios were reflected in foliar chemistry.

Despite this, differences in plot-level foliar N concentrations between disturbance regimes were relatively small and not significant. Among hardwoods, foliar N averaged

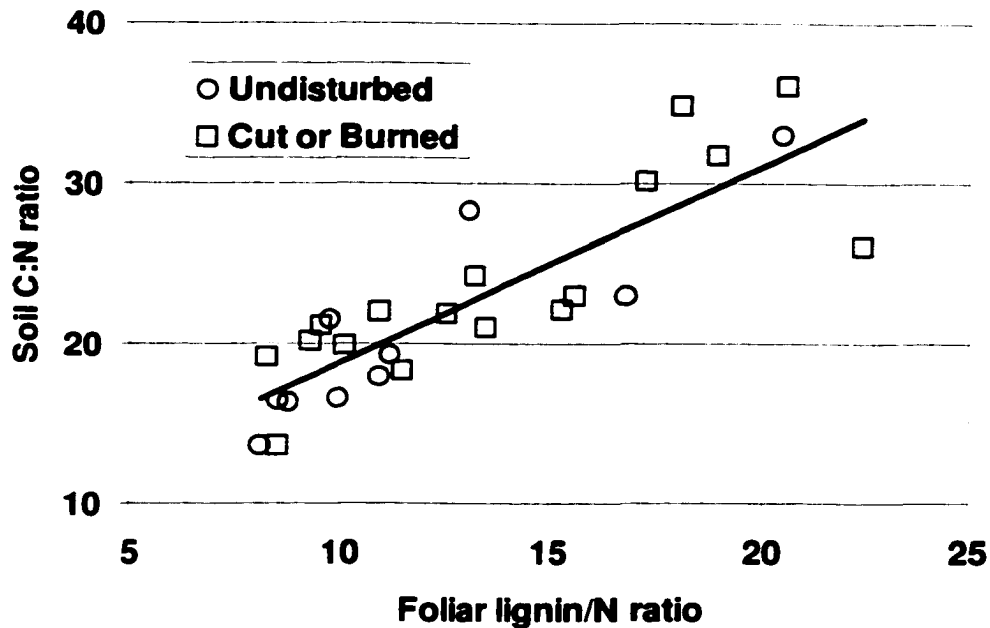


Figure 4.7. Soil C:N ratios in relation to mass-based foliar lignin:N ratios ($R^2 = 0.72$, $p < 0.001$, $SoilC:N = 1.2118 (Foliar\ Lig:N) + 6.7717$).

2.18% in undisturbed stands and 2.04% in disturbed stands, but again, this difference was not significant. That foliar chemistry appeared to capture disturbance effects on C:N ratios, but not N mineralization or nitrification may stem from the small magnitude of change in C:N ratio and the non-linearity of trends in N cycling, especially nitrification. Similarly, conifer foliar N averaged 1.32% and 1.35% in disturbed versus undisturbed stands, differences that were not significant.

Species interactions with N cycling and foliar chemistry

Another factor to consider in explaining variability surrounding trends between N cycling and foliar chemistry is the concurrent effect of species composition, which normally changes over the course of succession, and in our study, differed between

Table 4.4. Fractional species abundance in the canopies of sample plots by disturbance and forest type. Species included are: AB = American beech, BF = balsam fir, EH = eastern hemlock, Pb = paper birch, RM = red maple, SM = sugar maple, RS = red spruce and YB = yellow birch. Other species that occurred at low frequencies included white ash, mountain ash and striped maple.

	AB	BF	EH	PB	RM	SM	RS	YB	Other
Hardwood									
Undisturbed	0.30	0.00	0.00	0.03	0.03	0.47	0.05	0.08	0.04
Cut/Burned	0.16	0.02	0.07	0.15	0.12	0.28	0.02	0.11	0.08
Conifer									
Undisturbed	0.01	0.09	0.25	0.05	0.07	0.00	0.49	0.01	0.03
Cut/Burned	0.01	0.26	0.12	0.08	0.04	0.02	0.42	0.04	0.01

disturbed and undisturbed sites (Table 4.4). Among deciduous forests, disturbed stands had greater overall canopy diversity than undisturbed stands, with mixtures of sugar maple and beech, early to mid successional species such as paper birch and red maple, and a moderate presence of conifers (22 % on average). In undisturbed deciduous stands, overall canopy diversity was lower, conifers were less abundant in the canopy and sugar maple and/or beech had become dominant.

These differences are important because there were significant interactions between N cycling and the abundance of some tree species in the canopy, with sugar maple in particular showing a significant positive correlation with N mineralization and nitrification and a negative correlation with soil C:N ratios (Table 4.5). Because sugar maple abundance is related to disturbance history, it is difficult to assess whether trends in soil properties reflect the singular effects of one of these or are the result of an interaction between the two, i.e. whereby disturbance alters the length of time over which a particular plant-soil feedback can occur. However, an analysis for deciduous stands

Table 4.5. Regression coefficients (*P* values in parentheses) for relationships between species abundance in the canopy and soil C:N ratio (forest floor + mineral soil), net N mineralization and net nitrification ($\text{kg ha}^{-1} \text{ yr}^{-1}$) for three species that exhibited significant trends across hardwood (sugar maple) and conifer (red spruce and balsam fir) plots sampled.

	Sugar Maple (n = 12)		Red Spruce (n = 10)		Balsam Fir (n = 8)	
	coef. (P)	R²	coef. (P)	R²	coef. (P)	R²
C:N Ratio	-14.69 (0.01)	0.62	10.75 (0.08)	0.29	-18.03 (0.02)	0.46
Net N Min	82.323 (0.04)	0.35	-83.356 (0.03)	0.43	107.665 (0.03)	0.51
Net Nitr	3.757 -0.01	0.53	-3.604 -0.09	0.34	4.376 0.05	0.51

using stepwise linear regression of log transformed nitrification rates against foliar nitrogen, percent sugar maple in the canopy and a disturbance history interaction term indicated that disturbance history explained a greater amount of variation than did sugar maple abundance, which was not significant in the combined regression ($R^2 = 0.70$, Table 4.3), but was significant when the disturbance interaction variables were left out. This should not be taken to suggest that variation in nitrification is caused solely by direct disturbance effects, irrespective of associated changes in species composition, but it does suggest that there is at least some effect of disturbance that is not also explained by the increase in sugar maple.

Other species whose abundance in the canopy was correlated with soil characteristics were red spruce and balsam fir. Red spruce was inversely related with N mineralization and nitrification, and positively related with C:N ratios (Table 4.5).

Trends for balsam fir were opposite those of red spruce, being positively related to N mineralization and nitrification and negatively related to soil C:N ratio. Although nitrification was generally low among conifer stands, ranging from near zero to approximately 24% of N mineralized (Table 4.1), the percent of the canopy occupied by balsam fir was the strongest overall correlate of log-transformed nitrification rates, explaining 51% of the observed variation within conifer stands ($R^2 = 0.51$, $p < 0.04$). Because balsam fir also had the highest foliar N concentration among conifers, these trends were also reflected in patterns of foliar chemistry (Table 4.3).

Foliar N concentrations also exhibited interesting trends within and between species. For sugar maple, red maple, American beech and yellow birch, but not paper birch, foliar N increased with increasing N mineralization rates. Further, these trends showed distinct differences between species (Figure 4.8a). Yellow birch had the highest foliar N concentrations, followed by American beech, red maple and sugar maple. These trends were pronounced enough that sugar maple and red maple growing on rich sites often had foliar N concentrations similar to those of birch and beech on poorer sites. In addition, while there were no differences in plot-level foliar chemistry across disturbance treatments, there were differences within species. Sugar maple and beech both had significantly lower foliar N concentrations in disturbed than undisturbed stands (one-way analysis of variance at $P < 0.05$). Foliar N concentrations for red maple, yellow birch and paper birch also tended to be lower on heavily disturbed sites, but differences were not significant.

In contrast to the patterns observed among hardwoods, there were no significant trends between foliar N and N mineralization among conifers (Figure 4.8b). Hemlock

foliage was collected along a relatively small N cycling gradient, but additional data from a related study (Ollinger unpublished data) show no change in foliar N along a greater range of N cycling rates.

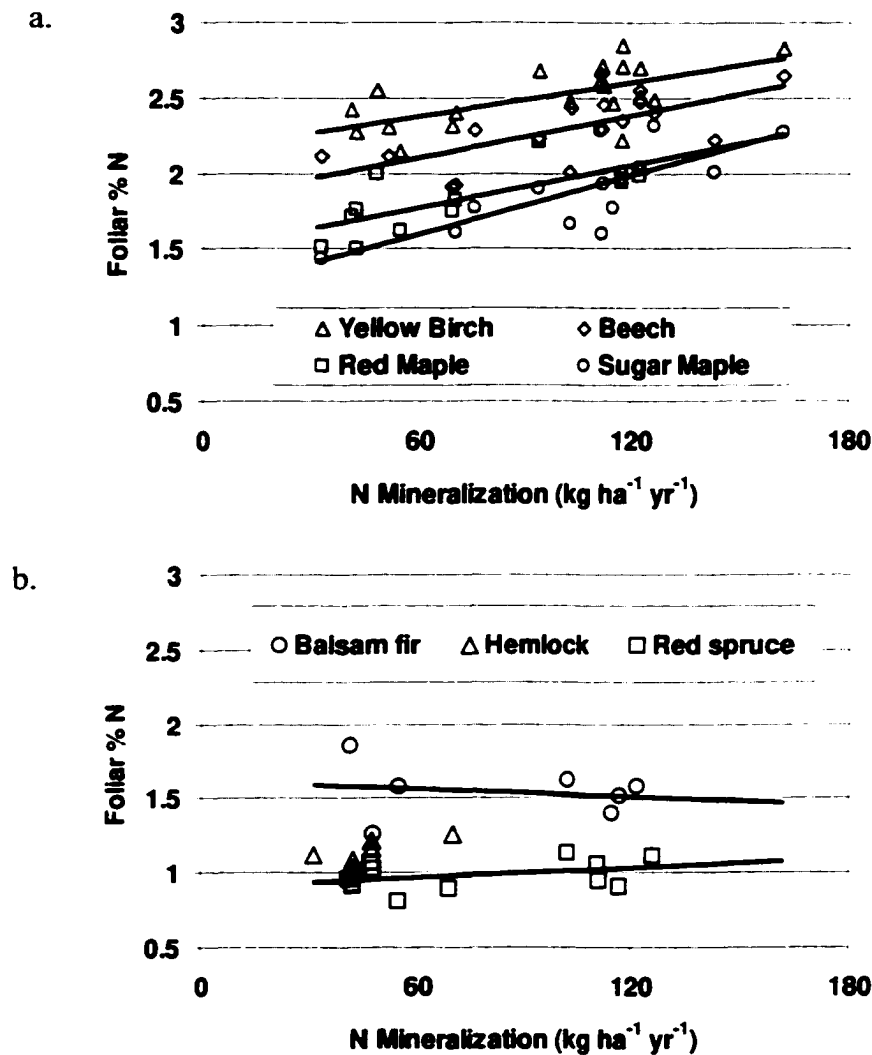


Figure 4.8. Mass-based foliar N concentrations for individual species within a) deciduous and b) coniferous forests in relation to N mineralization rates for plots on which they were sampled. Relationships were significant at $p < 0.05$ for all deciduous species except paper birch. Regression R^2 values were 0.42 for yellow birch, 0.49 for beech, 0.51 for red maple and 0.57 for sugar maple. Trends were significant for coniferous species.

Remote detection of canopy chemistry and soil C:N ratios

Previous remote sensing analyses have demonstrated that high spectral resolution data can be used to estimate canopy nitrogen and lignin concentrations with a high degree of accuracy (Wessman et al. 1988, Martin and Aber 1997). Using Partial Least Squares regression (PLS), we obtained a 2 factor calibration equation relating AVIRIS spectral data to measured canopy lignin:N ratios directly. The equation had a calibration $R^2=0.69$ and a standard error of calibration (SEC) of 2.3 or 16.7% of measured lignin:N ratios from Table 4.1. This level of accuracy is within that required to detect important spatial patterns over the range of canopy chemistry values experienced (Schimel 1995). Although greater calibration accuracy has been achieved for single remote sensing scenes covering relatively small areas, our calibration included 36 of the 56 scenes that cover the White Mountain region.

The ability to detect canopy lignin to nitrogen ratios with a reasonable level of accuracy allowed us to extend the relationship in Figure 4.7 to estimate spatial patterns of soil C:N ratios across the White Mountain region (Figure 4.9). Although 20 of the 30 plots used in this study were also sampled for foliar chemistry image calibration, the remaining 10 provide some means of assessing prediction accuracy against independent data. A plot of AVIRIS-predicted versus measured values (Figure 4.10) for these plots shows generally good agreement with a standard error of prediction of 2.34, or 12.8% of observed C:N ratios, but suggests a tendency towards overprediction at the low end of the range. Although we do not consider this small validation exercise to be adequate for such a large region, it does provide some confidence that hyperspectral image data can be used

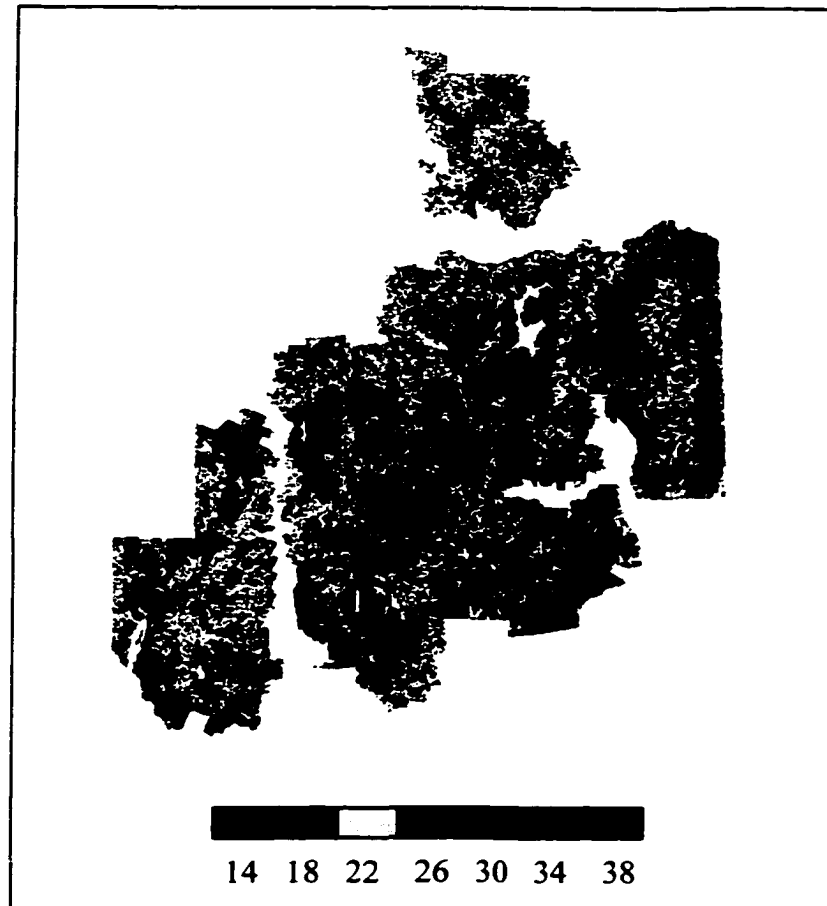


Figure 4.9. *Predicted soil C:N ratio for the White mountain National Forest, derived by combining the trend in figure 7 with AVIRIS-estimated foliar lignin:N ratio.*

to detect important spatial variability in soils through related patterns in canopy chemistry.

Figure 4.11 shows the distribution of predicted values over the entire White Mountain region, indicating that roughly 64% of the area is predicted to fall below 22, the observed threshold for nitrate production. Below this, we expect increasing, but variable rates of nitrification depending on additional factors such as disturbance history and species composition and perhaps others we have not addressed (e.g. soil mineralogy,

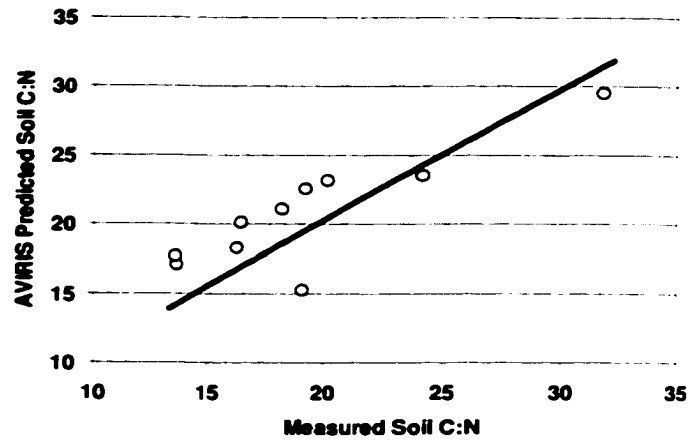


Figure 4.10. Soil C:N ratios as predicted from AVIRIS imagery (Figure 4.8) in relation to measured values at 10 plots that were not used in AVIRIS foliar chemistry calibrations. The line shows a 1:1 relationship.

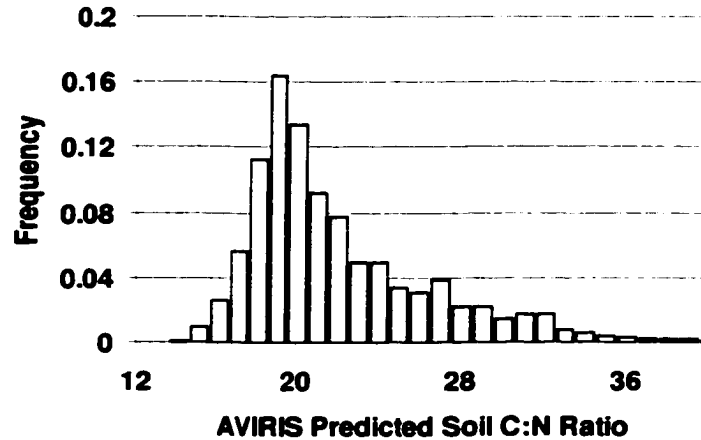


Figure 4.11. Distribution of predicted soil C:N ratios across the White Mountain National Forest. Approximately 63% of the region contains predicted values below the nitrification threshold of 22. Below that value we expect increasing nitrification with high variability caused by disturbance history and/or other factors that are not reflected in foliar lignin:N ratios.

Hornbeck et al. 1997). We view these results as preliminary given the lack of comprehensive validation and we anticipate that future improvement in image calibration can be achieved by more careful correction for atmospheric effects and within scene sun-sensor-target geometry effects (Smith 2000).

Discussion

Plant-soil interactions

Across the White Mountain study area, patterns of nitrification in soils were strongly related to rates of N mineralization and soil C:N ratios and these were broadly reflected in forest canopy chemistry. These results are consistent with previous analyses of N cycling and leaf chemistry (most of which have come from the western and mid-western U.S.) in demonstrating the coupled nature of carbon-nitrogen interactions between forest canopies and soils (e.g. Wessman et al 1988, Scott and Binkley 1997, Ferrari 1999), but are different in that foliar nitrogen and not lignin showed a greater degree of connection with soil N status. This could stem from differences between the chemistry of leaf litter, which has been the focus of many prior analyses, and that of whole-canopy green foliar chemistry, which we have examined here to evaluate its potential to serve as an indicator of ecosystem N status and for application with remote sensing.

We have also demonstrated that variation surrounding relationships between foliar chemistry and N cycling is related to differences in disturbance history. The same was not true for relationships between foliar chemistry and soil C:N ratios, indicating that foliar chemistry is a good predictor of C:N ratios across forest types and disturbance history gradients. This is due in part to the linear nature of foliar chemistry-soil C:N relationships and the relatively small difference in C:N ratios between disturbance regimes. In contrast, nitrification varied more dramatically between disturbance treatments and increased exponentially with both foliar N concentrations and soil C:N ratios. Despite the relatively strong overall relationship between foliar N and

nitrification, this non-linearity produces increasing variation at sites with high foliar N concentrations and low C:N ratios (see inset of Figure 4.6).

Although distinguishing cause from effect is an inherent problem in studies of plant-soil interactions, trends between N mineralization and foliar nitrogen concentrations within species suggest that some species are responsive to differences in site quality and that observed patterns of N cycling were not simply due to different combinations of species, each with characteristic and implast leaf traits. The increase in foliar N concentrations with increasing rates of N mineralization observed for most deciduous species is indicative of a positive feedback between plant and soil N status whereby plants respond to increased N availability in such a way that can further increase N cycling rates; by producing foliage with higher N contents, which leads to faster leaf litter turnover, narrower soil C:N ratios and increased N mineralization (e.g. Hobbie 1992). The higher rates of N mineralization in undisturbed versus disturbed hardwood stands is likely the result of this feedback being reiterated over longer periods of time than has occurred on heavily disturbed sites. This should emphasize the fact that plant-soil relations are interactive and can lead to changes in both over time.

These patterns should also be considered with respect to changes in species composition since individual species showed distinct patterns of foliar N along N cycling gradients. Sugar maple was the most dominant late successional species in deciduous forests among our sample set and yet it had the lowest foliar N concentration of all hardwood species examined. Based on this alone, we might expect undisturbed stands with high sugar maple abundance to have low foliar nitrogen, wider soil C:N ratios and low nitrification rates than early successional hardwood stands. However, sugar maple

on undisturbed stands had higher foliar N than on disturbed stands, reaching concentrations similar to those of early successional species on disturbed stands with lower N cycling rates. This, along with higher foliar N concentrations in co-occurring species (e.g. American beech and yellow birch), led to the small, but not significant increase in plot-level foliar N in undisturbed stands. The association between sugar maple abundance and nitrification is consistent with a number of recent studies that have linked sugar maple abundance with nitrate production (Goodale and Aber 2000, Lovett and Reuth 1999, Ferrari 1999, Finzi et al. 1998). In our study, we could not identify an effect of sugar maple that was separate from that of disturbance history. Others who have examined sugar maple more explicitly have indicated a significant species effect that did not appear to be related to differences in disturbance history (Lovett and Reuth 1999, Ferrari 1999).

In marked contrast to hardwood species, conifers had consistently lower and less plastic foliar N concentrations across relatively wide N cycling gradients. These patterns suggest a plant-soil interaction for conifers by which litter inputs can cause N cycling rates to decline over time (e.g. Pastor et al. 1987, van Cleve et al. 1993). However, the association between balsam fir abundance with elevated nitrification might represent exception. Although our sample size was relatively small (balsam fir occurred on 8 out of 11 conifer plots sampled) and most conifer stands had relatively low nitrification rates, balsam fir abundance was the best overall correlate, explaining 55% of the variation in nitrate production among stands dominated by conifers.

There are at least two possible explanations for the trends observed for balsam fir. The first is that balsam fir has a positive effect on N mineralization and nitrification,

relative to other conifer species it coexists with (primarily red spruce). Balsam-fir foliage does have relatively high N concentrations among conifers (Figure 4.8), but it also has high lignin and has previously been associated with inhibition and not stimulation of nitrification (Olson and Reiners 1983). The second is that balsam fir abundance and nitrification both reflect some other site property such as the severity or timing of past disturbance. Balsam fir is adapted to growth in disturbed environments, often occurring in areas where wind damage is common (Marchand et al. 1986). If disturbance leads to elevated rates of nitrification in these systems, a relationship with balsam fir abundance may be observed without implying a causal effect. Sasser and Binkley (1989) studied patterns of nitrogen cycling with stand development in wind-generated fir waves and found that nitrification was high following mortality and declined in regenerating stands, but then became elevated again in mature stands. These observations could reflect either possibility, but in combination with our data, suggest that differences between the foliar chemistry-N cycling interactions of spruce and fir should be considered when making generalizations about spruce-fir forest types.

Disturbance History

Differences in N cycling between sites that were heavily impacted by logging and/or fire and sites that were undisturbed or only selectively cut indicate significant long-term impacts of disturbance on present-day rates of N mineralization and nitrification. Model analyses have suggested that, in the absence of disturbance, maximum rates of N cycling would be determined by energy or moisture availability as they constrain plant growth and N turnover via organic matter inputs (Schimel et al. 1996, Aber et al. 1997). The fact that undisturbed or lightly cut forests in our study had

higher and less variable rates of N cycling may be an indication that these stands have reached such a state. Heavily disturbed stands, on the other hand, exhibited lower and more variable N cycling rates, presumably reflecting variation in the severity and/or timing of the disturbances experienced.

However, a related analysis of land use history in White Mountain forests found no differences in N cycling rates between old growth, cut and burned stands, but did find lower C:N ratios and elevated nitrification in old growth stands, consistent with our own results (Goodale and Aber 2000). The difference in results for N mineralization could be due to several factors. First, Goodale and Aber (2000) located plots adjacent to one another across known land use history boundaries. This was useful for reducing variation in unrelated factors (e.g. soil type, climate), but may have limited the severity of disturbance treatments sampled. We did not attempt to control for site factors, which could have introduced an unrecognized bias to our results, but also allowed us to sample from areas that may have been more heavily disturbed than areas near the edge of a given treatment (for example, if the edge of a burn represents an area where fire was waning in intensity). Another possible difference stems from our inclusion of lightly culled areas along with undisturbed stands. The decision to combine these two categories was based on current stand structural characteristics and evidence that cutting in these areas was very limited. Although the similarity between selectively cut sites and old growth sites in terms of current N status suggests that this decision was warranted, it is also possible that selective removal of conifers from some areas could actually have *improved* site quality and led to elevated rates of N mineralization over areas that were truly undisturbed. In either case, this discussion should serve to highlight the complexity of issues surrounding

disturbance history and the obvious limitations of summarizing such varied conditions into few broad categories.

Finally, a study conducted in the White Mountains by Thorne and Hamburg (1985) found decreasing nitrification potentials in soils along an old-field chronosequence, counter to the findings of both this study and those of Goodale and Aber (2000). The decrease in nitrification found by Thorn and Hamburg was related to declines in soil pH (and increases in soil C:N ratios) from initial values in young stands that were relatively high for soils of the region (e.g. Bormann and Likens 1979). This suggests that agricultural practices may have resulted in elevated soil pH and reduced soil C:N ratios and that the decline in nitrification potential reflected a return to conditions more characteristic of forest soils. Our study did not include agriculture as a disturbance treatment and, although nitrification rates were weakly correlated with forest floor pH, we did not observe a difference in pH between disturbance treatments.

Collectively, these results indicate that fundamentally different patterns of nitrogen cycling with stand development during secondary succession can result from differences in initial conditions that, in turn, stem from differences in the nature of the disturbance experienced. Such differences must be carefully considered before making generalizations about widespread effects of disturbance and subsequent patterns of nutrient cycling during stand development.

Remote detection of canopy chemistry and regional ecological analysis

Early work with hyperspectral remote sensing held much promise for its role in analyses of ecosystem biogeochemistry (Wessman et al. 1988). Although there have

been significant improvements in detector technology and application techniques since that time (e.g. ACCP 1994, Asner 1998), its use has been relatively limited, owing, in part, to the limited availability of hyperspectral image data. Nevertheless, interest in the approach has persisted, or even grown, as a result of the increasing scientific importance of terrestrial carbon and nitrogen cycles (e.g. Schimel 1995), leading to development of new hyperspectral sensors for upcoming orbital platforms (e.g. NASA's Hyperion on the EO-1 platform scheduled for launch in July, 2000).

Whereas previous hyperspectral analyses have been limited to single remote-sensing scenes covering relatively small areas, here we have demonstrated that applications across large, multi-scene landscapes are also possible. That the observed relationship between foliar chemistry and soil C:N ratios was consistent across a range of forest communities and disturbance histories suggests that patterns of soil C:N ratios across complex forested landscapes can be broadly characterized by patterns of canopy chemistry. A number of studies in both Europe and north America have identified soil C:N ratios as a key ecological variable and several, in addition to this one, have identified C:N ratios of between 22 and 24 as a critical threshold for nitrification and nitrate leaching (McNulty et al. 1991, Emmett et al. 1998, Lovett and Reuth 1999, Goodale and Aber 2000). Although our analysis also indicates that ancillary information regarding disturbance history, species composition and perhaps other variables will be important for making precise estimates of soil N transformations, the ability to detect fine-scale patterns of foliar chemistry and soil C:N ratios over large areas represents a useful step towards conducting regional biogeochemical analyses.

Whereas this study has focused on canopy chemistry and forest nitrogen status, future efforts will examine relationships between canopy chemistry and forest productivity. Establishment of such relationships would greatly enhance our ability to use canopy chemistry as a means of studying patterns of carbon-nitrogen relations in forest ecosystems.

Although high spectral resolution remote sensing cannot replace more conventional sensors that provide data over larger areas and at greater frequencies continued development of the approach we have applied here stands to benefit regional ecological analyses by making it possible to derive spatially-explicit data that could not be attained through even the most ambitious field campaigns nor through conventional remote sensing. If such efforts incorporate rigorous field analyses, they can perhaps even compliment broader-scale, coarser-resolution sensors by providing a much needed bridge between kilometer-scale grid cells and plot-based field measurements.

LIST OF REFERENCES

- Aber, J.D. 1979. A method for estimating foliage-height profiles in broad-leaved forests. *Journal of Ecology* 67:35-40.
- Aber, J.D., K. Nadelhoffer, P. Steudler, and J.M. Melillo. 1989. Nitrogen saturation in northern forest ecosystems. *Bioscience*. 48:921-934.
- Aber, J.D., J.M. Melillo and C.A. McClaugherty. 1990. Predicting long-term patterns of mass loss, nitrogen dynamics, and soil organic matter formation from initial fine litter chemistry in temperate forests. *Canadian Journal of Botany*. 68:2201-2208.
- Aber, J.D., and C.A. Federer. 1992. A generalized, lumped-parameter model of photosynthesis, evapotranspiration and net primary production in temperate and boreal forest ecosystems. *Oecologia*. 92: 463-474
- Aber, J.D., S.V. Ollinger, C.A. Federer, P.B. Reich, M.L. Goulden, D.W. Kicklighter, J.M. Melillo, and R.G. Lathrop. 1995. Predicting the effects of climate change on water yield and forest production in the northeastern U.S. *Climate Research*. 5:207-222.
- Aber, J.D., P.B. Reich, and M.L. Goulden. 1996. Extrapolating leaf CO₂ exchange to the canopy: a generalized model of forest photosynthesis validated by eddy correlation. *Oecologia*. 106:257-265.
- Aber, J.D. and C.T. Driscoll. 1997. Effects of land use, climate variation, and N deposition on N cycling and C storage in northern hardwood forests. *Global Biogeochemical Cycles*. 11:639-648.
- Aber, J.D., S.V. Ollinger, and C.T. Driscoll. 1997. Modeling nitrogen saturation in forest ecosystems in response to land use and atmospheric deposition. *Ecological Modelling*. 101:61-78.

Abrams, M.D., J.C. Schultz, and K.W. Kleiner. 1990. Ecophysiological response in mesic versus xeric hardwood species to an early-season drought in central Pennsylvania. *Forest Science*. 36:970-981.

ACCP. 1994. The Accelerated Canopy Chemistry Program: Final report to NASA-EOS-IWG. Aber, J.D. (ed.). National Aeronautics and Space Administration, Washington, DC.

Amthor, J.S., D.S. Gill, and F.H. Bormann. 1990. Autumnal leaf conductance and apparent photosynthesis by saplings and sprouts in a recently disturbed northern hardwood forest. *Oecologia*. 84:93-98.

Asner GP. 1998. Biophysical and biochemical sources of variability in canopy reflectance. *Remote Sensing of Environment* (64):234-53.

Aubuchon, R.R., D.R. Thompson, and T.M. Hinckley. 1978. Environmental influences on photosynthesis within the crown of a white oak. *Oecologia*. 35:295-306.

Bailey, S.W., J.W. Hornbeck, C.T. Driscoll and H.E. Gaudett. 1996. Calcium imports and transport in a base poor forest ecosystem as interpreted by Sr isotopes. *Water Resources Research*. 32: 707-719.

Baldocci, D.D., S.B. Verma and D.E. Anderson. 1987. Canopy photosynthesis and water-use efficiency in a deciduous forest. *Journal of Applied Ecology*. 24: 251-260.

Berg, B. and E. Matzner. 1997. Effects of N deposition on decomposition of plant litter and soil organic matter in forest systems. *Environmental Reviews*. 5:1-25.

Bolster, K.L., M.E. Martin and J.D. Aber. 1996. Interactions between precision and generality in the development of calibrations for the determination of carbon fraction and nitrogen concentration in foliage by near infrared reflectance. *Canadian Journal of Forest Research* 26:590-600.

Bormann, F.H. and G.E. Likens. 1979. *Pattern and Process in a Forested Ecosystem*. Springer-Verland. New York. 253p.

Burke, I.C., D.S. Shimel, C.M. Yonker, W.J. Parton, L.A. Joyce, and W.K. Laurenroth. Regional Modeling of grassland biogeochemistry using GIS. 1990. *Landscape Ecology*. 4: 45-54.

Carlyle, J.C., E.K. Sadanandan and M.W. Bligh. 1998. The use of laboratory measurements to predict nitrogen mineralization and nitrification in *Pinus radiata* plantations after harvesting. *Canadian Journal of Forest Research*. 28: 1213-1221.

Chamedes, W.L., P.S. Kasibhatla, J. Yienger and H.Levy II. 1994. Growth of continental-scale metro-agro-plexes, regional ozone pollution, and world food production. *Science*. 264:74-77.

Chapelka, A.H. and L.J. Samulson. 1998. Ambient ozone effects on forest trees of the eastern United States: a review. *New Phytologist*. 139:91-108.

Chen, C.W., W.T. Tsai, and L.E. Gomez. 1994. Modeling responses of ponderosa pine to interacting stresses of ozone and drought. *Forest Science*. 40:267-288.

Chittenden, A.K. 1905. Forest conditions of northern New Hampshire. USDA Bureau of Forestry, Bulletin No. 55. 100p.

Clapp, R.B. and G.M. Hornberger. 1978. Empirical equations for some soil hydraulic properties. *Water Resources Research*. 9: 1599-1604.

Comins, H.N. and R.E. McMurtrie. 1993. Long-term response of nutrient-limited forests to CO₂ enrichment; equilibrium behavior of plant-soil models. *Ecological Applications*. 3(4):666-681.

Curtis, P.S., C.S. Vogel, K.S. Pregitzer, D.R. Zak and J.A. Teeri. 1995. Interacting effects of soil fertility and atmospheric CO₂ on leaf area growth and carbon gain in *Populus x euroamericana* (Dode) Guinier. 1995. *New Phytologist*. 129:253-263.

Curtis, P.S. and X. Wang. 1998. A meta-analysis of elevated CO₂ effects on woody plant mass, form, and physiology. *Oecologia*. 113:299-313

Dise, N.B. and R.F. Wright. 1995. Nitrogen leaching in European forests in relation to nitrogen deposition. *Forest Ecology and Management*. 71:153-162.

Dobson, M.C., G.Taylor, and P.H. Freer-Smith. 1990. The control of ozone uptake by *Picea abies* (L.) Karst. and *P. sitchensis* (Bong.) Carr. during drought and interacting effects on shoot water relations. *New Phytologist*. 116:465-474.

- Drake, B.G. and M.A. Gonzalez-Meler. 1996. More efficient plants: a consequence of rising atmospheric CO₂? *Annual Review of Plant Physiology and Plant Molecular Biology*. 48:609-639.
- Edwards, G.S., S.D. Wullschleger, and J.M. Kelly. 1994. Growth and physiology of northern red oak: preliminary comparison of mature tree and seedling responses to ozone. *Environmental Pollution*. 83:215-221.
- Ellsworth, D.S., and P.B. Reich. 1993. Canopy structure and vertical patterns of photosynthesis and related leaf traits in a deciduous forest. *Oecologia*. 96:169-178.
- Ellsworth, D.S., R. Oren, C. Huang, N. Phillips and G.R. Hendrey. 1995. Leaf and canopy response to elevated CO₂ in a pine forest under free-air CO₂ enrichment. *Oecologia*. 104:139-146.
- Ellsworth, D.S. 1999. CO₂ enrichment in a maturing pine forest: are CO₂ exchange and water status in the canopy affected? *Plant, Cell and Environment*. 22:461-472.
- Emmett, B. A., D. Boxman, M. Bredemeier, P. Gunderson, O. J. Konaas, F. Moldan, P. Schleppei, A. Tietma, and R. F. Wright. 1998. Predicting the effects of atmospheric nitrogen deposition in conifer stands: evidence from the NITREX ecosystem-scale experiments. *Ecosystems* 1:352-360.
- Fahey, T.J. and W.A. Reiners. 1981. Fire in the forests of Maine and New Hampshire. *Bulletin of the Torrey Botanical Club*. 108:362-373.
- Fan, S., M. Gloor, J. Mahlman, S. Pacala, J. Sarmiento, T. Takahashi and P. Tans. 1998. A large terrestrial carbon sink in North America implied by atmospheric and oceanic carbon dioxide data and models. *Science*. 282(442-446).
- Farquhar, G.D. and S.C. Wong. 1982. An empirical model of stomatal conductance. *Australian Journal of Plant Physiology*. 11:191-210.
- Federer, C.A., and D. Lash. 1978. BROOK: A hydrologic simulation model for eastern forests. University of New Hampshire Water Resources Research Center Report 19.
- Federer, C.A. 1982. Frequency and intensity of drought in New Hampshire forests: Evaluation by the BROOK model. In: *Applied Modeling in Catchment Hydrology, Proceedings of the international symposium on rainfall-runoff modeling, May 1981, Water Resources Publications, Littleton, CO.*

Ferarri, J. B. 1999. Fine-scale patterns of leaf litterfall and nitrogen cycling in an old-growth forest. *Canadian Journal of Forest Research*. 29 (3):291-302.

Field, C., and H.A. Mooney. 1986. The Photosynthesis-nitrogen relationship in wild plants. In: Givnish, T. (ed.) *On the Economy of Plant Form and Function*. Cambridge University Press. pp. 25-55.

Field, C.B., R.B. Jackson and H.A. Mooney. 1995. Stomatal response to increased CO₂: implications from the plant to the global scale. *Plant, Cell and Environment*. 18:1214-1225.

Finzi, A.C., N van Breemen and C.D. Canham, 1998. Canopy tree-soil interactions within temperate forests: species effects on soil carbon and nitrogen. *Ecological Applications*. 8(2): 440-446.

Fogel, R. and K. Cromack Jr. 1977. Effect of habitat and substrate quality on douglas-fir litter decomposition in western Oregon. *Canadian Journal of Botany*. 55:1632-1640.

Foster, D. R. 1992. Land-use history (1730-1990) and vegetation dynamics in central New England, USA. *Journal of Ecology*. 80: 753-772.

Fredericksen, T.S., B.J. Joyce, J.M. Skelly, K.C. Steiner, T.E. Kolb, K.B. Kouterick, J.E. Savage, and K.R Snyder. 1994. Physiology, morphology, and ozone uptake of leaves of black cherry seedlings, saplings, and canopy trees. *Environmental Pollution*. 89:273-283.

Fuhrer, J. 1994. The critical level for ozone to protect agricultural crops - An assessment of data from European open-top chamber experiments. In: J. Fuhrer and B. Achermann (eds.) *Critical Levels for Ozone: a UN-ECE workshop report*. Swiss Federal Research Station for Agricultural Chemistry and Environmental Hygiene, Liebefeld-Bern, pp.42-57.

Gao B, K. Heidebrecht, F. Goetz. 1992. *Atmosphere Removal Program (ATREM) User's Guide*. Boulder, CO: Center for the Study of Earth from Space/CIRES, University of Colorado.

Goodale, C.L. and J.D. Aber. 2000. The long-term effects of land-use history on nitrogen cycling in northern hardwood forests. *Ecological Applications*. In Press.

Green R.O., M.L. Eastwood, C.M. Sarture, T.G. Chrien, M. Aronsson, B.J. Chippendale,

- J.A. Faust, B.E. Pavri, C.J. Chovit, M. Solis. 1998. *Imaging Spectrometry and the Airborne Visible/Infrared Imaging Spectrometer (AVIRIS). Remote Sensing of Environment* 65: 227-48.
- Guderian, R., D.T. Tingey, and R. Rabe. 1985. Effects of photochemical oxidants on plants. In Guderian (ed.) *Air Pollution by Photochemical Oxidants: Formation, Transport, Control, and Effects on Plants*. Springer-Verlag. Berlin Heidelberg, Germany.
- Gundersen, P., B.A. Emmett, O.J. Kjonas, C.J. Koopmans, and A. Tietema. 1998. Impact of nitrogen deposition on nitrogen cycling in forests: a synthesis of NITREX data. *Forest Ecology and Management*. 101:37-55.
- Hamilton, L.C. 1989. *Statistics with STATA*. Brooks/Cole Publishing. California, U.S.A.
- Heck, W.W., O.C. Taylor, and D.T. Tingey, editors. 1988. *Assessment of Crop Loss from Air Pollutants*. Elsevier Applied Science. New York, NY.
- Hinckley, T.M., R.G. Aslin, R.R. Aubuchon, C.L. Metcalf, and J.E. Roberts. 1978. Leaf conductance and photosynthesis in four species of the oak-hickory type. *Forest Science*. 24:73-84.
- Hobbie, S.E. 1992. Effects of plant species on nutrient cycling. *Trends in Ecology and Evolution*. 7(10): 336-339.
- Hogsett, W.E., M. Plocher, V. Wildman, D.T. Tingey, and J.P. Bennett. 1985. Growth response of two varieties of slash pine seedlings to chronic ozone exposures. *Canadian Journal of Botany*. 63:2369-2376.
- Holland, E.A. B.H. Braswell, J.F. Lamarque, A. Townsend, J. Sulzman, J.F. Muller, F. Dentener, G. Brasseur, H. Levy II, J.E. Penner and G.J. Roelofs. 1997. Variations in the predicted spatial distribution of atmospheric nitrogen deposition and their impact on carbon uptake by terrestrial ecosystems. *Journal of Geophysical Research*. 102:15,849-15,866.
- Hornbeck, J.W., S.W. Bailey, D.C. Buso, and J.B. Shanley. 1997. Streamwater chemistry and nutrient budgets for forested watersheds in New England: variability and management implications. *Forest Ecology and Management*. 93:73-89.

Houghton, R.A., J.L. Hackler and K.T. Lawrence. 1999. The U.S. carbon budget: contributions from land-use change. *Science*. 285:574-578.

Hruschka, W. 1987. Data Analysis: Wavelength Selection Methods, p 35-56, in P. Williams and K. Norris (eds.), *Near-Infrared Technology in the Agricultural and Food Industries*. American Association of Cereal Chemists, St. Paul, Minnesota.

Jarvis, A.J. and W.J. Davies. 1998. The coupled response of stomatal conductance to photosynthesis and transpiration. *Journal of Experimental Botany*. 49:399-406.

Kingsley, N.P. 1985. A forester's atlas of the northeast. USDA Forest Service General Technical Report NE-95.

Kronzucker, H.J., M. Yaesh and A.D.M. Glass. 1997. Conifer root discrimination against soil nitrate and the ecology of forest succession. *Nature*. 385: 59-61

Kull, O., A. Sober, M.D. Coleman, R.E. Dickson, J.G. Isebrands, Z. Gagnon, and D.F. Karnosky. 1996. Photosynthetic responses of aspen clones to simultaneous exposures to ozone and CO₂. *Canadian Journal of Forest Research*. 26:639-648.

Laisk, A., O.Kull., and H. Moldau. 1989. Ozone concentration in leaf intercellular air spaces is close to zero. *Plant Physiology*. 90:1163-1167.

Lathrop, R.G. and J.A. Bognar. 1994. Development and validation of AVHRR-derived regional land cover data for the northeastern U.S. Region. *International Journal of Remote Sensing*. 15: 2695-2702

Lathrop, R.G., J.D. Aber and J.A. Bognar. 1995. Spatial variability of a digital soils map in a regional modeling context. *Ecological Modeling*. 82:1-10.

Laurence, J.A., R.J. Kohut, and R.G. Amundson. 1993. Use of TREGRO to simulate the effects of ozone on growth of red spruce seedlings. *Forest Science*. 39:453-464.

Laurence, J.A., R.G. Amundson, A.L. Friend, E.J. Pell, and P.J. Temple. 1994. Allocation of carbon in plants under stress: an analysis the ROPIS experiments. *Journal of Environmental Quality*. 23:412-417.

Lewis, J.D., D.T. Tissue and B.R. Strain. 1996. Seasonal response of photosynthesis to elevated CO₂ in loblolly pine (*Pinus taeda* L.) over two growing seasons. *Global change biology*. 2:103-114.

Likens, G.E., C.T. Driscoll, and D.C. Buso. 1996. Long-term effects of acid rain: response and recovery of a forest ecosystem. *Science*. 272:244-246.

Lloyd, J. The CO₂ dependence of photosynthesis, plant growth responses to elevated CO₂ concentrations and their interactions with soil nutrient status, II. Temperate and boreal forest productivity and the combined effects of increasing CO₂ concentrations and increased nitrogen deposition at a global scale. *Functional Ecology*. 13:439-459.

Lorimer, C.G. 1977. The presettlement forest and natural disturbance cycle of northeastern Maine. *Ecology*. 58: 139-148.

Lovett, G.M. and H. Reuth. 1999. Soil nitrogen transformations in beech and maple stands along a nitrogen deposition gradient. *Ecological Applications*. 9(4): 1330-1344.

Magill, A.H., M.R. Downs, K.J. Nadelhoffer, R.A. Hallett, And J.D. Aber. 1996. Forest ecosystem response to four years of chronic nitrate and sulfate additions at Bear Brook Watershed, Maine, USA. *Forest Ecology and Management*. 84:29-37.

Magill, A.H., J.D. Aber, J.J. Hendricks, R.D. Bowden, J.M. Melillo and P. Steudler. 1997. Biogeochemical response of forest ecosystems to simulated chronic nitrogen deposition. *Ecological Applications*. 7:402-415.

Marchand, P.J., F.L. Goulet and T.C. Harrington. 1986. Death by attrition: a hypothesis for wave mortality of subalpine *Abies balsamea*. *Canadian Journal of Forest Research*. 16:591-596.

Marks, P.L. 1974. The role of pin cherry (*Prunus pensylvanica* L.) in the maintenance of stability in northern hardwood ecosystems. *Ecological Monographs*. 44: 73-88.

Martin, M.E. and J.D. Aber. 1997. High spectral resolution remote sensing of forest canopy lignin, nitrogen and ecosystem processes. *Ecological Applications*. 7:431-443.

Martin, M.E., M.L. Smith, S.V. Ollinger, R.A. Hallett, C.L. Goodale, and J.D. Aber. 1999. Applying AVIRIS at the Sub-regional Scale: Forest Productivity and Nitrogen and Cation Cycling. In *Summaries of the Eighth JPL Airborne Earth Science Workshop*. R.O Green editor. Jet Propulsion Lab, Pasadena CA. pp 275-280.

McClaugherty, C.A. and B. Berg. 1987. Cellulose, lignin and nitrogen concentrations as rate regulating factors in late stages of forest litter decomposition. *Pedobiologia*. 30:101-112.

McGuire, A.D., J.M. Melillo, L.A. Joyce, D.W. Kicklighter, A.L. Grace, B. Moore III, and C.J. Vorosmarty. 1992. Interactions between carbon and nitrogen dynamics in estimating net primary production for potential vegetation in North America. *Global Biogeochemical Cycles*. 6: 101-124.

McLaughlin, S.B., P.A. Layton, M.B. Abrams, N.T. Edwards, P.J. Hanson, E.G. O'Neill, and W.K. Roy. 1994. Growth response of 53 open-pollinated loblolly pine families to ozone and acid rain. *Journal of Environmental Quality*. 23:247-257.

McLaughlin, S.B., and D.J. Downing. 1995. Interactive effects of ambient ozone and climate measured on growth of mature forest trees. *Nature*. 374:252-254.

McLellan, T., Martin, M.E., Aber, J.D., Melillo, J.M., Nadelhoffer, K.J., and Dewey, B. 1991. Comparison of wet chemistry and near infrared reflectance measurements of carbon-fraction chemistry and nitrogen concentration of forest foliage. *Canadian Journal of Forest Research* 21: 1689-1693.

McMurtrie, R.E. and Y.P. Wang. 1993. Mathematical models of the photosynthetic response of tree stands to rising CO₂ concentrations and temperature. *Plant, Cell and Environment*. 16:1-13.

McNulty, S.G., J.D. Aber, and R.D. Boone. 1991. Spatial changes in forest floor and foliar chemistry in spruce-fir forests across New England. *Biogeochemistry*. 14:13-29.

Melillo, J.M., J.D. Aber and J.M. Muratore. 1982. Nitrogen and lignin control of hardwood leaf litter decomposition dynamics. *Ecology*. 63:621-626.

Mooney, H.A. and W.E. Winner. 1991. Partitioning response of plants to stress. In H.A. Mooney et al. (ed.) *Response of Plants to Multiple Stress*. Academic Press, San Diego, CA. pp. 129-141.

Munger, J.W., S.C. Wofsy, P.S. Bakwin, S. Fan, M.L. Goulden, B.C. Daube, A.H. Goldstein, K. Moore, and D. Fitzjarrald. 1996. Atmospheric deposition of reactive nitrogen oxides and ozone in a temperate deciduous forest and a sub-arctic woodland. 1. Measurements and mechanisms. *Journal of Geophysical Research*. 101:12639-12657.

Murdoch, P.S. and J.L. Stoddard. 1992. The role of nitrate in the acidification of streams in the Catskill Mountains of New York. *Water Resources Research*. 28:2707-2720.

Nadelhoffer, K.J. J.D. Aber and J.M. Melillo, 1983. Leaf-litter production and soil organic matter dynamics along a nitrogen availability gradient in Southern Wisconsin (U.S.A.). *Canadian Journal of Forest Research*. 13:12-21.

Nadelhoffer, K.J., J.D. Aber, and J.M. Melillo. 1985. Fine roots, net primary productivity, and soil nitrogen availability: a new hypothesis. *Ecology*. 66(4):1377-1390.

Nadelhoffer, K.J. M.R. Downes and B. Fry. 1999. Sinks for ^{15}N -enriched additions to an oak forest and a red pine plantation. *Ecological Applications*. 9(1):72-86.

Neilson, R.P. 1995. A model for predicting continental-scale vegetation distribution and water balance. *Ecological Applications*. 5: 362-385.

National Research Council. 1992. *Rethinking the Ozone Problem in Urban and Regional Air Pollution*. National Academy Press, Washington, D.C.

Newman, S.D., M.E. Soulia, J.D. Aber, B. Dewey and A. Ricca. 1994. Analysis of forest foliage I: Laboratory procedures for proximate carbon fractionation and nitrogen determination. *Journal of Near Infrared Spectroscopy*. 2: 5-14.

Ollinger, S.V., J.D. Aber, G.M. Lovett, S.E. Millham, R.G. Lathrop, and J.M. Ellis. 1993. A spatial model of atmospheric deposition for the northeastern U.S. *Ecological Applications* 3:459-472.

Ollinger, S.V., J.D. Aber, C.A. Federer, G.M. Lovett, and J. Ellis. 1995. Modeling physical and chemical climatic variables across the northeastern U.S. for a Geographic Information System. USDA Forest Service General Technical Report NE-191.

Ollinger, S.V., J.D. Aber, and P.B. Reich. 1997. Simulating ozone effects on forest productivity: interactions among leaf-, canopy- and stand-level processes. *Ecological Applications*. 7(4): 1237-1251.

Ollinger, S.V., J.D. Aber, and C.A. Federer. 1998. Estimating regional forest productivity and water yield using an ecosystem model linked to a GIS. *Landscape Ecology*. 13:323-334.

Olson, R.K. and W.A. Reiners. 1983. Nitrification in subalpine balsam fir soils: tests for inhibitory factors. *Soil biology and biochemistry* 15: 413-418.

Parton, W.J., J.W.B. Stewart, and C.V. Cole. 1988. Dynamics of C, N, P and S in grassland soils: a model. *Biogeochemistry*. 5: 109-131

Pastor, J., J.D. Aber, C.A. McClaugherty, and J.M. Melillo. 1984. Aboveground production and N and P cycling along a nitrogen mineralization gradient on Blackhawk Island, Wisconsin. *Ecology*. 65:256-268.

Pastor, J., R.H. Gardner, V.H. Dale, and W.M. Post. 1987. Successional changes in nitrogen availability as a potential factor contributing to spruce declines in boreal North America. *Can. J. For. Res.* 17: 1394-1400.

Pell, E. J., N. Eckerdt, and A.J. Enyedi. 1992. Timing of ozone stress and resulting status of ribulose biphosphate carboxylase/oxygenase and associated net photosynthesis. *New Phytologist*. 120:397-405.

Pell, E.J., P.J. Temple, A.L. Friend, H.A. Mooney, and W.E. Winner. 1994. Compensation as a plant response to ozone and associated stresses: an analysis of ROPIS experiments. *Journal of Environmental Quality*. 23:429-436.

Peterjohn, W.T., M.B. Adams, and F.S. Gilliam. 1996. Symptoms of nitrogen saturation in two central Appalachian hardwood forest ecosystems. *Biogeochemistry*. 35:507-522.

Pettersson, R. and A.J.S. McDonald. 1992. Effects of elevated carbon dioxide concentration on photosynthesis and growth of small birch plants (*Betula pendula* Roth.). *Plant, Cell and Environment*. 15:911-919.

Pye, J.M. 1988. Impact of ozone on the growth and yield of trees: a review. *Journal of Environmental Quality*. 17:347-360.

Raich, J.W. and K.J. Nadelhoffer. 1989. Belowground carbon allocation in forest ecosystems: global trends. *Ecology*. 70:1346-1354.

Raich, J.W., E.B. Rastetter, J.M. Melillo, D.W. Kicklighter, P.A. Steudler, B.J. Peterson, A.L. Grace, B. Moore III, and C.J. Vorosmarty. 1991. Potential net primary productivity in South America: Application of a global model. *Ecological Applications*. 1: 399-429.

Reich, P.B., and J.P. Lassoie. 1984. Effects of low level O₃ exposure on leaf diffusive conductance and water-use efficiency in hybrid poplar. *Plant, Cell and Environment*. 7:661-668.

Reich, P.B., and J.P. Lassoie. 1985. Influence of low concentrations of ozone on growth, biomass partitioning and leaf senescence in young hybrid poplar plants. *Environmental Pollution*. 39:39-51.

Reich, P.B., and R.G. Amundson. 1985. Ambient levels of ozone reduce net photosynthesis in tree and crop species. *Science*. 230:566-570.

Reich, P.B. 1987. Quantifying plant response to ozone: a unifying theory. *Tree Physiology*. 3: 63-91

Reich, P.B., D.S. Ellsworth, B.D. Kloeppel, J.H. Fownes, and S.T. Gower. 1990. Vertical variation in canopy structure and CO₂ exchange of oak-maple forests: influence of ozone, nitrogen, and other factors on simulated canopy carbon gain. *Tree Physiology*. 7:329-345.

Reich, P.B., B. Kloeppel, D.S. Ellsworth, and M.B. Walters. 1995. Different photosynthesis- nitrogen relations in deciduous and evergreen coniferous tree species. *Oecologia*. 104:24-30.

Reich, P.B., D.F. Grigal, J.D. Aber, and S.T. Gower. 1997. Nitrogen mineralization and productivity in 50 hardwood and conifer stands on diverse soils. *Ecology*. 78:335-347.

Reiners, W.A. and G.E. Lang. 1979. Vegetational patterns and processes in the balsam fir zone , White Mountains, New Hampshire. *Ecology*, 60: 403-417.

Running, S.W., and S. Gower. 1991. FOREST-BGC, a general model of forest ecosystem processes for regional applications. II. Dynamic carbon allocation and nitrogen budgets. *Tree Physiology*. 9: 147-160.

Sasser, C.L. and D. Binkley. 1989. Nitrogen mineralization in high-elevation forests of the Appalachians. II. Patterns with stand development in fir waves. *Biogeochemistry*. 7:147-155.

SCS. 1991. State soil geographic data base (STATSGO) data users guide. U.S. Soil Conservation Service Miscellaneous Publication 1492.

Schimel, D.S. 1995. Terrestrial biogeochemical cycles: global estimates with remote sensing. *Remote Sensing and Environment*. 51:49-56.

Schimel, D.S., B.H. Braswell, R. McKeown, D.S. Ojima, W.J. Parton, and W. Pulliam. 1996. Climate and Nitrogen controls on the geography and timescales of terrestrial biogeochemical cycling. *Global Biogeochemical Cycles*. 10: 677-692.

Scott, N.A. and D. Binkley. 1997. Foliage litter quality and annual net N mineralization: comparison across North American forest sites. *Oecologia*. 111:151-159.

Shenk, J. and M. Westerhaus. 1991. Population structuring of near infrared spectra and modified partial least squares regression. *Crop Science* 31:1548-1555.

Sinclair, T.R., C.B. Tanner and J.M. Bennet. 1984. Water-use efficiency in crop production. *Bioscience*. 34: 36-40.

Skarby, L., G. Wallin, G. Sellden, P.K. Karlsson, S. Ottosson, S. Sutinen, and P. Grennfelt. 1995. Tropospheric ozone - a stress factor for Norway spruce in Sweden. In: Staff, H. and Tyler, G. (eds.), *Effects of Acid Deposition and Tropospheric Ozone on Forest Ecosystems in Sweden*. *Ecological Bulletins (Copenhagen)* 44:133-146.

Slack, J.R., and J.M. Landwehr. 1992. *Hydro-Climatic Data Network (HCDN): A U.S. Geological Survey streamflow dataset for the United States for the study of climate variations, 1874-1988*. U.S. Geological Survey Open-File Report 92-129. Reston, VA.

Smith, M.L. 2000. Landscape-scale prediction of forest productivity by hyperspectral remote sensing of canopy nitrogen. University of New Hampshire Ph.D. Thesis.

Sprugel, D.G. 1984. Density, biomass, productivity, and nutrient-cycling changes during stand development in wave-regenerated balsam fir forests. *Ecological Monographs*. 54: 165-186.

Stump, L.M. and D. Binkley. 1993. Relationships between litter quality and nitrogen availability in Rocky Mountain forests. *Canadian Journal of Forest Research*. 23: 492-502.

Taylor, G. E. Jr., and P.J. Hanson. 1992. Forest trees and tropospheric ozone: role of canopy deposition and leaf uptake in developing exposure-response relationships. *Agriculture, Ecosystems and Environment*. 42:255-273.

Thorne, J.F. and S.P. Hamburg. 1985. Nitrification potentials of an old-field chronosequence in Campton, New Hampshire. *Ecology*. 66: 1333-1338.

Thorne, L., and G.P. Hanson. 1972. Species differences in rates of vegetal ozone absorption. *Environmental Pollution*. 3:303-312.

Tietema, A. and C. Beier. 1995. A correlative evaluation of nitrogen cycling in the forest ecosystems of the EC projects NITREX and EXMAN. *Forest Ecology and Management*. 71:142-152.

Tjoelker, M.G., J.C. Volin, J. Oleksyn, and P.B. Reich. 1995. Interaction of ozone pollution and light effects on photosynthesis in a forest canopy experiment. *Plant, Cell and Environment*. 18:895-905.

Townsend, A.R., B.H. Braswell, E.A. Holland and J.E. Penner. 1996. Spatial and temporal patterns in terrestrial carbon storage due to deposition of fossil fuel nitrogen. *Ecological Applications*. 6(3):806-814.

Turner, D.P., G.J. Koerper, M.E. Harmon and J.J. Lee. 1995. A carbon budget for forests of the conterminous United States. *Ecological Applications*. 5(2):421-436.

Van Cleve, K., J. Yarie, R. Erickson and C.T. Dyrness. 1993. Nitrogen mineralization and nitrification in successional ecosystems on the Tanna River floodplain, interior Alaska. *Canadian Journal of Forest Research*. 23:970-978.

VEMAP. 1995. Vegetation/ecosystem modeling and analysis project: Comparing biogeography and biogeochemistry models in a continental-scale study of terrestrial ecosystem responses to climate change and CO₂ doubling. *Global Biogeochemical cycles*. 9: 407-437.

Vitousek, P. M., and W. A. Reiners. 1975. Ecosystem succession and nutrient retention: a hypothesis. *Bioscience* 25(6):376-381.

Vitousek, P.M., J.R. Gosz, C.C. Grier, J.M. Melillo, W.A. Reiners and R.L. Told. 1979. Nitrate losses from disturbed ecosystems. *Science*. 204: 469-474.

Vitousek, P.M. and R.W. Howarth. 1991. Nitrogen limitation on land and sea: how can it occur? *Biogeochemistry*. 13: 87-115.

Volin, J.C., M.G. Tjoelker, J. Oleksyn, and P.B. Reich. 1993. Light environment alters response to ozone stress in seedlings of *Acer saccharum* Marsh. and hybrid *Populus* L. II. Diagnostic gas exchange and leaf chemistry. *New Phytologist*. 124:637-646

Volin, J.C., P.B. Reich, and T.J. Givnish. 1998. Elevated carbon dioxide ameliorates the effects of ozone on photosynthesis and growth: species respond similarly regardless of photosynthetic pathway or plant functional group. *New Phytologist*. 138:315-325.

Wang, D., D.F. Karnosky, and F.H. Bormann. 1986. Effects of ambient ozone on the productivity of *Populus tremuloides* Michx. grown under field conditions. *Canadian Journal of Forest Research* 16:47-55.

Weinstein, D.A. and R.D. Yanai. 1994. Integrating the effects of multiple stresses on plants using the simulation model TREGRO. *Journal of Environmental Quality*. 23:418-428.

Wessman, C.A., J.D. Aber, D.L. Peterson and J.M. Melillo. 1988. Remote sensing of canopy chemistry and nitrogen cycling in temperate forest ecosystems. *Nature*. 333:154-156.

Whittaker, R.H., F.H. Borman, G.E. Likens, and T.G. Siccama. 1974. The Hubbard Brook ecosystem study: forest biomass and production. *Ecological Monographs*. 44: 233-254.

Wofsy, S.C., M.L. Goulden, J.W. Munger, S.M. Fan, P.S. Bakwin, B.C. Daube, S.L. Bassow, F.A. Bazzaz. 1993. Net exchange of CO₂ in a mid-latitude forest. *Science*. 279:1314-1317.

Yin, X. 1992. Variation in foliar nitrogen concentration by forest type and climatic gradients in North America. *Canadian Journal of Forest Research*. 23:1587-1602.

Zak, D.R., G.E. Host and K.S. Pregitzer. 1989. Regional variability in nitrogen mineralization, nitrification, and overstory biomass in northern Lower Michigan. *Canadian Journal of Forest Research*. 19:1521-1526.